

2007

Dynamics and Divergences in Electromagnetic Backgrounds

Jameson, Paul

<http://hdl.handle.net/10026.1/2054>

<http://dx.doi.org/10.24382/4349>

University of Plymouth

All content in PEARL is protected by copyright law. Author manuscripts are made available in accordance with publisher policies. Please cite only the published version using the details provided on the item record or document. In the absence of an open licence (e.g. Creative Commons), permissions for further reuse of content should be sought from the publisher or author.

Dynamics and Divergences in Electromagnetic Backgrounds

A thesis submitted to the University of Plymouth in partial fulfillment
for the degree of

Doctor of Philosophy

Paul Jameson

School of Mathematics and Statistics

Faculty of Technology

19/11/2007

University of Plymouth
Library

9007965811

THESIS 5.80.1433

JABT.

This copy of the thesis has been supplied on the condition that anyone who consults it recognises that its copyright rests with the author and that no quotation from the thesis or information derived from it may be published without prior consent.

Abstract

Dynamics and Divergences in Electromagnetic Backgrounds

Paul Jameson

This thesis investigates the behaviour of a charge which is subjected to either an electromagnetic background created by a laser or a background which is hidden behind the resolution limitations of accelerator experiments. When a charge interacts with an intense laser beam its dynamics changes. The resulting trajectory of a non-relativistic particle is solved in this thesis without having to employ the dipole approximation. Many fundamental features of this trajectory are analysed including the drift velocity and the appearance of higher harmonic oscillations. In contrast, the interaction between a charge and an unobserved electromagnetic background leads to the infrared catastrophe. This has plagued field theories since the early nineteenth century. The standard theoretical response to such soft and collinear infrared divergences which are present in quantum field theories is the Lee-Nauenberg theorem. In this thesis a new class of collinear divergences associated with particles which are both soft and collinear will be discussed within the Coulomb scattering process. We show that all infrared singularities may be cancelled by the Lee-Nauenberg theorem but only if severe restrictions are placed on the normalisation of states and experimental set-up.

TABLE OF CONTENTS

<i>Introduction</i>	1
<i>Part I The Motion of a Charge Subjected to the Background Created by a Laser Beam</i>	
<i>1. Introduction</i>	6
<i>2. Methods and Concepts</i>	13
2.1 Plane Waves	13
2.2 Mechanics	15
2.3 Constrained Dynamics	20
2.3.1 The Dirac-Bergmann Algorithm	22
2.3.2 Lagrangian Reparametrisation Invariance	26
2.3.3 Light-Cone Coordinates	30
2.4 Canonical Transformations and Hamilton Jacobi Theory	31
<i>3. Non-Relativistic Dynamics beyond the Dipole Approximation</i>	37
3.1 Dipole Approximated Solution and Thomson Scattering	37
3.2 Parametric Solution	39
3.2.1 The Dirac Parametrisation method and Hamilton-Dirac Equation	40
3.2.2 Canonical Transformation to a Free System	43
3.2.3 Light-Cone Gauge Fixing and the Parametric Solution	46
3.2.4 Orbit of a Particle in a Weak Plane Wave Background	48
3.3 The Orbit of a Particle in a Monochromatic Plane Wave	49
3.3.1 Trajectory as a Function of the Laboratory Frame's Time	51
3.3.2 Modular Properties of the Orbits	58
3.4 Analysis of the Trajectory	59
3.5 Concluding Remarks	63

4. Relativistic Charge Subjected to the Background of a Laser	65
4.1 Parametric Solution	66
4.2 Solution in terms of the Average Rest Frame's Time	74
4.3 Parameter Region between Dipole and Relativistic Solutions	78
 Part II Unobserved Backgrounds and Infrared Divergences	83
1. Introduction	84
2. Yang Mills Theory	91
3. The Infrared Problem - Asymptotic Dynamics	95
4. From Bloch-Nordsieck to Lee-Nauenberg	99
4.1 The Virtual Process	100
4.2 Soft Emission and the Eikonal Approximation	102
4.3 Collinear Divergences and the Lee-Nauenberg Theorem	107
4.3.1 Processes with just Final State Degeneracies	115
4.4 Summation of Soft Divergences to all Orders	117
5. Lee-Nauenberg for Soft and Regular Collinear Infrared Divergences	125
6. Δ Collinear Divergences and Lee-Nauenberg theorem	134
6.1 Collinear Emission - $P_{0,1}$	136
6.2 Collinear Absorption - $P_{1,0}$	139
6.3 Collinear Emission and Absorption - $P_{1,1}$	142
6.4 Collinear Emission + Disconnected - $P_{1,2}$	148
6.5 Further $P_{n,m}$ Processes which Contribute to the Cross-Section at NLO	154
6.6 Cancelling Collinear Divergences and Energy Weighting	157
 Conclusion	171
 Appendix	175
A. Non-relativistic Symmetries	176
A.1 Gauge Transformations	176
A.2 Galilean Boosts	177

<i>B. General Boundary Conditions</i>	<i>178</i>
<i>C. Jacobian Elliptic Functions</i>	<i>180</i>
<i>D. Feynman Rules for QED</i>	<i>184</i>
<i>E. Some Collinear Approximations</i>	<i>186</i>

LIST OF FIGURES

<i>Part I</i>	6
1.1 Progress in laser technology	7
4.1 Parametric relativistic trajectory for a linearly polarised laser beam .	73
4.2 Domain in which the non-relativistic trajectory is applicable	80
4.3 Trajectory for a non-relativistic particle beyond the dipole approximation	82
 <i>Part II</i>	 84
1.1 Some processes which contribute to the Coulomb scattering cross-section	86
4.1 Tree-level Coulomb scattering	100
4.2 Next to leading order virtual contribution to Coulomb scattering . . .	100
4.3 Soft photon emission	103
4.4 Semi-hard collinear emission by the out-going electron	109
4.5 Collinear absorption by the in-coming electron	111
4.6 LEP process $e^+e^- \rightarrow q\bar{q} \rightarrow \text{jets}$	116
4.7 Coulomb scattering including hard virtual processes	117
4.8 Example virtual photon contribution	118
5.1 Emission and absorption processes	128
5.2 Disconnected process and its associated Feynman rule	129
5.3 Emission combined with a disconnected photon – $P_{1,2}$	129
5.4 Absorption combined with a disconnected photon – $P_{2,1}$	132
6.1 Emission of a photon by the in-state electron which is collinear with the in-state electron	137
6.2 Interference between emission by the in-state and out-state electrons .	139
6.3 Absorption collinear with the out-going electron	140
6.4 Emission and absorption by the in-state electron	143

6.5	Emission combined with a disconnected process, $P_{1,2}$, with momenta labels	148
6.6	Possible contractions of photon lines	150
6.7	Absorption and disconnected – $P_{2,1}$	154
6.8	Processes contributing to a symmetric cancellation of collinear divergences	165

LIST OF TABLES

<i>Part II</i>	84
6.1 Cross-section contribution for all processes contributing at NLO to Coulomb scattering	161
<i>Appendix</i>	176
D.1 Feynman rules for QED	185

ACKNOWLEDGEMENTS

I would like to express my sincere thanks to David McMullan and Tom Heinzl of the University of Plymouth for their supervision and assistance during this research. I would like to include Martin Lavelle who has provided valuable advise on the infrared research. I want to express my gratitude to Arsen Khvedelidze for his guidance on the laser research. Thanks to the Joint Institute for Nuclear Research, Dubna for their hospitality. My gratitude to Stephen Jameson and Antony Ilderton for thoroughly proof reading several sections of this thesis. Finally I would like to thank my colleague Peter Jerney and my wife Eleanor Jameson for their support during my studies.

Author's Declaration

At no time during the registration for the degree of Doctor of Philosophy has the author been registered for any other University award. This programme of advanced study was financed with the aid of a studentship from the Particle Physics and Astronomy Research Council.

Word Count: 39834

Publications:

Infrared Divergences from Soft and Collinear Gauge Bosons, Proceedings for the Ninth Workshop on Non-Perturbative Quantum Chromodynamics, Paris, June 2007. A copy of this paper can be found at the end of the thesis.

In Preparation:


Particles Dynamics in a Strong Laser Field beyond the Dipole Approximation, with A. Khvedelidze.

Infrared Divergences from Soft and Collinear Gauge Bosons, with D. McMullan and M. Lavelle.

Presentations and Conferences Attended:

Ninth Workshop on Non-Perturbative Quantum Chromodynamics, l'Institut Astrophysique de Paris, 4-8th June 2007.

QCD 06 - 13th International QCD Conference, Montpellier, 3-7th July 2006.

Signed... 

Dated... 23/1/2008

INTRODUCTION

This thesis investigates the effects which an electromagnetic background has on charges. The background might be manifest, as in the case of a laser, or hidden behind the resolution limitation of experimental detectors. The physical implications of such backgrounds are significant but, to a large extent, poorly understood. The aim of this thesis is to develop a greater understanding of the behaviour of a charge in both a laser and an unobserved electromagnetic background. There will be two themes to this thesis. First we consider the motion of a classical charged particle when it is subjected to the intense electromagnetic background of a laser. Following this the infrared singularities which manifest themselves in quantum field theories will be investigated. Although there is a significant overlap between the two projects the methods developed are quite distinct so each project will be essentially self-contained. Therefore this thesis is structured in two parts followed up by an overall conclusion.

The word laser is an acronym which stands for ‘light amplification by stimulated emission of radiation’. Typical lasers emit light with a well defined wavelength in a narrow beam. This contrasts with more traditional light sources, such as the incandescent light bulb, which emits radiation over a wide spectrum of wavelengths into a large solid angle. A laser is designed and calibrated for a particular purpose which gives it certain properties. Some of these properties are discussed within part I. The first working laser was demonstrated in May 1960 by Theodore Maiman at Hughes Research Laboratories. Once lasers were said to be a ‘solution’ without a problem but today they have become a multi-billion dollar industry. The most widespread use of lasers is in optical storage devices such as the compact disc and DVD players, in which the laser scans the surface of the disc. Other common applications of lasers are bar code readers and laser pointers. In industry, lasers are used for cutting steel and other metals and for inscribing patterns. Lasers are also commonly used in various fields in science, especially spectroscopy, typically because

of their well-defined wavelength or short pulse duration in the case of pulsed lasers. Lasers are also used for military and medical applications. Recent rapid technology developments have lead to great interest in lasers from particle physicists. Some exciting laser phenomena are discussed in the introduction to part I.

The infrared catastrophe originated in classical field theories and appears when considering classical bremsstrahlung, i.e. the radiation produced by a charge which is suddenly accelerated. It is shown, on page 40 of [1], that although the total amount of energy radiated by the charge is finite the total number of light quanta (photons) required to emit this energy is infinite which leads to infrared divergent cross-sections. A solution to this problem was recognised during one of the earliest papers on QED by Bloch and Nordsieck [2]. These authors found that singularities also appear in some QED cross-sections provided there is more than one interaction vertex, i.e. beyond leading order in perturbation theory. Bloch and Nordsieck found that by adding to the bremsstrahlung process the cross-section contribution from a virtual photon the overall cross-section is finite. Within an experiment there may be low energy unobserved photons accompanying charges. Our detectors cannot distinguish between processes containing low energy photons and those without. They are referred to as degenerate processes. Since Bloch and Nordsieck released their original paper on the infrared problem in QED other types of infrared singularities have been found and new methods to deal with these divergences have been discovered. Much work has been done on the physical interpretation of these divergences [3]. The greatest advance in our understanding of the infrared properties of QED came during the 1960's through the work of Kinoshita [4], Lee and Nauenberg [5] and Chung [6]. These authors addressed different questions regarding the infrared and their conclusions are somewhat different. Chung wanted to go beyond the cross-section approach of Bloch and Nordsieck and develop an infrared finite S -matrix description of scattering. Lee and Nauenberg adopted a more conservative approach

and extended the Bloch-Nordsieck mechanism to cover all infrared divergences with the aid of calculations by Kinoshita. Today the Lee-Nauenberg theorem is widely accepted as the method used to remove infrared singularities from cross-sections and the approach taken by Chung is relatively unknown.

The presence of *symmetries* within the Lagrangian, which describes the system, is an important aspect for both projects. Transformations of the canonical variables under which the Lagrangian is invariant has important consequences for the system. Examples of this, discussed within this thesis, are the Lorentz and their non-relativistic counterpart Galilean transformations, gauge transforms and reparametrisation invariance. Constraints is another issue which spans both topics which leads to physical effects such as Gauss' law in QED and the mass-shell condition for relativistic mechanics, $E^2 = m^2c^4 + \mathbf{p}^2c^2$. We will see that both the laser background and the unobserved background lead to a mass-shift effect.

The remainder of this introduction will serve to inform the reader which parts of this thesis are already scientifically well known and which parts are original contributions by the author of this thesis. The motion of a relativistic charged particle in the electromagnetic background of a laser has been previously studied by many authors [7, 8]. However, for the motion of a non-relativistic charge the 'dipole approximation' is often used, which neglects the influence of the magnetic field of the laser on the charge. The non-relativistic theory has many uses. For instance, it is ideally suited to describe atoms where particles are bound together by a potential. Potentials do not account for the relativistic retardation effect so they are fundamentally non-relativistic. During part I chapter 3 we derive the previously unknown trajectory for the motion of a non-relativistic particle without having to apply the dipole approximation. This has the effect of making the non-relativistic theory applicable to a greater range, in terms of the intensity and frequency, of laser. During chapter 4, we proceed to show exactly what lasers the non-relativistic

trajectory can be applied to. Often the relativistic trajectory is given in a parametric form, where the trajectory is described by the proper time. An observer who sees that the particle is moving at a velocity which approaches the speed of light would need to know the relationship between the time measured on his clock and the proper time in order to predict the motion of the charge. Only once in the literature is the trajectory written in terms of the reference frame's time [9]. The method used by Sengupta to derive the three dimensional trajectory is complicated but in chapter 4 we find an alternative, somewhat simpler, method. The relativistic and non-relativistic trajectories are then compared.

Part II aims to give a thorough description of the widely accepted method, proposed by Lee and Nauenberg, to remove infrared singularities to processes with both final and initial degeneracies. After introducing the different types of infrared divergences and the physical reason why these divergences occur in QED, we proceed in part II chapter 4 to analyse the Bloch-Nordsieck and Lee-Nauenberg approach to Coulomb scattering. Subtleties associated with low energy photons have been pointed out by Lavelle and McMullan [10] and, using Coulomb scattering as an explicit example, they found many hidden assumptions of the Lee-Nauenberg proposition which are reviewed in chapters 4 and 5. In [10] the authors also commented on a class of infrared divergences which Lee and Nauenberg omitted in their original calculations. In chapter 6 we show how to systematically include all degenerate processes and prove that the requirement to simultaneously cancel all types of infrared divergences at the level of the cross-section leads to dramatic restrictions on the way states are normalised and experiments are conducted. This allows us to question the physical significance of the Lee-Nauenberg proposition.

Part I

THE MOTION OF A CHARGE SUBJECTED TO THE BACKGROUND CREATED BY A LASER BEAM

1. INTRODUCTION

By the end of the 20th century Quantum Electrodynamics had been proven to correctly describe the interaction between light and charged matter within a vacuum. It had passed many high precision tests [11]. Perturbative QED is successful despite not taking into account the *coherence*¹ of the photons. Until the development of the laser, photon sources could only produce incoherent photons, one at a time. Perturbative QED only considers a *single photon* interacting with a *single charge* at a time, which was adequate.

Since the mid 1980's a huge amount of development has been conducted into laser technology, as may be seen from figure 1.1. The lasers which are manufactured for research today are capable of producing petawatt intensity short attosecond pulses of light. The physics which occurs in a strong field is rather different compared to the physics within a vacuum. To reinforce this statement we consider an example, using values obtained from [12]. If we have an optical frequency laser operating with an intensity of $10^{19}\text{W}/\text{cm}^2$, an isolated electron within the electromagnetic field has an energy of interaction of approximately 10^6eV . The energy of a single photon of this laser is approximately 1eV so the electron must have interacted with at least 10^6 photons. The rest energy of an electron is 511keV so the electron must be a relativistic particle. The laser clearly provides a physical environment which is quite foreign to conventional low intensity accelerator physics but still capable of achieving high energies. Research in this field opens up the possibility of exploring fundamental physics in a new environment which may be used to enhance our understanding of the

¹ Coherence is the property of wave-like states that enables them to exhibit interference.

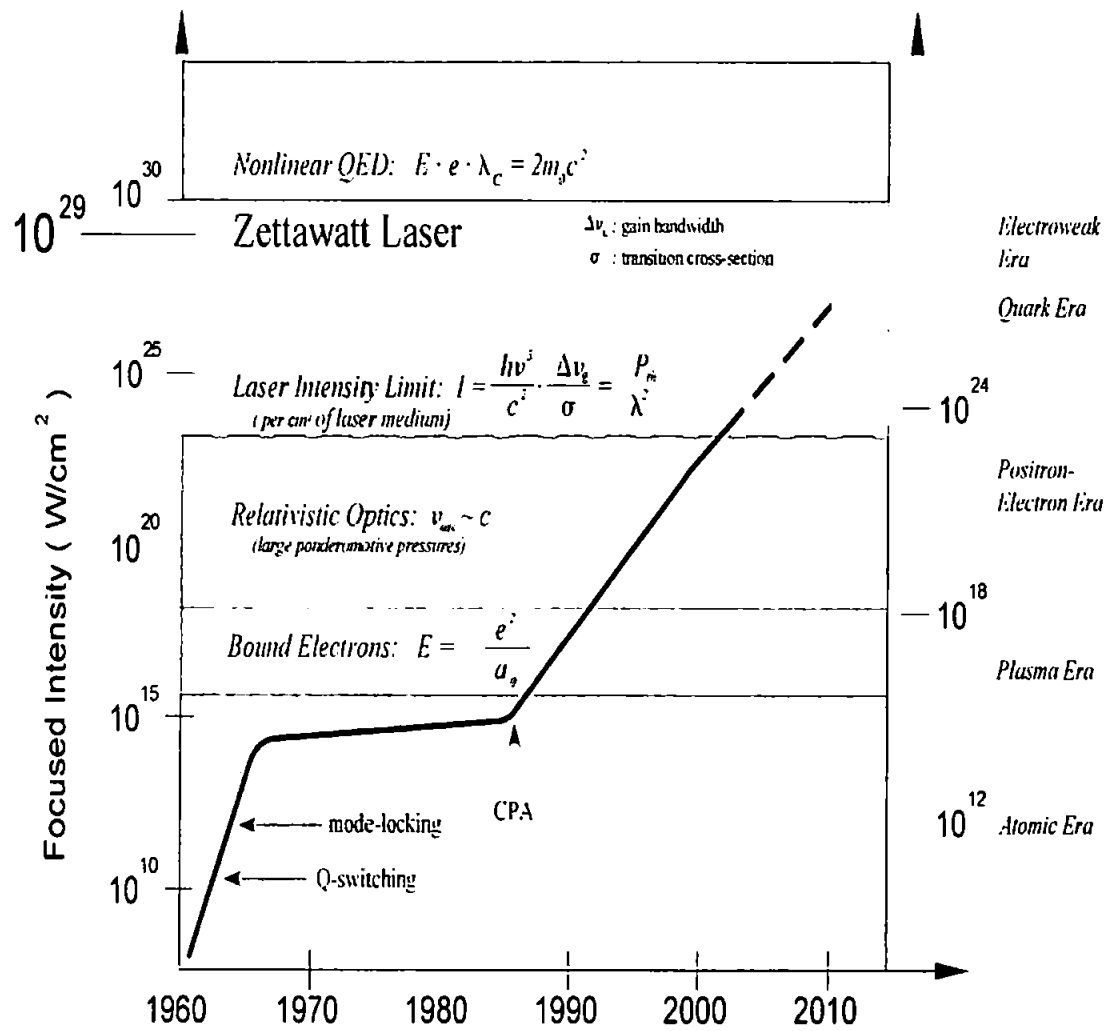


Fig. 1.1: Progress in laser technology (Source: Tajima, Mourou 2002)

world (see e.g. [13–16] and recent surveys [17], [18]). Multi-photon experiments have shown us that it is necessary to modify the conventional single particle description of the radiation-matter interaction. QED must be applied in an environment other than the vacuum in order to extend its predictive power.

Many exciting experimental consequences are predicted when using strong enough fields, such as spontaneous pair creation, light-by-light scattering, multiphoton effects in Thomson scattering, the mass-shift and drift velocity. Pair creation has been observed at SLAC E-144 in 1997 [19]. In this experiment plane wave laser field photons γ_L are probed by another high energy photon γ . Through the reaction

$$\gamma + n\gamma_L \rightarrow e^+ e^- \quad (1.1)$$

the n laser photons collide, by means of virtual particles, with the high energy photon to produce an electron-positron pair. More intense lasers lead to a faster transition rate per probe photon [20]. If the field strength reaches the *critical field* the field will become unstable and pairs will be produced spontaneously. The critical field is defined as the field in which an electron gains energy, across a Compton wavelength, equal to its rest mass [21, 22]. The rate for spontaneous pair creation² is much lower [20] than that produced during the SLAC experiment because we cannot produce fields close enough to the critical field.

Pair creation and light-by-light scattering are obviously quantum effects. However, the probabilities of these occurring without stimulation for current lasers is low. Many of the most interesting predictions are classical in nature, such as the modification to Thomson scattering, mass-shift and the drift velocity. It is these classical phenomena which we will study in the following material.

During this thesis we will be studying the motion of a charge within strong and weak electromagnetic backgrounds. Classically interactions between a charged

² Pair creation from a constant electric field

particle and a laser beam have been studied in the past. Known non-relativistic solutions take $v \ll c$ and the *dipole approximation*³ is used. The dipole approximation has two implications:

1. the influence of the magnetic portion of the Heaviside-Lorentz force on the charge is neglected;
2. the position of the charge in the field no longer modifies the trajectory.

This then leads to the well known Thomson scattering [7, 23] cross-section formula

$$\sigma_T = \frac{8\pi}{3} \left(\frac{e^2}{mc^2} \right)^2. \quad (1.2)$$

The dipole approximated solution for the motion of a charge will be reviewed in section 3.1.

New research conducted by the author has shown that it is possible to go beyond the dipole approximation and this will be covered in chapter 3. A solution to the trajectory for a non-relativistic particle is derived which takes into account the position of the charge within the field and the full Heaviside-Lorentz force. We keep $\mathcal{O}(v/c)$ but drop the “truly relativistic” second order effects $\mathcal{O}(v^2/c^2)$, such as the relativistic correction to the kinetic energy through the Darwin term and the spin-orbital coupling effects on the Lagrangian. Reiss [12, 24] has shown that there is an intermediate region with a wide range of parameters (in laser intensity and frequency) where the leading contribution to the deviation from the dipole approximated solution comes solely from the magnetic field effect. The terms $\mathcal{O}(v^2/c^2)$ can be still be neglected. Reiss’ observation motivated us to fill this gap in the theory. Such an approach is attractive for the description of laser-atom interactions, where the whole formalism is intrinsically non-relativistic (see [25] and

³ The name “dipole” was given because the formula for dipole radiation [7] is used when one comes to study the scattering of the light by the charge

references within). The widely used numerical technique becomes cumbersome when passing to the fully four dimensional relativistically covariant description. This work may be important for the study of atoms in laser backgrounds because potentials are intrinsically non-relativistic. Several partially relativistic approaches have been conducted previously which include the effect of the magnetic field [12, 26] but do not go fully beyond the dipole approximation.

The motion of the electron in a laser beam has the relativistic energy which is given by [8, 12]:

$$E = mc^2 - \frac{e^2 \langle A_\mu A^\mu \rangle}{2mc^2}, \quad (1.3)$$

where $\langle A_\mu A^\mu \rangle$ is the time-averaged square of the electromagnetic four-vector potential. The first term is the relativistic rest energy of the particle and the second term is called the ‘ponderomotive potential’ U_p which is a relativistic invariant. The laser *intensity parameter* can be defined as

$$\eta^2 := \frac{4U_p}{mc^2}. \quad (1.4)$$

This quantity arose many years ago [27–29]. It was found that η^2 may be viewed as a *mass-shift* effect. The normal mass of the electron appears to be modified by the laser. The mass-shift will be derived in chapter 4 and we will find that the effective mass is given by the formula

$$m^{*2} = m^2(1 + \eta^2). \quad (1.5)$$

When the interaction energy U_p is of the order of the rest energy, the mass-shift effect is large and the effects of the field are relativistic in nature. Relativistic effects become important when the field is sufficiently strong and it has been suggested [12, 24] that the required laser intensity corresponds to $\eta^2 \approx 0.1$.

The fully relativistic theory, which is valid for all values of the intensity parameter, has been solved⁴. However, the solution is usually written in a parametric form where the trajectory of the charge is described by the proper time. If the charge is moving at a velocity close to the speed of light in the frame we are considering then the proper time will be significantly different to the observers time. The four dimensional parametric solution can be improved by writing the trajectory in a three dimensional form $\mathbf{x}(t)$ if the relationship between the time and proper time is invertible. The explicit solution $\mathbf{x}(t)$ is much more complicated than the parametric solution. Sengupta [9] found the three dimensional solution and showed that the oscillation frequency for the relativistic solution is not the same as the incident frequency of the laser but depends upon the intensity. The orbit of the particle includes all harmonic oscillations⁵ and as a result of this the classical Thomson cross-section, (3.4), is modified for high-intensity laser beams (see e.g., the basic references [8, 37–40] and for the recent direct experimental observation of second harmonics [41]). Higher harmonics are not predicted when the simple dipole approximation is used for a non-relativistic particle but, by going beyond this approximation, we will see that all harmonics are present in the orbit. In section 4.2 the method used by Sengupta to find the three dimensional relativistic solution [9] will be improved upon.

The material in part I is organised as follows. Background topics which are required to comprehend the solutions for both relativistic and non-relativistic problems are presented in chapter 2. The plane waves we use to model the laser beam are discussed. Systems which describe the interaction of a charge with a laser beam contain constraints so we will explain how to deal with these through

⁴ To the best of our knowledge, J. Frenkel was the first person to present the parametric relativistic solution [30]. Since that publication this problem has been studied many times in different contexts. For the principal references see the reviews [17, 18], original papers [27–29, 31–35] and the textbooks [1, 7, 36].

⁵ If the frequency of a wave is ω then the harmonics have frequency, $n\omega$, where n is any positive integer.

the Dirac-Bergmann algorithm [42–44]. Finally canonical transformations, which will be used to simplify many problems and enable us to determine trajectories, will be covered. Chapter 3 considers the motion of a non-relativistic charge in the electromagnetic background of a laser. At first the dipole approximation is used but, following this, we derive a new result using a novel method which does not require this approximation. In chapter 4 we consider a fully relativistic particle. Its parametric trajectory is derived and then we find an alternative method to derive the three dimensional solution. Finally we consider the parameter region in which the non-relativistic solution we discovered without having to resort to the dipole approximation can accurately describe the motion of the particle.

Much of the original research presented in chapters 3 and 4 has been discovered in collaboration with Dr A. Khvedelidze from the Joint Institute for Nuclear Research, Dubna, Russia. A publication is in preparation regarding the material covered in chapter 3.

2. METHODS AND CONCEPTS

2.1 Plane Waves

The electromagnetic field in a vacuum is determined from Maxwell's equations [7, 23] with charge density $\rho = 0$ and current density $\mathbf{j} = 0$

$$\nabla \times \mathbf{E} = -\frac{1}{c} \frac{\partial \mathbf{B}}{\partial t}, \quad \nabla \cdot \mathbf{E} = 0, \quad (2.1)$$

$$\nabla \times \mathbf{B} = \frac{1}{c} \frac{\partial \mathbf{E}}{\partial t}, \quad \nabla \cdot \mathbf{B} = 0. \quad (2.2)$$

A non-zero field may exist without the presence of charges but it must be time varying (see [7] p108).

A wave equation for the gauge potentials can be derived from Maxwell's equations. We define the gauge potential from the fields in the usual way

$$\mathbf{E} = \nabla \phi - \frac{1}{c} \frac{\partial \mathbf{A}}{\partial t}, \quad \mathbf{B} = \nabla \times \mathbf{A}. \quad (2.3)$$

By making the radiation gauge choice, $\phi = 0$ and $\nabla \cdot \mathbf{A} = 0$, and using the first of Maxwell's equations in (2.2) it can be seen that

$$\nabla^2 \mathbf{A} - \frac{1}{c^2} \frac{\partial^2 \mathbf{A}}{\partial t^2} = 0, \quad (2.4)$$

which is called the wave equation. The wave equation is also called d'Alembert's equation. This may also be derived using the Lorentz gauge condition $\partial_\mu A^\mu = 0$ [7].

A *plane wave* is a special form of an electromagnetic wave where the fields depend

on only one spatial coordinate, which we take to be the \hat{z} direction, and time. The wave equation (2.4) becomes

$$\frac{\partial^2 \mathbf{A}}{\partial z^2} - \frac{1}{c^2} \frac{\partial^2 \mathbf{A}}{\partial t^2} = 0. \quad (2.5)$$

To solve this equation we introduce the variables $\xi = t - z/c$ and $\eta = t + z/c$ and re-write the wave equation as

$$\frac{\partial^2 \mathbf{A}}{\partial \xi \partial \eta} = 0. \quad (2.6)$$

If the gauge potential depends solely on either ξ or η the equation is solved. Conventionally we choose $\mathbf{A} = \mathbf{A}(\xi)$. These plane waves are interpreted as an electromagnetic field propagating along the positive \hat{z} direction.

For plane waves the Coulomb gauge condition reduces to

$$\nabla \cdot \mathbf{A} = \frac{\partial A_z}{\partial z} = 0. \quad (2.7)$$

From this condition it can be seen that (2.5) predicts a constant electric field. Since there can be no overall electric field when the charge and current density are zero so we set $A_z = 0$. The vector potential is perpendicular to the propagation direction. Using these gauge choices the fields (2.3) become

$$\mathbf{E} = -\frac{1}{c} \frac{\partial \mathbf{A}}{\partial \xi}, \quad \mathbf{B} = \hat{z} \times \mathbf{E}. \quad (2.8)$$

The fields are perpendicular to the propagation direction of the plane wave, \hat{z} and to each other.

If the wave is a periodic function of time it is said to be *monochromatic*. Let ω_L be the frequency of the wave, the time dependence of the wave is of the form $\cos(\omega_L t + \alpha)$.

If we have a monochromatic plane wave the wave equation (2.5) becomes

$$\frac{\partial^2 \mathbf{A}}{\partial z^2} + \frac{\omega_L^2}{c^2} \mathbf{A} = 0. \quad (2.9)$$

The vector potential is a function of $\omega_L(t - z/c)$. The wave is said to be *linearly polarised* if the gauge potential is zero in the x or y direction and *circularly polarised* if the amplitude for the A_x and A_y components are the same. For linear polarisation the electric field vector's components E_x and E_y are in phase, so the direction of the electric field vector is constant, this is also true for the magnetic field. The components of the electric field are 90 degrees out of phase for circular polarisation. To an observer stationed at the laser it appears that the electric field rotates in a clockwise direction about the \hat{z} direction.

An electromagnetic monochromatic plane wave represents the simplest way to model a laser field. This is a reasonable assumption providing the transverse directions of the laser beam are much larger than the dimensions of the system considered. In reality most lasers have a focal spot of a few optical wavelengths.

2.2 Mechanics

The Lagrangian Formulation

In classical mechanics the equations of motion follow from the principle of least action [45, 46]. Let $x = \{x_1, x_2, \dots, x_n\}$ be a collection of coordinates and \dot{x} be the velocities at time t . The action is defined as

$$S = \int_{t_1}^{t_2} dt \mathcal{L}[x(t), \dot{x}(t), t], \quad (2.10)$$

where \mathcal{L} is the Lagrangian. For the systems we will consider the Lagrangian depends explicitly on the time.

There are many different routes a particle can take between two points. The principle of least action states that there is only one path the particle follows which joins point A at time t_1 to point B at time t_2 . This is called the classical path and it yields a stationary value for the action $\delta S = 0$. This principle implies the Euler-Lagrange equations of motion

$$\frac{\partial \mathcal{L}}{\partial x^i} - \frac{d}{dt} \frac{\partial \mathcal{L}}{\partial \dot{x}^i} = 0. \quad (2.11)$$

If \mathcal{L} is quadratic in \dot{x} there are n second order equations of motion in total for the system. To obtain an exact solution $2n$ initial conditions must be specified.

In the Lagrange formulation of mechanics the state of the system is represented by a point in an n -dimensional configuration space with n coordinates x^i . This point traverses a path in configuration space as 'time' evolves according to the solution of the Euler-Lagrange equations. Physically the velocities \dot{x}^i are not separate degrees of freedom so the system has n degrees of freedom.

The Hamiltonian Formulation

From a mathematical viewpoint in the Lagrangian formulation the x 's and \dot{x} 's have been treated as independent variables. Therefore it can be argued that there are $2n$ independent variables describing the Lagrange formulation. In the Hamiltonian formulation the system is described using the coordinates x^i and the conjugate momenta defined by

$$p^i(t) = \frac{\partial \mathcal{L}(x, \dot{x}, t)}{\partial \dot{x}^i}. \quad (2.12)$$

The quantities x and p are known as canonical variables and the system is described within *phase space*.

If the Lagrangian of a system does not contain a given coordinate then the coordinate is said to be *cyclic* [46]. The conjugate momentum to a cyclic coordinate

is conserved since the Euler-Lagrange equation reduces to

$$\frac{dp_i}{dt} = 0. \quad (2.13)$$

Systems with more cyclic coordinates tend to be easier to solve because more of the initial conditions are known.

The transition from Lagrange's to Hamilton's formulation corresponds to a change of variables from (x, \dot{x}, t) to (x, p, t) . The procedure for switching variables is known as a Legendre transformation [46]. Define the function

$$H_c(x, p, t) = \dot{x}^i p_i - \mathcal{L}(x, \dot{x}, t), \quad (2.14)$$

known as the Hamiltonian. This is considered as a function of (x, p, t) providing (2.12) may be inverted to express the velocities in terms of phase space variables. The differential of H_c is

$$dH_c = \frac{\partial H_c}{\partial x_i} dx_i + \frac{\partial H_c}{\partial p_i} dp_i + \frac{\partial H_c}{\partial t} dt = \dot{x}^i dp_i + p_i d\dot{x}^i - \frac{\partial \mathcal{L}}{\partial \dot{x}_i} d\dot{x}_i - \frac{\partial \mathcal{L}}{\partial x_i} dx_i - \frac{\partial \mathcal{L}}{\partial t} dt. \quad (2.15)$$

The terms proportional to $d\dot{x}_i$ vanish due to the definition of conjugate momenta (2.12). By using the definition of the conjugate momenta in the Euler-Lagrange equations (2.11) it can be seen that

$$\frac{\partial \mathcal{L}}{\partial x^i} = \dot{p}_i. \quad (2.16)$$

Now from (2.15) Hamilton's equations of motion can be derived by equating coefficients of dx_i and dp_i to find

$$\dot{x}^i = \frac{\partial H_c}{\partial p_i}, \quad \dot{p}^i = -\frac{\partial H_c}{\partial x_i}. \quad (2.17)$$

They take the form of $2n$ first order equations of motion. They require one initial condition per equation to solve. The n second order equations (2.11) are replaced by (2.17) in the transition from a Lagrangian to Hamiltonian formulation for a given system.

From Hamilton's equations of motion it can be seen that the Hamiltonian takes on the rôle of generator of time evolution. Consider an arbitrary function A which depends on the coordinates and momenta, then the derivative with respect to time

$$\dot{A}(x, p) = \{A, H\}. \quad (2.18)$$

Here the Poisson brackets have been introduced which are defined in the standard way

$$\{A, B\} = \frac{\partial A}{\partial x^i} \frac{\partial B}{\partial p_i} - \frac{\partial A}{\partial p_i} \frac{\partial B}{\partial x^i}. \quad (2.19)$$

Therefore (2.17) may be re-written as

$$\dot{x}^i = \{x^i, H_c\}, \quad \dot{p}^i = \{p^i, H_c\}. \quad (2.20)$$

Both forms of Hamilton's equations (2.17) and (2.20) will be used in the following material.

The Hamiltonian for each problem must be constructed from the Lagrangian formulation using the following steps:

1. Choose a set of coordinates x^i (e.g cartesian, polar etc) and write down the Lagrangian for the system in question;
2. Derive the conjugate momentum using (2.12) as a function of x^i , \dot{x}^i and t ;
3. Write down the Hamiltonian using (2.14);
4. Invert the conjugate momenta formula to make the velocities, \dot{x}^i the subject of

the formula. They will be functions of $\{x, p, t\}$;

5. Eliminate the \dot{x}^i 's from the Hamiltonian so it depends only on phase space variables and time;
6. Hamilton's equations of motion may be used.

The laser systems considered in this thesis contain constraints which prevents steps 4, 5 & 6 from being done. The modification of the Legendre transforms due to constraints will be discussed in section 2.3.

For many systems the Hamiltonian is the total energy $H_c = T + V$, where T and V are the kinetic and potential energies. Often energy is conserved within a system hence the Hamiltonian is frequently a conserved quantity. Time dependent external forces, such as laser beams, may add energy to a system in which case the Hamiltonian is not conserved since it is a function of time. The Hamiltonian is only equal to the total energy if the forces are *conservative*¹. If a part of the Lagrangian potential term is of degree one in the velocities the system is not conservative, an example of this would be a non-relativistic particle interacting with an external electromagnetic source. Later, in section 2.3.2, we will study systems in which the canonical Hamiltonian vanishes. The Hamiltonian will be conserved but it is not the total energy.

Free Non-Relativistic Particle

The free particle is the simplest system which may be solved completely. Later, we will use a canonical transform (see section 2.4) to reduce more complex systems to the free system. Now, we will review the relevant material.

¹ A force is defined as being conservative if the work done moving from point A to B is the same for all possible paths from A to B . The potential V is a function of $x(t)$ only, not the velocities. The system does not lose energy through frictional (e.g. the damped harmonic oscillator) or other external forces.

For a non-relativistic particle the free theory is governed by the Lagrangian or Hamiltonian

$$\mathcal{L} = \frac{m}{2} \dot{\mathbf{x}}^2, \quad H_c = \frac{1}{2m} \mathbf{p}^2, \quad (2.21)$$

where the three momentum $\mathbf{p} = m\dot{\mathbf{x}}$. The Lagrangian is homogeneous to degree two in the velocities so it is purely kinetic energy. The Hamiltonian is the total energy of the system and is conserved. All of the coordinates \mathbf{x} are cyclic, so we know the canonical momenta are constants. Solving the Euler-Lagrange or Hamilton's equations (2.17) are straightforward

$$\dot{\mathbf{x}} = \frac{\mathbf{p}}{m}, \quad \dot{\mathbf{p}} = 0, \quad \text{so} \quad \mathbf{x} = \frac{\mathbf{p}t}{m} + \mathbf{c}. \quad (2.22)$$

The particle moves at an uniform velocity. To obtain a complete solution we need three more initial conditions which give values for the constant vector \mathbf{c} .

2.3 Constrained Dynamics

Many of the problems we will deal with contain constraints [44]. A system with n degrees of freedom is governed by Lagrange function $\mathcal{L}(x^i, \dot{x}^i; t)$ where $i = 1, 2, \dots, n$. This leads to the Euler-Lagrange (2.11) equations of motion

$$\begin{aligned} \frac{\partial \mathcal{L}}{\partial x^i} &= \frac{d}{dt} \frac{\partial \mathcal{L}}{\partial \dot{x}^i} \\ &= W_{ik} \ddot{x}^k + \frac{\partial^2 \mathcal{L}}{\partial \dot{x}^i \partial x^k} \dot{x}^k + \frac{\partial^2 \mathcal{L}}{\partial \dot{x}^i \partial t}, \end{aligned} \quad (2.23)$$

where we have defined the Hessian matrix

$$W_{ik} = \frac{\partial^2 \mathcal{L}}{\partial \dot{x}^i \partial \dot{x}^k}. \quad (2.24)$$

The accelerations \ddot{x}^k may only be uniquely determined by the positions and velocities if W_{ik} can be inverted. Now define the Hessian, $W = \det(W_{ik})$, this is a very important quantity because it determines if there are constraints within a system. In a constrained system the coordinates and the conjugate momenta are not independent. Constrained systems have the property that $W = 0$ and, as we will shortly see, this means the Legendre transform from the Lagrangian formulation to the Hamiltonian formulation of mechanics is not unique. As an example of this take a free classical relativistic particle which is described by the Lagrangian, $\mathcal{L} = m\sqrt{\dot{x}^2(\tau)}$. Here the dot represents differentiation with respect to the proper time, τ . The Hessian,

$$W = \frac{m}{(\sqrt{\dot{x}^2})^3} \det [\dot{x}^2 \delta_{ik} - \dot{x}_i \dot{x}_k] = 0, \quad (2.25)$$

therefore this is a constrained system.

A matrix rank is the number of independent rows or columns. For constrained systems $W = 0$ implies that the matrix rank, r of W_{ik} is less than n . If W_{ik} were to be reduced to row echelon form it would have $n - r$ rows of zero's. This leads to $n - r$ Euler-Lagrange equations which do not contain accelerations. There are still r equations which contain accelerations and only these shall be called 'equations of motion'.

There are many examples of constraints within mechanics and field theory. In relativistic mechanics the mass-shell condition $p^2 = (mc)^2$ is the constraint, associated with the example in (2.25), and for electromagnetism the momentum conjugate to A_0 vanishes which is another constraint. Dirac set up the formalism to treat constraints consistently [42–44].

2.3.1 The Dirac-Bergmann Algorithm

The Dirac-Bergmann algorithm [42–44] treats constraints within the Hamiltonian formalism of classical mechanics. Starting with the definition of the canonical momenta

$$p_i = \frac{\partial \mathcal{L}(x_i, \dot{x}_i)}{\partial \dot{x}^i}, \quad i = 1, 2, \dots, n, \quad (2.26)$$

it can be seen that the Hessian matrix is equal to $\partial p_i / \partial \dot{x}^j$. Reduce the Hessian matrix to row echelon form so it contains rows of zeros if there are constraints. Let the first r rows of the Hessian matrix be non-zero. Define indices $a, b = 1, 2, \dots, r$ and $\rho, \sigma = (r+1), (r+2), \dots, n$ so, for some values of i we find $W_{ai} \neq 0$ and $W_{\rho i} = 0$ for all i . Since $W_{\rho i} = 0$ it can be seen that p_ρ does not depend on \dot{x}^j . Overall, the conjugate momenta are functions of

$$p_a = p_a(x, \dot{x}_b, \dot{x}_\rho; p_i) \quad \text{and} \quad p_\rho = p_\rho(x_i, p_i) \quad (2.27)$$

By inverting the equation for p_a and since p_ρ does not depend on \dot{x}^j we find

$$\dot{x}^a = f^a(x_i, p_b, \dot{x}_\rho). \quad (2.28)$$

With constraints present the Hamiltonian may not be written as a function of $\{x, p, t\}$. Substituting (2.28) into the definition of conjugate momenta (2.26) it can be seen that $p_i = g_i(x_i, p_b, \dot{x}_\rho)$. For $i = \rho$ the function g cannot depend on the velocities \dot{x}_ρ from (2.27), therefore

$$p_\rho = g_\rho(x_i, p_b). \quad (2.29)$$

This gives $(n - r)$ relations between the coordinates and momenta which are called *primary constraints*.

The next step is to transform from a velocity phase space to a phase space with coordinates x_i, p_a and \dot{x}_ρ . The canonical Hamiltonian

$$\begin{aligned} H_c &= p_i \dot{x}^i - L(x, \dot{x}) \\ &= p_a f^a(x, p_b, \dot{x}_\rho) + g_\rho(x, p_a) \dot{x}^\rho - L(x, f_a(x, p_b, \dot{x}_\rho), \dot{x}_\rho), \end{aligned} \quad (2.30)$$

Using this the constrained version of Hamilton's equations of motion (2.17) may be derived. For a constrained system the differential of H_c will lead to three differentials dx_i, dp_a and $d\dot{x}_\rho$ instead of the two found in (2.15). By using the definition of the conjugate momenta (2.12) and equating coefficients of dx_i, dp_a and $d\dot{x}_\rho$ the constrained equations of motion are

$$\frac{\partial H_c}{\partial \dot{x}^\rho} = g_\rho - p_\rho = 0, \quad (2.31)$$

$$f^a = \frac{\partial H_c}{\partial p_a} - \dot{x}^\rho \frac{\partial g_\rho}{\partial p_a}, \quad (2.32)$$

$$\frac{\partial L}{\partial x^i} = -\frac{\partial H_c}{\partial x^i} + \dot{x}^\rho \frac{\partial g_\rho}{\partial x^i}. \quad (2.33)$$

The final two equations are reminiscent of Hamilton's equations but have additional terms which depend on the constraint. There are only $(n + r)$ equations of motion, (2.32) and (2.33), in the singular case and $(n - r)$ constraints (2.31) for the $2n$ variables. The constraints restrict the motion to a subspace Γ_p of the full phase space Γ . The hypersurface Γ_p is defined by these constraints.

The Hamiltonian H_c and the equations of motion are defined on Γ_p . It is desirable to describe the dynamics on Γ , the physical phase space (x, p) . Therefore we want to define a function on the whole phase space, which is equivalent to H_c in the subspace Γ_p . To proceed with the Dirac-Bergmann algorithm for dealing with constraints a discussion on switching a function between the two phase spaces is needed. Let $F(x, p)$ be a function defined on the full phase space. It is called

'weakly zero' (denoted \approx) if $F|_{\Gamma_p} = 0$ and 'strongly zero' (denoted \simeq) if, additionally, $(\partial F/\partial x^i, \partial F/\partial p^i)|_{\Gamma_p} = 0$. A primary constraint on Γ_p is a weakly vanishing function, $G_\rho(x, p)$, on the whole phase space

$$G_\rho(x, p) = -g_\rho(x, p_a) + p_\rho \approx 0, \quad (2.34)$$

but they are *not* strongly zero. On the subspace Γ_p this is the constraint equation $g_\rho(x, p_a) = p_\rho$.

The relationship between weakly zero and strongly zero functions may be derived by studying the variation of a weakly zero function. If $F \approx 0$ then $\delta F \approx 0$, we find

$$\delta F = \frac{\partial F}{\partial x^i} \delta x^i + \frac{\partial F}{\partial p^i} \delta p^i = \left[\frac{\partial F}{\partial x^i} + \frac{\partial F}{\partial p_\rho} \frac{\partial g_\rho}{\partial x^i} \right] \delta x^i + \left[\frac{\partial F}{\partial p^a} + \frac{\partial F}{\partial p_\rho} \frac{\partial g_\rho}{\partial p^a} \right] \delta p^a. \quad (2.35)$$

Note that $\delta p_\rho = \delta g^\rho(x, p_a)$ which depends on δx^i and δp^a . The expressions in square brackets must be weakly vanishing. Substituting $g_\rho = p_\rho - G_\rho$ and using $G_\rho \approx 0$ it can be shown that

$$\frac{\partial}{\partial x^i} \left(F - G_\rho \frac{\partial F}{\partial p_\rho} \right) \approx 0 \quad \text{and} \quad \frac{\partial}{\partial p^i} \left(F - G_\rho \frac{\partial F}{\partial p_\rho} \right) \approx 0. \quad (2.36)$$

Here in the second part of equation (2.36) the index a has been replaced with i because $\partial G_\rho/\partial p_\sigma = \delta_\rho^\sigma$. It can be seen that if $F \approx 0$ then $F \simeq G_\rho \partial F/\partial p_\rho$. A weakly vanishing function is a linear combination of the weakly vanishing functions defining the hypersurface Γ_p . A constant term could not be added to F because that is not weakly vanishing.

It is possible to define a function H' on Γ which is weakly equal to H_c . Since H_c does not depend on p_ρ studying the variation of these functions by substituting

them into (2.36) it can be seen that

$$\frac{\partial}{\partial x^i} \left(H' - g_\rho \frac{\partial H'}{\partial p_\rho} \right) \approx \frac{\partial H_c}{\partial x^i} \quad \text{and} \quad \frac{\partial}{\partial p^i} \left(H' - g_\rho \frac{\partial H'}{\partial p_\rho} \right) \approx \frac{\partial H_c}{\partial p^i}. \quad (2.37)$$

Introduce $H = \left(H' - g_\rho \frac{\partial H'}{\partial p_\rho} \right)$ which, as may be seen from the previous equation, is strongly equal to H_c . Using the equations of motion (2.32), (2.33) and $g_\rho = p_\rho - G_\rho$ the previous equations may be re-written as

$$\begin{aligned} \dot{x}^i &\approx \frac{\partial H}{\partial p_i} + \dot{x}^\rho \frac{\partial G_\rho}{\partial p_i} \approx \{x^i, H + \dot{x}^\rho G_\rho\}, \\ \frac{\partial L}{\partial x^i} &\approx -\frac{\partial H}{\partial x^i} - \dot{x}^\rho \frac{\partial G_\rho}{\partial x^i} \approx \{p^i, H + \dot{x}^\rho G_\rho\}, \end{aligned} \quad (2.38)$$

the Poisson brackets, defined in (2.19), are calculated as if the x 's and p 's are independent. Only after calculating the brackets may we impose the constraints. Since the Poisson brackets contain only derivatives with respect to phase space variables we may use $H \simeq H_c$ and $\partial L / \partial x^i = \dot{p}^i$ in (2.38) to give

$$\dot{x}^i \approx \{x^i, H_c + \dot{x}^\rho G_\rho(x, p)\}, \quad \dot{p}^i \approx \{p^i, H_c + \dot{x}^\rho G_\rho(x, p)\}. \quad (2.39)$$

Since G_ρ only vanishes weakly it still influences the dynamics on the full phase space. The \dot{x}^ρ are arbitrary functions which we will refer to as Lagrange multipliers λ^ρ .

We define the primary Hamiltonian in order to rewrite the equations of motion in terms of one evolution operator

$$H_p(x, p) := H_c + \lambda^\rho G_\rho, \quad (2.40)$$

where λ^ρ is a multiplier function. The equation of motion for any phase-space

function A defined on the whole phase space Γ is

$$\dot{A}(x, p) \approx \{A, H_p\}. \quad (2.41)$$

Note that the equations of motion are now only weak equations, however they bear more similarity to the equations dealt with for unconstrained systems making them advantageous. The constraints $G_r \approx 0$ should be preserved in time² therefore $\dot{G}_r \approx 0 \approx \{G_r, H_c\} + \mu^\rho \{G_r, G_\rho\}$.

2.3.2 Lagrangian Reparametrisation Invariance

During chapters 3 and 4 we will be interested in reparametrisation invariant systems so this Lagrangian symmetry will be examined now. The general properties of reparametrisation invariant systems will be illustrated using the system governing the motion of a free relativistic particle as an example,

$$\mathcal{L}(s) = mc \sqrt{\dot{x}_\mu(s) \dot{x}^\mu(s)}. \quad (2.42)$$

Here s is the arc length parameter of the trajectory or the proper time and since the Lagrangian has units of energy $\dot{x}^2 = c^2$. The conjugate momenta is

$$p^\mu = mc \frac{\dot{x}^\mu}{\sqrt{\dot{x}_\nu \dot{x}^\nu}}, \quad (2.43)$$

this leads to a vanishing canonical Hamiltonian $H_c = 0$. We have seen in (2.25) this system is singular, it obeys the mass-shell constraint $p^2 = (mc)^2$. Therefore the time evolution of this system is generated entirely by the mass-shell constraint as one can see from (2.41).

Note that the Lagrangian function (2.42) is homogeneous to the first degree in

² This may generate new ‘secondary’ constraints and although this discussion is not needed for this thesis it is important for example in QED where it leads to Gauss’ law [44].

the velocity, so it has the property

$$L(\alpha \dot{x}^\mu) = \alpha L(\dot{x}^\mu). \quad (2.44)$$

This equation is an example of a more general theorem due to Euler [47] which states that

$$\dot{x}_i \frac{\partial f}{\partial \dot{x}_i} = n f(\dot{x}). \quad (2.45)$$

Integer n is the degree of homogeneity in the velocities \dot{x}^i of f . Homogeneity of the Lagrangian will now be used to show that the action is invariant under a reparametrisation of the world-line $s \rightarrow s'(s)$. Using (2.44), the effect of a parameter change on the Lagrangian (2.42) is

$$L\left(\frac{dx^\mu}{ds}\right) = L\left(\frac{dx^\mu}{ds'} \frac{ds'}{ds}\right) = \frac{ds'}{ds} L\left(\frac{dx^\mu}{ds'}\right). \quad (2.46)$$

The action,

$$S = \int ds L\left(\frac{dx^\mu}{ds}\right) = \int ds' L\left(\frac{dx^\mu}{ds'}\right), \quad (2.47)$$

is invariant, providing the endpoints remain unchanged, the mapping $s \rightarrow s'(s)$ is one-to-one and

$$ds'/ds > 0, \quad (2.48)$$

so time flows forwards. If any Lagrangian is homogeneous (2.44) and degree one in the velocities, using Euler's theorem (2.45) we find

$$\frac{\partial L}{\partial \dot{x}^\mu} = \frac{\partial}{\partial \dot{x}^\mu} \left(\frac{\partial L}{\partial \dot{x}^\nu} \dot{x}^\nu \right) = W_{\mu\nu} \dot{x}^\nu + p_\mu \quad \Rightarrow \quad W_{\mu\nu} \dot{x}^\mu = 0. \quad (2.49)$$

The matrix $W_{\mu\nu}$ has zero modes so therefore any Lagrangian which is homogeneous degree one is singular.

In the free relativistic theory the reparametrisation invariance is generated by the

mass-shell constraint $\theta \equiv p^2 - (mc)^2$ however for different systems there will be a different constraint. The constraint should generate a change in x^μ (notated by δx^μ) so that $x^\mu + \delta x^\mu$ is equivalent to a reparametrisation. Using the Poisson brackets³ $\{x^\mu, p^\nu\} = -g^{\mu\nu}$ the effect of the constraint on the coordinates is

$$\delta x^\mu(s) = \{x^\mu, \theta \delta \epsilon\} = \dot{x}^\mu \delta s = x^\mu(s + \delta s) - x^\mu(s) = x^\mu(s') - x^\mu(s), \quad (2.50)$$

where $\delta s = 2m\delta\epsilon$. Therefore, $x^\mu(s) + \delta x^\mu(s) = x^\mu(s')$, as required.

If a Lagrangian contains a reparametrisation invariance a single trajectory can be described by an infinite number of different parameters. Any of these parameters can be used to describe the trajectory but a particular choice must be made. The method of singling out one parameter is called gauge fixing. This amounts to splitting the four dimensional space-time into a continuum of hypersurfaces. Each hypersurface has a different value for the parameter and time evolution is the movement between hypersurfaces. For example, Minkowski space is decomposed into hypersurfaces of equal time, $s = \text{constant}$, so at each instant in time the universe appears three dimensional.

All of the properties discussed for the free relativistic system hold for all reparametrisation invariant systems [48]. To summarise, any system which has a vanishing canonical Hamiltonian is reparametrisation invariant and the Lagrangian is singular. A constraint generates this invariance and must be gauge fixed to choose one evolution parameter to describe the system.

³ During this thesis the metric is defined as $g^{\mu\nu} = \text{diag}(1, -1)$.

Parameterising Systems

In non-relativistic systems motion is normally described by giving the canonical variables as functions of the time. For a system with no constraints the action reads

$$S[\mathbf{x}(t), \mathbf{p}(t)] = \int_{t_1}^{t_2} dt \left(\mathbf{p}_i(t) \frac{d\mathbf{x}^i(t)}{dt} - H_c \right), \quad (2.51)$$

where H_c is the canonical Hamiltonian. Now introduce time as a canonical variable depending on some parameter s and replace the action by

$$S^*[t(s), p_t(s), \mathbf{x}(s), \mathbf{p}(s), \lambda(s)] = \int_{s_1}^{s_2} ds \left(p_t \dot{t} + \mathbf{p}_i \dot{\mathbf{x}}^i - \lambda(p_t + H_c) \right), \quad (2.52)$$

here the ‘dot’ represents differentiation with respect to the parameter s and λ is a Lagrange multiplier. The two systems (2.51) and (2.52) are equivalent. Through extremising the action with respect to p_t we find that $\dot{t} - \lambda = 0$ and equation (2.52) becomes

$$\int_{s_1}^{s_2} ds \left(\mathbf{p}_i \dot{\mathbf{x}}^i - \dot{t} H_c \right) = \int_{t_1}^{t_2} dt \left(\mathbf{p}_i(t) \frac{d\mathbf{x}^i(t)}{dt} - H_c \right), \quad (2.53)$$

providing t is a monotonic function of s , i.e. its inverse exists. The extended system (2.52) has an extra canonical pair compared to (2.51). The canonical Hamiltonian of the extended system is always equal to zero, as can be seen from (2.40), so it is reparametrisation invariant. By extremising the action with respect to the Lagrange multiplier, λ we find

$$\mathcal{H} := p_t + H_c \approx 0, \quad (2.54)$$

this is called the energy constraint and is responsible for generating the reparametrisation invariance.

The dynamics of the system (2.52) is contained entirely within the constraint (2.54). When calculating the effect of the parametrisation on any function F of the

canonical variables the equations of motion (2.41) become

$$\dot{A} \approx \epsilon \lambda \{A, p_t + H_c\}. \quad (2.55)$$

Any Lagrangian may be cast into a reparametrisation invariant form but it is especially useful when considering systems with an explicit time dependence. The parametrisation removes many awkward time derivatives [42] and, as we shall see in section 2.4, makes shifting from one set of canonical variables to another simpler. The reduced/original phase space may be reached again by gauge fixing the reparametrisation $s = t$. The constraint (2.54) has two roles:

1. generator of the evolution of system (2.55);
2. generator of the local symmetry transformation induced by the reparametrisation (2.50).

2.3.3 Light-Cone Coordinates

Often in laser physics it is beneficial to use the light-cone coordinates which are defined as

$$\xi := t - \frac{z}{c}, \quad \text{and} \quad \vartheta := t + \frac{z}{c}. \quad (2.56)$$

Note that the light-cone coordinate ξ is the variable used to solve the plane wave equation (2.5). In this section we will derive the light cone coordinates canonical pairs and study gauge fixing for parameterised systems. Excluding constraints the Lagrangian for a parameterised system is

$$\mathcal{L} = p_t \dot{t} + p_i \dot{x}^i, \quad (2.57)$$

where the dot represents differentiation with respect to parameter s . As discussed, there are many different ways to gauge fix this parameter. Two different gauge fixing

will now be presented, the ‘normal’ Minkowski gauge fixing $s = t$ and a light-cone gauge fixing.

To discretise space-time into slices of equal time we gauge fix the parameter $s = t$. Then $\dot{t} = 1$ and the gauge fixed Lagrangian is

$$\mathcal{L}_{\text{GF}} = \mathbf{p}_i \dot{\mathbf{x}}^i + p_t. \quad (2.58)$$

It can be seen that the canonical Hamiltonian, $H_c = -p_t$. The term which is a product of canonical coordinates are canonical pairs and they have the commutation relation, $\{p^i, x^j\} = -\delta^{ij}$.

The Lagrangian (2.57) can be written in light-cone coordinates

$$\mathcal{L} = \mathbf{p}_i^\perp \dot{\mathbf{x}}_\perp^i + \frac{1}{2} (p_t - cp_z) \left(\dot{t} + \frac{\dot{z}}{c} \right) + \frac{1}{2} (p_t + cp_z) \left(\dot{t} - \frac{\dot{z}}{c} \right), \quad (2.59)$$

where $\dot{\mathbf{x}}_\perp^i = (\dot{x}, \dot{y})$ and $\mathbf{p}_i^\perp = (p_x, p_y)$. For light-cone gauge fixing $s = \xi$ so $\dot{\xi} = 1$ and the Lagrangian becomes

$$\mathcal{L}_{\text{GF}} = \frac{1}{2} p^- \dot{\vartheta} + \mathbf{p}_i^\perp \dot{\mathbf{x}}_\perp^i + \frac{1}{2} p^+, \quad (2.60)$$

here the light cone momenta have been defined. The final term expresses the light-cone energy, $p^+ = p_t + cp_z$, and the commutation relations can be read off from the Lagrangian's terms $\{p^-, \vartheta\} = -2$.

2.4 Canonical Transformations and Hamilton Jacobi Theory

Canonical Transformations

For many problems in theoretical physics the equations of motion are complicated. However the free particle system, described in section 2.2, maybe easily solved. In

this situation all the coordinates are cyclic and the conjugate momenta are constants of motion. It is possible to reduce a system, with an equation of motion that is hard to solve, into a solvable system via a canonical transformation [1, 46] .

The Hamiltonian formalism gives an equal status to all phase space variables. For example a change of variables from cartesian to polar coordinates must also transform the momenta. A system can be described by more than one set of canonical variables and all choices are equally valid, but one set may be more convenient for the problem under consideration. Moving to a set of variables which leaves the Hamiltonian with more cyclic coordinates will, in general, make the system simpler to solve [46]. The act of transforming from one set of phase space variables to another will now be discussed. The coordinates and momenta (x_i, p_i) are transformed to the new set (X_i, Π_i) with transform equations

$$X_i = X_i(x_i, p_i; t) \quad \text{and} \quad \Pi_i = \Pi_i(x_i, p_i; t) . \quad (2.61)$$

These equations are assumed to be invertible.

If the new variables (X_i, Π_i) are to be of interest to us, they must also be canonical coordinates. They must be conjugate to each other and there must exist a new function which plays the role of the Hamiltonian, $K_c(X_i, \Pi_i; t)$. The Poisson brackets remain invariant [44] under a canonical transformation and the new variables obey the Hamilton's equations of motion

$$\dot{X}_i = \frac{\partial K_c}{\partial \Pi_i}, \quad \dot{\Pi}_i = -\frac{\partial K_c}{\partial X_i} . \quad (2.62)$$

The principle of least action must be satisfied by both sets of variables. This is achieved if both sets are related by the equation

$$\kappa (p_i \dot{x}_i - H_c) = \Pi_i \dot{X}_i - K_c + \frac{dS}{dt} . \quad (2.63)$$

Here κ is a scale transform; during this thesis we are only interested in the case $\kappa = 1$. According to the principle of least action the variation of the phase space coordinates vanish at the end of the path. Let function S depends on both old and new phase space variables. A derivative with respect to time of the S will vanish in the action since it is evaluated at the endpoints. The function S can be used to specify the exact form of the canonical transform when half its variables belong to the old set of phase space coordinates and half to the new. It then acts as a bridge between the two sets and is called the *generating function* of the canonical transformation.

For the canonical transforms used in chapters 3 and 4, the generating function is chosen to be a function of the old coordinates and the new momenta. Let

$$S = S_2(x, \Pi; t) - X_i \Pi_i, \quad (2.64)$$

which leads to

$$p_i \dot{x}_i - H_c = -\dot{\Pi}_i X_i - K_c + \frac{dS_2}{dt}. \quad (2.65)$$

The derivative

$$\frac{dS_2}{dt} = \frac{\partial S_2}{\partial t} + \dot{x}_i \frac{\partial S_2}{\partial x_i} + \dot{\Pi}_i \frac{\partial S_2}{\partial \Pi_i}, \quad (2.66)$$

allows (2.65) to be re-written as

$$K_c = H_c + \frac{\partial S_2}{\partial t} + \dot{x}_i \left(\frac{\partial S_2}{\partial x_i} - p_i \right) + \dot{\Pi}_i \left(\frac{\partial S_2}{\partial \Pi_i} - X_i \right). \quad (2.67)$$

The new Hamiltonian, K_c , is a function of new variables X and Π but not $\dot{\Pi}$. Therefore the $\dot{\Pi}$ dependence in this equation must vanish. Similarly the old Hamiltonian is not a function of \dot{x} so its dependence must also vanish. This is satisfied if

$$p_i = \frac{\partial S_2}{\partial x_i}, \quad X_i = \frac{\partial S_2}{\partial \Pi_i}, \quad (2.68)$$

leaving the equation

$$K_c = H_c + \frac{\partial S_2}{\partial t}. \quad (2.69)$$

Now p and X are known as a function of x and Π through the generating equations (2.68). If these functions are invertible the canonical transform may be completed, i.e. we may write new canonical variable as functions of old and vice versa.

Hamilton-Jacobi Theory

The canonical transformation is specified if the exact form of the generating function is known since it relates the old and new Hamiltonians. In following chapters we will face problems where the initial Hamiltonian is known and we choose a new Hamiltonian where the equations of motion can be easily solved. The challenge will be to find the generating function which specifies the canonical transformation. Writing explicit variables in (2.69) we have

$$K_c \left(\frac{\partial S_2}{\partial \Pi_i}, \Pi; t \right) = H_c \left(x_i, \frac{\partial S_2}{\partial x_i}; t \right) + \frac{\partial S_2(x_i, \Pi_i; t)}{\partial t}. \quad (2.70)$$

This equation is known as the Hamilton-Jacobi equation. It is a partial differential equation in n coordinates and one time variable. It can be shown that the solution to the Hamilton-Jacobi equation is equivalent to the classical action [46].

Before considering the canonical transformation we had to solve $2n$ ordinary differential equations (2.17) to derive the motion. To know the transformation to a solvable system we need to solve the partial differential Hamilton-Jacobi equation, which is notoriously difficult. At first glance it seems like not a great deal has been achieved, but, for systems with cyclic coordinates, it is possible to separate the variables in (2.70). Assume x_1 is cyclic so its conjugate momenta p_1 is a constant γ . From (2.68) we know that

$$\gamma = \frac{\partial S_2}{\partial x_1}, \quad (2.71)$$

so we propose the solution

$$S_2(x_i, \Pi_i; t) = \gamma x_1 + \mathcal{F}(x_2, x_3 \dots, x_n, \Pi_i; t) . \quad (2.72)$$

By conducting a canonical transform to the free theory we can relate the constant new momenta Π_1 with γ . The generating function may be separated into a term for each cyclic coordinate in the system.

The Hamilton-Jacobi theory will now be applied to systems which are explicit functions of time. As mentioned, in section 2.3.2, it is useful to introduce a parameter into the system to remove awkward time derivatives in (2.70). Let the following system have an explicit time dependence

$$\mathcal{L}(\mathbf{p}, \mathbf{x}, t) = \mathbf{p} \cdot \dot{\mathbf{x}} - H_c(\mathbf{p}, \mathbf{x}, t) . \quad (2.73)$$

This system is then parameterised to become the equivalent system

$$\mathcal{L}^*(\mathbf{p}, \mathbf{x}, t, p_t) = p_t \dot{t} + \mathbf{p} \cdot \dot{\mathbf{x}} - \lambda(p_t + H_c((\mathbf{p}, \mathbf{x}, t, p_t))) , \quad (2.74)$$

which does not have any explicit parameter dependence. The time, t , has been promoted to be a proper canonical coordinate and it has the conjugate momenta p_t . The canonical Hamiltonian of the parameterised system $H_c = 0$ and the system's evolution is governed by the constraint (2.54), which is

$$\mathcal{H}(p_t, t, \mathbf{p}, \mathbf{x}) = p_t + H_c \approx 0 . \quad (2.75)$$

The post canonical transformation system may also be parameterised so $K_c = 0$ and it obeys the constraint $\mathcal{H}_0 \approx 0$. Due to the parametrisation the Hamilton-Jacobi

equation (2.70) becomes

$$\frac{\partial S_2}{\partial s} = 0. \quad (2.76)$$

The generating function has no explicit parameter dependence. Note that a factor of $\partial s/\partial t$ is extracted for the change of variables in the action (2.53). The generating function still specifies the canonical transform between the constraints $\mathcal{H} \rightarrow \mathcal{H}_0$

$$\mathcal{H} \left(\frac{\partial S_2}{\partial t}, t, \frac{\partial S_2}{\partial \mathbf{x}}, \mathbf{x} \right) = \mathcal{H}_0 \left(\Pi_t, \frac{\partial S_2}{\partial \Pi_t}, \Pi, \frac{\partial S_2}{\partial \Pi} \right) \approx 0. \quad (2.77)$$

The time derivatives which made the Hamilton-Jacobi equation difficult to solve have been removed. By making a sensible choice for the new constraint the time evolution in the extended phase space may be solved through the constrained equations of motion (2.55) providing (2.77) can be solved for the generating function⁴.

⁴ If we cannot solve for the generating function then the canonical transform between the two systems cannot be specified.

3. NON-RELATIVISTIC DYNAMICS BEYOND THE DIPOLE APPROXIMATION

All required background material has been covered so we may now move on to consider a particle's motion under the influence of a laser's electromagnetic background. In section (3.1) the simple dipole approximation will be reviewed and following that we will go beyond the dipole approximation. This can only be achieved using the parametrisation techniques discussed in the previous chapter. Constraints are introduced into the system through the parametrisation of the non-relativistic system. Section 3.2 derives the parametric solution of the trajectory for a non-relativistic particle beyond the dipole approximation. In section 3.3 an elliptically polarised monochromatic plane wave is introduced which will allow us to write the trajectory as a function of the Galilean time and eliminate the parameter. In section 3.4 the trajectory is analysed in the lab frame and a frame in which the particle is, on average, at rest.

3.1 *Dipole Approximated Solution and Thomson Scattering*

Consider Thomson scattering [23, 49]. A free non-relativistic electron which is at rest is subjected to a linearly polarised monochromatic plane wave¹ whose phase² is $\omega_L t - \mathbf{k}_L \cdot \mathbf{x} \approx \omega_L t$. This is called the *dipole approximation* which we discussed in the

¹ The electromagnetic plane wave represents the simplest way to mathematically model a laser field. This is a reasonable assumption providing the transverse directions of the laser beams are much larger than the dimensions of the system considered.

² The non-relativistic nature of the wave phase approximation becomes apparent when differentiating $\omega_L c t \gg \omega_L \mathbf{n} \cdot \mathbf{x}$ with respect to t .

introduction to part I. The vector $\mathbf{k}_L = \omega_L \mathbf{n}/c$ is called the wave vector, ω_L is the frequency of the plane wave and \mathbf{n} is an unit vector in the direction of the wave's propagation. The dipole approximation neglects the influence of the magnetic part of the Heaviside-Lorentz force,

$$\mathbf{F} = e \mathbf{E} + \frac{e}{c} \mathbf{v} \times \mathbf{B} \simeq e \mathbf{E}. \quad (3.1)$$

For a plane wave the fields' amplitudes $|\mathbf{E}_0| = |\mathbf{B}_0|$. By neglecting the magnetic portion of the force we are insisting that the electron's motion must be completely non-relativistic, $v \ll c$. The electric field is

$$\mathbf{E} = \mathbf{E}_0 \cos \omega_L t, \quad (3.2)$$

and therefore, according to (3.1), the electron executes simple harmonic motion at the same wave frequency as the laser, ω_L , along the electric field direction

$$\mathbf{x} = -\frac{e}{m\omega_L^2} \mathbf{E}_0 \cos \omega_L t. \quad (3.3)$$

By using the Larmor radiation formula [23] the frequency independent Thomson cross-section may be derived

$$\sigma_T = \frac{8\pi}{3} \left(\frac{e^2}{mc^2} \right)^2. \quad (3.4)$$

According to (3.3) the maximum velocity of the electron is $v_{\max} = e|\mathbf{E}_0|/m\omega_L$ and therefore the motion is non-relativistic providing

$$\eta^2 := \frac{v_{\max}^2}{c^2} = \frac{e^2}{\omega_L^2 m^2 c^2} |\mathbf{E}_0|^2 = \frac{2}{\pi} \frac{e^2 \lambda_L^2}{m^2 c^5} I \simeq 9.17 \times 10^{-8} \lambda_L^2 I \ll 1, \quad (3.5)$$

where λ_L is the radiation's wavelength and the beam's intensity $I := c|\mathbf{E}_0|^2/8\pi$ has been introduced. The parameter η is called the *laser intensity* and is dimensionless.

3.2 Parametric Solution

We now investigate the derivation of the particle's trajectory again, but this time we do not use the dipole approximation. A non-relativistic point particle with mass m and electric charge $-e$ moving in an external electric field \mathbf{E} and magnetic field \mathbf{B} is influenced by the full Heaviside-Lorentz force. The particle's trajectory $\mathbf{x}(t)$ can be determined from Newton's equations of motion

$$m \frac{d^2 \mathbf{x}(t)}{dt^2} = e \mathbf{E}(t, \mathbf{x}(t)) + \frac{e}{c} \frac{d\mathbf{x}}{dt} \times \mathbf{B}(t, \mathbf{x}(t)). \quad (3.6)$$

The nonlinear equations (3.6) can be reproduced within the conventional variational principle of least action from the following “non-relativistic”³ Lagrangian function⁴

$$\mathcal{L} \left(\mathbf{x}, \frac{d\mathbf{x}}{dt}, t \right) = \frac{m}{2} \frac{d\mathbf{x}}{dt} \cdot \frac{d\mathbf{x}}{dt} + \frac{e}{c} \frac{d\mathbf{x}}{dt} \cdot \mathbf{A}(t, \mathbf{x}(t)) - e \Phi(t, \mathbf{x}(t)), \quad (3.7)$$

if the external electric field \mathbf{E} and magnetic field \mathbf{B} are defined in terms of the gauge potential $A^\mu(t, \mathbf{x}) = (\Phi(t, \mathbf{x}), \mathbf{A}(t, \mathbf{x}))$ in the standard way (2.3). We intend to solve (3.6) for the special case of an idealised laser field described by the electromagnetic *monochromatic plane wave*. However, before restricting to this special case, we consider the more general plane wave background [7] discussed in section 2.1, with a gauge potential of the form

$$A_\mu(\mathbf{x}, t) = A_\mu(\xi). \quad (3.8)$$

³ Note that the name “non-relativistic” is somewhat misleading because the Lagrangian (3.7) is not Galilean invariant. It possess an approximate Galilean symmetry for small velocities which is discussed in [50] and Appendix A.

⁴ Note the discussion in [51, 52] considering the possible artifacts which arise from a partial relativistic treatment, as well as the necessity to consider the radiation damping effects [53–55]

Here A_μ is a 4-vector which depends only on the light-cone coordinate

$$\xi = t - \frac{\mathbf{n} \cdot \mathbf{x}}{c}, \quad (3.9)$$

and \mathbf{n} is a constant unit 3-vector pointing in the direction of the wave's propagation.

We impose the axial gauge⁵ on the potentials

$$\mathbf{n} \cdot \mathbf{A} = 0. \quad (3.10)$$

It will be shown that the Lagrangian (3.7) with a plane wave background (3.8) is classically integrable and its solution can be represented in a parametric integral form. First the system must be parameterised [42] and a canonical transformation [46] to the free theory must be carried out using the methods from classical Hamilton-Jacobi theory [56–58] as well as the Dirac constraint formalism [42, 43].

3.2.1 The Dirac Parametrisation method and Hamilton-Dirac Equation

Due to the explicit time dependence of the electromagnetic wave potential the Lagrangian (3.7) describes a *non-autonomous* system. To deal with non-autonomous systems it is often useful to use the method of time re-parametrisation (see sections 2.3.2 and 2.3.2 and [57], page 90 or [58], page 235) which is known to particle physicists as the Dirac “parametrisation trick” [42, 43]. The system is then generally covariant and awkward time derivatives, which we would otherwise have faced, are removed.

This approach will be summarised since it has been discussed in [42] and section 2.3.2 and then applied to system (3.7). Starting from an arbitrary Lagrangian system with Lagrangian $\mathcal{L}(\mathbf{x}(t), d\mathbf{x}/dt, t)$ the configuration space is extended by considering

⁵ This gauge choice is also the Coulomb gauge which reduces for a plane wave to $\mathbf{n} \cdot \mathbf{A} = \text{constant}$. Since there can be no net electric field, as can be seen from (2.7) and related discussions, we set the constant equal to zero.

the time t as a new dynamical variable, $t(s)$ which, together with the other “spatial” coordinates $\mathbf{x}(s)$, depends upon an auxiliary evolution parameter s . The dynamics of the extended system is determined by the degenerate homogeneous (degree one) time-reparametrisation invariant Lagrangian \mathcal{L}^* which is constructed from the initial Lagrangian by the definition:

$$\mathcal{L}^*\left(\mathbf{x}(s), t(s), \dot{\mathbf{x}}(s), \dot{t}(s)\right) := \left(\frac{dt}{ds}\right) \mathcal{L}\left(\mathbf{x}(s), \frac{d\mathbf{x}}{ds} / \frac{dt}{ds}, t(s)\right) \quad (3.11)$$

From now on a “dot” over any variable denotes a derivative with respect to the evolution parameter s . We require that $t(s)$ is a monotonic, increasing function of the new evolution parameter s :

$$\frac{dt}{ds} > 0. \quad (3.12)$$

Any system with the Lagrangian \mathcal{L}^* is generally covariant so it is invariant under an arbitrary change of the evolution parameter

$$s \rightarrow s' = f(s). \quad (3.13)$$

The extended phase of the system (3.11) consists of $3 + 1$ canonical pairs

$$\mathbf{Z}(s) := \begin{bmatrix} \mathbf{x}(s), & \mathbf{p}(s) \\ t(s), & p_t(s) \end{bmatrix}, \quad p_t := \frac{\partial \mathcal{L}^*}{\partial \dot{t}(s)}, \quad \mathbf{p} := \frac{\partial \mathcal{L}^*}{\partial \dot{\mathbf{x}}(s)}, \quad (3.14)$$

but due to the parametrisation invariance symmetry (3.13) the dynamics on the new phase space are constrained by (2.54).

According to the Hamilton-Dirac description [42, 43], the constraint (2.54) plays a twofold role. First, it is the generator of the local symmetry transformation of the phase space coordinates (3.14) which is induced by the time reparametrisation (3.13). Second, it generates the evolution of the extended system. The canonical

Hamiltonian derived from the Lagrangian \mathcal{L}^* is identically zero and the dynamics are encoded within the constraint (2.54). The Hamilton-Dirac equations of motion (2.55) for the extended phase space are

$$\dot{\mathbf{Z}} = \lambda(s)\{\mathbf{Z}, \mathcal{H}\}, \quad (3.15)$$

where $\lambda(s)$ is an arbitrary function. The freedom associated with the Lagrange multiplier $\lambda(s)$ reflects the fact that we can use any evolution parameter. This freedom needs to be fixed by imposing an additional constraint, in the form of a gauge condition,

$$\chi(s, \mathbf{x}, t) = 0.$$

The solution to (3.15) either coincides with the classical trajectory of the initial Lagrangian \mathcal{L} (gauge $\chi := t - s$) or, by using any other admissible gauge, will be canonically equivalent to it [42].

Applying this method to the system (3.7) the Lagrangian is transformed to

$$\mathcal{L}^*(\mathbf{x}, \dot{\mathbf{x}}, t, \dot{t}) = \frac{m}{2} \left(\frac{\dot{\mathbf{x}}}{\dot{t}} \right)^2 \dot{t} + \frac{e}{c} \dot{\mathbf{x}} \cdot \mathbf{A}(\xi) - e \dot{t} \Phi(\xi). \quad (3.16)$$

The time reparametrisation invariant Hamiltonian dynamics of the non-relativistic particle is governed by the following Hamiltonian constraint

$$\mathcal{H} := p_t + e\Phi + \frac{1}{2m} \left(\mathbf{p} - \frac{e}{c} \mathbf{A} \right)^2 = 0. \quad (3.17)$$

The strategy that we will use to find the parametric form of the trajectory of a non-relativistic particle in an electromagnetic plane background will now be outlined. A canonical transformation to the free theory is conducted by using the Hamilton-Jacobi method discussed in section 2.4. A solution to the equation of motion (3.15) is constructed by using the free theory and the canonical transformation equations [46].

Fixing the parametrisation invariance with a suitable gauge allows us to derive the Lagrange multiplier function $\lambda(s)$ and complete the derivation.

3.2.2 Canonical Transformation to a Free System

Using the constrained Hamilton-Jacobi method (2.77) a canonical transformation from system (3.16), denoted \mathbf{Z} , to a free system \mathbf{Z}_0 is constructed. The notation that will be used for pre and post canonical transformation variables are

$$\mathbf{Z} = \begin{bmatrix} \mathbf{x}(s), & \mathbf{p}(s) \\ t(s), & p_t(s) \end{bmatrix} \longleftrightarrow \mathbf{Z}_0 = \begin{bmatrix} \mathbf{X}(s), & \mathbf{\Pi}(s) \\ T(s), & \Pi_T(s) \end{bmatrix}. \quad (3.18)$$

In order for \mathbf{Z}_0 to be a free system the constraint (3.17) must be transformed into the constraint for a free theory

$$\mathcal{H} \rightarrow \mathcal{H}_0 = \Pi_T + \frac{1}{2m} \mathbf{\Pi}^2 = 0. \quad (3.19)$$

This canonical transformation “absorbs” the electromagnetic field so \mathcal{H}_0 generates free evolution and according to the transformed version of (3.15) we find

$$T(s) = T_0 + \int_0^s du \lambda(u), \quad \mathbf{X}(s) = \mathbf{X}_0 + \frac{\mathbf{\Pi}}{m} \int_0^s du \lambda(u), \quad (3.20)$$

where Π_T and $\mathbf{\Pi}$ are now constants of motion determined by the initial conditions imposed here at $s = 0$. Note that the constraint (3.19) has modified the un-parameterised results obtained in section 2.2. If we know the “absorbing transformation” $\mathbf{Z} \rightarrow \mathbf{Z}_0$ we have found the solution to the initial interacting system.

The explicit form of the “absorbing” transformation (3.18) can be found using the generating function method (section 2.4 and [56,57]) where the generating function S_2 depends upon the old coordinates (t, \mathbf{x}) and new momenta $(\Pi_T, \mathbf{\Pi})$. We introduce the

notation that if a vector has a “ \perp ”/“ \parallel ” subscript means it is perpendicular/parallel to the wave vector \mathbf{n} . The system has cyclic coordinates \mathbf{x}_\perp and $(x_\parallel + t)$ so the generating function, using (2.72), must be of the form

$$S_2(t, \mathbf{x}, \Pi_T, \Pi) = t \Pi_T + \mathbf{x} \cdot \Pi + \mathcal{F}(\xi, \Pi). \quad (3.21)$$

The unknown function, $\mathcal{F}(\xi, \Pi)$ will now be determined. Write the old momenta p_t and \mathbf{p} , using (2.68), as functions of transformed coordinates

$$p_t = \frac{\partial S_2}{\partial t} = \Pi_T + \frac{d\mathcal{F}}{d\xi}, \quad (3.22)$$

$$\mathbf{p} = \frac{\partial S_2}{\partial \mathbf{x}} = \Pi - \frac{\mathbf{n}}{c} \frac{d\mathcal{F}}{d\xi}. \quad (3.23)$$

We now decompose all three dimensional vectors into components which are perpendicular and parallel to the wave propagation direction \mathbf{n} e.g. $\Pi = \Pi_\perp + \Pi_\parallel \mathbf{n}$. Finally, by using the gauge condition (3.10), we see that the constraint (3.17) will reduce to the free constraint (3.19) if the function \mathcal{F} is a solution to the equation

$$\left[\frac{1}{c} \frac{d\mathcal{F}}{d\xi} + (mc - \Pi_\parallel) \right]^2 = (mc - \Pi_\parallel)^2 + W(\xi, \Pi_\perp), \quad (3.24)$$

where

$$W(\xi, \Pi_\perp) := -\frac{e^2}{c^2} \mathbf{A}_\perp^2 + 2 \frac{e}{c} \mathbf{A}_\perp \cdot \Pi_\perp + 2me\Phi. \quad (3.25)$$

The solution to (3.24) for \mathcal{F} must be real in order to derive a real trajectory. This means that the left hand side of (3.24) must satisfy the inequality

$$(mc - \Pi_\parallel)^2 + W(\xi, \Pi_\perp) \geq 0. \quad (3.26)$$

Imposing the boundary condition $\mathcal{F}(0, \Pi) = 0$ we have the solution

$$\mathcal{F}(\xi, \Pi) = -c(mc - \Pi_{\parallel})\xi \pm c \int_0^{\xi} du \sqrt{(mc - \Pi_{\parallel})^2 + W(u, \Pi_{\perp})}. \quad (3.27)$$

Later, we will see this boundary condition sets the particle to be at the origin when $t = 0$. Inequality (3.26) must be satisfied for all values of integration variable u . The importance of this restriction will be seen when we analyse the trajectory for a monochromatic wave. Observe the \pm sign choice in (3.27). This occurs because the energy constraint does not contain information regarding the direction of the particle, only the shape of the trajectory. This choice is fixed by choosing the positive sign for the remainder of the calculation.

Using (3.27) and equations (3.22) and (3.23) one can determine an expression for the new momenta as a function of the initial canonical coordinates. The momentum canonically conjugated to the new spatial coordinates \mathbf{X} are

$$\Pi_{\perp} = \mathbf{p}_{\perp}; \quad \Pi_{\parallel} = mc + \sqrt{(mc - p_{\parallel})^2 - W(\xi, \mathbf{p}_{\perp})}, \quad (3.28)$$

and the conjugate to the new time coordinate T is

$$\Pi_T = p_t - c \left[(mc - p_{\parallel}) + \sqrt{(mc - p_{\parallel})^2 - W(\xi, \mathbf{p}_{\perp})} \right]. \quad (3.29)$$

Using the generating equations (2.68)

$$T = \frac{\partial S}{\partial \Pi_T} = t, \quad (3.30)$$

$$\mathbf{X} = \frac{\partial S}{\partial \Pi} = \mathbf{x} + \frac{\partial \mathcal{F}}{\partial \Pi} \Big|_{\Pi = \Pi(t, \mathbf{x}, \mathbf{p})}. \quad (3.31)$$

one can find the new coordinates as a function of the old ones. The time coordinate

is unchanged

$$T = t, \quad (3.32)$$

but, after using (3.28), the new three dimensional coordinates are

$$\mathbf{X}_\perp = \mathbf{x}_\perp + e \frac{1}{|mc - p_\parallel|} \int_0^\xi du \mathbf{A}_\perp(u), \quad (3.33)$$

$$X_\parallel = x_\parallel + c\xi + c \frac{1}{|mc - p_\parallel|} \int_0^\xi du \sqrt{(mc - p_\parallel)^2 - W(u, \mathbf{p}_\perp)}. \quad (3.34)$$

The first half of the canonical transformation is complete, we have written the new canonical coordinates as a function of the old.

Equations (3.28) express three constants of motion. The first two coincide with the transversal momenta \mathbf{p}_\perp . The third one, Π_\parallel , can be interpreted as the longitudinal momenta of the particle in the asymptotic region where the interaction with the electromagnetic field is negligible. Experimentally the laser pulse only lasts for a short time period. From the expressions (3.29) and (3.28) we see that the “light-cone energy” represents another constant of motion

$$\frac{p_t}{c} + p_\parallel = \frac{\Pi_T}{c} + \Pi_\parallel = \text{constant}. \quad (3.35)$$

In order to obtain the parametric solution to the Hamilton-Dirac equations, (3.15) the equations, (3.33) and (3.34) need to be inverted. We want to express the old coordinates as a function of the parameter s and the constants of motion. In order to do this the system must be fixed using an appropriate gauge.

3.2.3 Light-Cone Gauge Fixing and the Parametric Solution

The observation that the light cone energy (3.35) is a constant suggests a natural gauge fixing condition (see (2.60) and related discussion). The evolution parameter s can be identified with the canonical variable conjugate to the light cone energy,

(3.9) which is our gauge

$$\chi := t(s) - \frac{x_{\parallel}(s)}{c} - s = 0. \quad (3.36)$$

To find the form of the multiplier function, the equations of motion for the new coordinates (3.20) can be subtracted from each other to give

$$T - \frac{X_{\parallel}}{c} = (1 - \frac{\Pi_{\parallel}}{mc}) \int_0^s du \lambda(u), \quad (3.37)$$

where the initial conditions T_0 and \mathbf{X}_0 have been set equal to zero. By using the canonical transformation equations (3.32)-(3.34) and this gauge fixing condition we find that the Lagrange multiplier is

$$\int_0^s du \lambda(u) = mc \int_0^s du \frac{1}{\sqrt{(\Pi_{\parallel} - mc)^2 + W(u, \Pi_{\perp})}}. \quad (3.38)$$

When the canonical transformation equations (3.32)-(3.34) and this definition of the Lagrange multiplier are substituted into (3.20) the following trajectory may be derived

$$t(s) = mc \int_0^s du \frac{1}{\sqrt{(\Pi_{\parallel} - mc)^2 + W(u, \Pi_{\perp})}}, \quad (3.39)$$

$$x_{\parallel}(s) = -cs + mc^2 \int_0^s du \frac{1}{\sqrt{(\Pi_{\parallel} - mc)^2 + W(u, \Pi_{\perp})}}, \quad (3.40)$$

$$\mathbf{x}_{\perp}(s) = c \int_0^s du \frac{\Pi_{\perp} - \frac{e}{c} \mathbf{A}_{\perp}(u)}{\sqrt{(\Pi_{\parallel} - mc)^2 + W(u, \Pi_{\perp})}}. \quad (3.41)$$

Formulas (3.39)-(3.41) give the parametric solution for a non-relativistic particle's trajectory in an arbitrary plane wave background. They are analogous to the well-known parametric solution of the corresponding relativistic problem (cf. [1, 7, 36]).

The four dimensional parametric solution can be further improved by expressing

the three dimensional trajectory as a function of the Galilean time, $\mathbf{x}(t)$. It is necessary to invert (3.39) and find s as function of t , but this is not possible for an arbitrary plane wave background. Sections 3.2.4 and 3.3 are dedicated to solving the three dimensional trajectory.

3.2.4 Orbit of a Particle in a Weak Plane Wave Background

We will sketch the possibility to solve the trajectory in terms of the galilean time for an arbitrarily “weak” plane wave in the leading order of an intensity expansion.

According to (3.39)-(3.41), if s as a function of t is known, $s = f^{-1}(t)$, the classical trajectory can be written in the form of an integral

$$\mathbf{x}_{\perp}(t) = \frac{\Pi_{\perp}}{m} t - \frac{e}{mc} \int_0^t dt' \mathbf{A}_{\perp}(f^{-1}(t')), \quad (3.42)$$

and

$$z(t) = ct - cf^{-1}(t), \quad (3.43)$$

These formulae, where the function f^{-1} is to be determined from (3.39), gives the non-relativistic particle’s trajectory as a function of the Galilean time in an arbitrary plane wave background.

A “naive” non-relativistic limit for the solution of a particle’s trajectory follows from (3.42) and (3.43) if we assume the validity of a $1/c$ expansion in the denominator of the integrand in the expression (3.39). For small enough laser field intensities the charged particle’s classical trajectory $\mathbf{x}(t)$, as a function of the Galilean time t , can then be found.

We denote by $\langle \dots \rangle$ the time averaging of some quantity over one period and the dimensionless intensity parameter (3.5) is written in the form

$$\eta^2 = -2 \frac{e^2}{m^2 c^4} \langle A_{\mu} A^{\mu} \rangle. \quad (3.44)$$

The metric is defined as $g_{\mu\nu} = \text{diag}(+1, -1)$ and if the laser is described by a monochromatic plane wave we find $\langle \mathbf{A}^2 \rangle = c^2 |\mathbf{E}_0|^2 / 2\omega_L^2$. If mc is much larger than the momenta, $mc - \Pi_{\parallel} \approx mc$ and $\Pi_{\perp}/mc \approx 0$. Assuming a weak background field the leading term of an intensity expansion of the denominator in (3.39) gives

$$t(s) = s + \frac{1}{2} \eta^2 \int_0^s du \mathbf{a}_{\perp}^2(u). \quad (3.45)$$

In (3.45) the normalised potential, $\mathbf{a}_{\perp} := \mathbf{A}_{\perp} / \sqrt{\langle \mathbf{A}_{\perp}^2 \rangle}$ has been introduced.

Therefore, for a background with a small intensity, the auxiliary time s can be described as a series in the intensity with the lowest order contribution

$$s = t - \frac{1}{2} \eta^2 \int_0^t du \mathbf{a}_{\perp}^2(u). \quad (3.46)$$

The 3 dimensional trajectory of a charged particle subjected to a weak electromagnetic plane wave background is thus given by

$$\mathbf{x}_{\perp}(t) = \frac{\mathbf{\Pi}_{\perp}}{m} t - \frac{c}{2} \eta \int_0^t du \mathbf{a}_{\perp}(u) + \dots, \quad (3.47)$$

$$z(t) = \frac{1}{4} c \eta^2 \int_0^t du \mathbf{a}_{\perp}^2(u) + \dots. \quad (3.48)$$

Higher order corrections can be obtained in a similar way by using the well-known Lagrange expansion method over a small parameter [59].

In section 3.3 it will be shown how to solve the three dimensional trajectory for a monochromatic plane wave.

3.3 The Orbit of a Particle in a Monochromatic Plane Wave

Let the monochromatic plane wave have an arbitrary polarisation, choose its propagation to be in the z -direction and let its frequency be ω_L . The gauge potential

in (3.39) - (3.41) which describes this wave is

$$A^\mu := a(u) \left(0, \varepsilon \cos(u), \sqrt{1 - \varepsilon^2} \sin(u), 0 \right), \quad u = \omega_L \left(t - \frac{z}{c} \right). \quad (3.49)$$

The parameter $0 \leq \varepsilon \leq 1$ measures the polarisation. The values, $\varepsilon = 0$ and $\varepsilon = 1$, correspond to linear polarisation while $\varepsilon^2 = 1/2$ is circular polarisation. To model a laser beam the profile function $a(u)$ is assumed to be smooth and slowly varying (on the scale of oscillations) and vanishing as $u \rightarrow \pm\infty$. For the remainder of this calculation, for simplicity, the pulse function is chosen to be a constant, $a(u) := a$. Formally this corresponds to a laser with an infinite length pulse.

The solution to the equations of motion for the particle depends upon the laser field characteristics as well as the particle's initial/boundary conditions. The laser field is specified by its frequency ω_L , polarisation ε and the gauge invariant dimensionless intensity parameter (3.44) which, for our choice of monochromatic wave potential, is

$$\eta^2 = \left(\frac{ea}{mc^2} \right)^2. \quad (3.50)$$

Recall that the solution (3.39)-(3.41) is written with the initial conditions for the coordinates so that

$$\mathbf{x}(0) = 0. \quad (3.51)$$

The initial velocity $\mathbf{v}(0) := d\mathbf{x}/dt(t=0)$ is related to the dimensionless constants of motion

$$\beta_+ := 1 - \frac{\Pi_{\parallel}}{mc}, \quad \boldsymbol{\beta}_{\perp} = (\beta_1, \beta_2) := \frac{\boldsymbol{\Pi}_{\perp}}{mc}, \quad (3.52)$$

via the relations

$$\mathbf{v}_{\perp}(0) = c\boldsymbol{\beta}_{\perp} - c\eta\boldsymbol{\epsilon}_{\perp}, \quad (3.53)$$

$$v_z(0) = c - c\sqrt{\beta_+^2 - \eta^2\varepsilon^2 + 2\eta\boldsymbol{\epsilon}_{\perp} \cdot \boldsymbol{\beta}_{\perp}}, \quad (3.54)$$

where for the electromagnetic background choice (3.49) when $t = 0$ the polarisation vector, $\epsilon_{\perp} = (\epsilon, 0)$. Recall that the system possesses a Galilean symmetry for small velocities (see Appendix A) so by choosing the constants $v(0)$ we pass to a certain frame of reference. To simplify the trajectory a transverse boost allows us to pass to a reference frame where the transverse velocity⁶ is

$$\beta_{\perp} = 0, \quad (3.55)$$

After this boost the particle's longitudinal velocity is

$$\beta_z = \frac{v_z(0)}{c} = 1 - \sqrt{\beta_+^2 - \eta^2 \epsilon^2}, \quad (3.56)$$

The velocity must be real so $\beta_+^2 > \eta^2 \epsilon^2$.

With this specific choice of constants we shall find x, y and z as functions of the Galilean time t . Here we note also that due to the 2π periodicity of the monochromatic gauge potential below we treat all canonical coordinates as functions of a point on a circle given in trigonometric parametrisation with the domain $-\pi/2 \leq u \leq \pi/2$.

3.3.1 Trajectory as a Function of the Laboratory Frame's Time

The condition (3.26) which, as we will see, guarantees the monotonic character (3.12) of the function $t(s)$ and forces the trajectory to be real must be fulfilled. For the monochromatic plane wave (3.49) the inequality (3.26) with initial conditions (3.55) can be rewritten as

$$1 - \mu^2 \sin^2 u > 0, \quad (3.57)$$

⁶ As it will be shown, fixing $\beta_{\perp} = 0$, corresponds to zero average transverse velocity, $\langle v_{\perp} \rangle = 0$.

where

$$\mu^2 := (1 - 2\varepsilon^2) \frac{\eta^2}{(1 - \beta_z)^2}. \quad (3.58)$$

Therefore, one can define three allowed domains

$$(I) \quad 0 < \mu^2 < 1, \quad (II) \quad \mu^2 > 1, \quad (III) \quad \mu^2 < 0.$$

It will be shown that the solution in region (I) which we call the “*fundamental domain*” determines the solution in all the other regions. It will be demonstrated that the particle’s trajectory in the fundamental domain will reproduce the trajectory in region (II) if the parameter $\mu \rightarrow 1/\mu$ in the “*fundamental solution*”. Similarly, if $\mu \rightarrow i\mu$ in the fundamental solution we reproduce the trajectory found in region (III). Besides these there are two other cases

$$\mu^2 = 0, \quad \text{and} \quad \mu^2 = 1.$$

The solution for both of these parameter values can also be derived from the fundamental solution. Note that $\mu^2 = 0$ corresponds to either circular polarisation or a free particle. Each of these domains and values will now be studied

Parameters in the Fundamental Domain, (I) : $0 < \mu^2 < 1$.

The inequality (3.57) is true for all the values of u between $-\pi/2 \leq u \leq \pi/2$.

Equations (3.39) and (3.41) can be rewritten as

$$t(s) = \frac{1}{\omega_L(1 - \beta_z)} \int_0^{\omega_L s} du \frac{1}{\sqrt{1 - \mu^2 \sin^2 u}}, \quad (3.59)$$

$$x(s) = -\frac{c}{\omega_L} \sqrt{\frac{\varepsilon^2}{1 - 2\varepsilon^2}} \arcsin \left[\sqrt{\mu^2} \sin(\omega_L s) \right], \quad (3.60)$$

$$y(s) = \frac{c}{\omega_L} \sqrt{\frac{1 - \varepsilon^2}{1 - 2\varepsilon^2}} \ln \left[\frac{\sqrt{\mu^2} \cos(\omega_L s) + \sqrt{1 - \mu^2 \sin^2(\omega_L s)}}{1 + \sqrt{\mu^2}} \right], \quad (3.61)$$

and the component in the wave propagation direction (3.40) is

$$z(s) = ct(s) - cs. \quad (3.62)$$

This is the parametric solution to the equation of motion with parameter s from the principal interval

$$-\frac{\pi}{2} \leq \omega_L s \leq \frac{\pi}{2}. \quad (3.63)$$

Thanks to the work of L. Euler, A.M. Legendre, N.H. Abel and C.G.J. Jacobi, we know how to invert (3.59). The evolution parameter s may be described as a function of the Galilean time t , using the Jacobian *amplitude* function (C.1), [59,60]

$$\omega_L s = \text{am}(\omega'_L t, \mu), \quad (3.64)$$

with *modulus* μ and the non-relativistically Doppler shifted frequency

$$\omega'_L := \omega_L (1 - \beta_z). \quad (3.65)$$

For the values of s from the interval (3.63), using (3.64), it can be seen that the Galilean time is a well defined increasing function between the interval

$$-\mathbb{K}(\mu) \leq \omega'_L t \leq \mathbb{K}(\mu), \quad (3.66)$$

where \mathbb{K} is the “real” quarter period of the Jacobian elliptic functions (C.7). Therefore one can consider the transformation from the evolution parameter s to the time t as well-defined change of coordinates on a circle. The useful properties of the Jacobian functions are discussed in appendix C.

Substitute the expression for the evolution parameter in terms of Galilean time (3.64) into (3.60), (3.61) and (3.62). Then, using Jacobian property (C.2), we arrive

at the trajectory for a charged particle moving in the electromagnetic background of a monochromatic elliptically polarised plane wave for the fundamental domain of parameters

$$\begin{aligned} x_F(t) &= -\frac{c}{\omega_L} \sqrt{\frac{\epsilon^2}{1-2\epsilon^2}} \arcsin [\mu \operatorname{sn}(\omega'_L t, \mu)] , \\ y_F(t) &= \frac{c}{\omega_L} \sqrt{\frac{1-\epsilon^2}{1-2\epsilon^2}} \ln \left[\frac{\mu \operatorname{cn}(\omega'_L t, \mu) + \operatorname{dn}(\omega'_L t, \mu)}{1+\mu} \right] \end{aligned} \quad (3.68)$$

and

$$z_F(t) = ct - \frac{c}{\omega_L} \operatorname{am}(\omega'_L t, \mu) . \quad (3.69)$$

The subscript “ F ” is written to emphasize that (3.67)-(3.69) corresponds to the trajectories with the modulus from the fundamental interval $0 < \mu^2 < 1$. We have discovered the trajectory of a non-relativistic particle subjected to a laser’s electromagnetic background without using the dipole approximation. The *fundamental solution* will be analysed in great detail shortly and we will discuss the type of laser it is applicable to in section 4.3.

Solution with Parameters in Domain (II) : $\mu^2 > 1$.

In this domain there are two peculiarities which need to be taken into account. Firstly, when $\mu^2 > 1$ the inequality (3.57) is only satisfied when

$$\underline{\mu}^2 \geq \sin^2 u , \quad \text{where} \quad \underline{\mu} := \frac{1}{\mu} . \quad (3.70)$$

This means that the upper limit, $\omega_L s$, for the integral in (3.59), lies within the smaller interval

$$-\frac{\pi}{2} < -\arcsin(\underline{\mu}) \leq \omega_L s \leq \arcsin(\underline{\mu}) < \frac{\pi}{2} . \quad (3.71)$$

Second, the standard integral representation for the amplitude function (C.1) is defined for a modulus which is in the interval $0 < \mu^2 < 1$. Some simple mathematical manipulations are required to transform the integral (3.59) into a form where its integrand depends upon the inverse of the parameter $\underline{\mu}$, which can be defined as the modulus of the amplitude function. So (3.59) becomes

$$t(s) = \frac{1}{\omega'_L \underline{\mu}} \int_0^{\arcsin(\underline{\mu} \sin(\omega s))} du \frac{1}{\sqrt{1 - \underline{\mu}^2 \sin^2 u}}. \quad (3.72)$$

The relationship between the evolution parameter s and the time t for this domain is given by

$$\omega_L s = \arcsin(\underline{\mu} \operatorname{sn}(\omega'_L \underline{\mu} t, \underline{\mu})). \quad (3.73)$$

As required, when the parameter s is contained within the interval (3.71) the relation (3.73) defines a monotonic increasing function on the interval

$$-\mathbb{K}(\underline{\mu}) \leq \omega'_L \underline{\mu} t \leq \mathbb{K}(\underline{\mu}), \quad (3.74)$$

On substituting (3.73) and relation (C.2) into the parametric form of the trajectory (3.60)-(3.62) we find

$$x(t) = -\frac{c}{\omega_L} \sqrt{\frac{\varepsilon^2}{1 - 2\varepsilon^2}} \operatorname{am}(\omega'_L \underline{\mu} t, \underline{\mu}), \quad (3.75)$$

$$y(t) = \frac{c}{\omega_L} \sqrt{\frac{1 - \varepsilon^2}{1 - 2\varepsilon^2}} \ln \left[\frac{\operatorname{cn}(\omega'_L \underline{\mu} t, \underline{\mu}) + \underline{\mu} \operatorname{dn}(\omega'_L \underline{\mu} t, \underline{\mu})}{\underline{\mu} + 1} \right], \quad (3.76)$$

and

$$z(t) = ct - \frac{c}{\omega} \arcsin(\underline{\mu} \operatorname{sn}(\omega'_L \underline{\mu} t, \underline{\mu})). \quad (3.77)$$

These formulae describe the particle's trajectory for parameters in the domain, $\mu^2 > 1$.

Solution with Parameters in Domain, (III) : $\mu^2 < 0$.

For this domain the inequality (3.57) is true for all values in the interval $-\pi/2 \leq u \leq \pi/2$. Introduce the positive parameter, κ^2 where $\mu^2 := -\kappa^2$. The relation (3.59) reads

$$t(s) = \frac{1}{\omega'_L} \int_0^{ws} du \frac{1}{\sqrt{1 + \kappa^2 \sin^2 u}}, \quad (3.78)$$

while the solutions for the spatial coordinates are

$$x(s) = -\frac{c}{\omega'_L} \frac{\eta\varepsilon}{\kappa} \operatorname{arcsinh} [\kappa \sin(\omega_L s)], \quad (3.79)$$

$$y(s) = \frac{c}{\omega'_L} \frac{\sqrt{1 - \varepsilon^2}}{i\kappa} \ln \left[\frac{\kappa \cos(\omega_L s) + i\sqrt{1 + \kappa^2 \sin^2(\omega_L s)}}{i + \kappa} \right]. \quad (3.80)$$

Again, we must perform a change of integration variables to (3.78), in order to obtain the integral in terms of a Jacobian amplitude function with modulus from (0,1). This guarantees that the amplitude function is single-valued. It is straightforward to check that (3.78) is equivalent to

$$t(s) = \frac{1}{\omega'_L \kappa'} \int_0^{\phi(s)} du \frac{1}{\sqrt{1 - \frac{\kappa^2}{\kappa'^2} \sin^2 u}}, \quad (3.81)$$

where the upper limit of the integral is

$$\phi(s) := \arcsin \left(\frac{\kappa' \sin(\omega s)}{\sqrt{1 + \kappa^2 \sin^2(\omega s)}} \right) \quad \text{and} \quad \kappa'^2 = 1 + \kappa^2. \quad (3.82)$$

We have now achieved our goal, the modulus of $\kappa/\kappa' \in (0, 1)$, for all values of $\mu^2 < 0$. Therefore, the inverse to (3.81) reads

$$\phi(s) = \operatorname{am} (\omega'_L \kappa' t, \kappa/\kappa'), \quad (3.83)$$

or in terms of the evolution parameter we find

$$\kappa' \sin(\omega_L s) = \frac{\text{sn}(\omega'_L \kappa' t, \kappa/\kappa')}{\text{dn}(\omega'_L \kappa' t, \kappa/\kappa')}. \quad (3.84)$$

Using (3.84), one can rewrite the particle's trajectory in terms of the Jacobian elliptic functions with modulus κ/κ'

$$x(t) = -\frac{c}{\omega'_L} \frac{\eta \varepsilon}{\kappa} \arcsin \left[\frac{\kappa}{\kappa'} \frac{\text{sn}(\omega'_L \kappa' t, \kappa/\kappa')}{\text{dn}(\omega'_L \kappa' t, \kappa/\kappa')} \right], \quad (3.85)$$

$$y(t) = +\frac{c}{\omega_L} \frac{\eta \sqrt{1 - \varepsilon^2}}{i\kappa} \ln \left[\frac{1 - i\kappa \text{cn}(\omega'_L \kappa' t, \kappa/\kappa')}{(1 - i\kappa) \text{dn}(\omega'_L \kappa' t, \kappa/\kappa')} \right], \quad (3.86)$$

$$z(t) = ct - \frac{c}{\omega} \arcsin \left[\frac{1}{\kappa'} \frac{\text{sn}(\omega'_L \kappa' t, \kappa/\kappa')}{\text{dn}(\omega'_L \kappa' t, \kappa/\kappa')} \right]. \quad (3.87)$$

Equations (3.85)-(3.87) describe the particle's trajectory in a background characterised by $\mu^2 < 0$. The solution is well defined on the interval

$$-\mathbb{K}(\kappa/\kappa') < \omega'_L \kappa' t < \mathbb{K}(\kappa/\kappa'). \quad (3.88)$$

Parameter values $\mu^2 = 0$ & $\mu^2 = 1$.

Note that vanishing modulus, $\mu^2 = 0$, corresponds to a circularly polarised monochromatic plane wave, $\varepsilon^2 = 1/2$, or no electromagnetic background, $\eta^2 = 0$. If $\mu^2 = 0$, then the parametric solution (3.39) which determines the time t as a function of the auxiliary parameter s takes on the simple form

$$t(s) = \frac{s}{1 - \beta_z}. \quad (3.89)$$

The equations (3.41) for the spatial orthogonal components reduce to

$$x(s) = -\frac{1}{\sqrt{2}} \frac{c}{\omega'_L} \eta \sin \omega_L s, \quad y(s) = -\sqrt{2} \frac{c}{\omega'_L} \eta \sin^2 \frac{\omega_L s}{2}. \quad (3.90)$$

Therefore the three dimensional trajectory in terms of the Galilean time for $\mu^2 = 0$ is given by

$$x(t) = -\frac{1}{\sqrt{2}} \frac{c}{\omega'_L} \eta \sin(\omega' t), \quad y(t) = -\sqrt{2} \frac{c}{\omega'_L} \eta \sin^2\left(\frac{\omega'}{2} t\right), \quad z(t) = c\beta_z t. \quad (3.91)$$

From these expressions we see that for a circularly polarised monochromatic wave all of the nonlinear effects disappear and one can choose to be in a frame of reference where the particle's motion is purely harmonic. The laser frequency ω'_L is Doppler shifted (3.65).

Finally, for completeness, we derive the orbit for $\mu^2 = 1$. The equation (3.39) gives

$$t(s) = \frac{1}{\omega'_L} \operatorname{arctanh}(\sin \omega_L s), \quad (3.92)$$

and from (3.41) it follows that

$$x(s) = -\sqrt{\frac{\varepsilon^2}{1-2\varepsilon^2}} cs, \quad y(s) = \sqrt{\frac{1-\varepsilon^2}{1-2\varepsilon^2}} \frac{c}{\omega_L} \ln(\cos \omega_L s). \quad (3.93)$$

All parameter values have been considered for the particle's trajectory in a generic monochromatic plane wave. In the next subsection we will briefly outline how each of the different trajectories may be related to the fundamental solution.

3.3.2 Modular Properties of the Orbits

As shown above the trajectories' dependence on the polarisation and intensity of the radiation background is contained in the modulus of the elliptic Jacobian functions. The doubly periodic elliptic functions have a remarkable property which relates functions with different moduli. An elliptic function with periods w_1 and w_2 can be algebraically expressed in terms of another elliptic function(s) with periods w'_1 and w'_2 .

In our trajectories the modular transformation manifests itself as an *intensity duality* between the motion in backgrounds with different laser intensities. The solutions in the fundamental domain may be connected to the trajectory with an arbitrary intensity using the modular transformation. Using the relations between the Jacobian functions whose moduli are inverse to each other, given in formulae (C.21), one can verify that the trajectory (3.75)-(3.77) with $\mu^2 > 1$ follow from the fundamental solution (3.67)-(3.69) by the transformation $\mu \rightarrow 1/\mu$:

$$\mathbf{x}(t|\mu) = \mathbf{x}_F(t|1/\mu), \quad (3.94)$$

Similarly if $\mu^2 < 0$, the trajectories (3.85)-(3.87) are connected to the fundamental solution by the shift transformation (C.20) where we transform $\mu \rightarrow i\mu/\sqrt{1-\mu^2}$:

$$\mathbf{x}(t|\mu) = \mathbf{x}_F\left(t\left|\frac{i\mu}{\sqrt{1-\mu^2}}\right.\right). \quad (3.95)$$

Note that the special cases of trajectories with $\mu^2 = 0$ and $\mu^2 = 1$, which were considered in section 3.3.1 coincides with the corresponding limits of the fundamental solution taking into account that the Jacobian functions are degenerate to the trigonometric (C.11) and hyperbolic functions (C.10) for moduli $\mu = 0$ and $\mu = 1$, respectively.

3.4 Analysis of the Trajectory

The trajectory has now been evaluated as a function of the Galilean time for all values of μ . For each value of μ we have seen that, due to the properties of the Jacobian functions, we need only consider the fundamental solution. We will now analyse this solution in greater detail.

From the fundamental solution, (3.67)-(3.69), one can derive the velocity

$$v_x(t) = -c\eta\varepsilon \operatorname{cn}(\omega'_L t, \mu), \quad (3.96)$$

$$v_y(t) = -c\eta\sqrt{1-\varepsilon^2} \operatorname{sn}(\omega'_L t, \mu), \quad (3.97)$$

$$v_z(t) = c - c(1-\beta_z) \operatorname{dn}(\omega'_L t, \mu). \quad (3.98)$$

Using the properties of the Jacobian functions (see equations (C.9) in Appendix C) it can be seen that components of the velocity which are in the plane orthogonal to the waves propagation are periodic with the period

$$T_P := \frac{4\mathbb{K}}{\omega'_L} = \frac{2\pi}{\omega_P}. \quad (3.99)$$

In the direction parallel to the wave's propagation the oscillation period is $T_P/2$. The frequency of the particle's motion, ω_P , differs from the frequency of a laser field, ω_L , by

$$\omega_P = \frac{\pi}{2\mathbb{K}} \omega'_L. \quad (3.100)$$

There are two differences between the particle's frequency and the laser's frequency. The former is Doppler shifted, which is a purely kinematical non-relativistic effect, and it depends on the laser's intensity η . Intensity dependence can be seen because the quarter period may be expanded as a function of the parameter μ (C.16). The particle oscillates at a frequency which depends on the laser's intensity in a nonlinear way. For low intensity lasers, $\eta \ll 1$, the period of the particle's oscillation can be represented by using the expansion, (C.16) to find that

$$T_P = \frac{2\pi}{\omega'_L} \left[1 + \left(\frac{1}{2}\right)^2 \frac{1-2\varepsilon^2}{(1-\beta_z)^2} \eta^2 + \left(\frac{1 \cdot 3}{2 \cdot 4}\right)^2 \frac{(1-2\varepsilon^2)^2}{(1-\beta_z)^4} \eta^4 + \dots \right]. \quad (3.101)$$

In contrast to the non-relativistic dipole approximated result, the relativistic

solution (see chapter 4) predicts that a laser pulse will cause a particle to move in the direction of the laser's propagation [9, 61, 62]. This leads to an overall net velocity which is called the *drift velocity* of the particle. The size of the relativistic drift velocity is proportional to the laser's intensity. With the initial condition $\Pi_{\perp} = 0$ the mean velocity for the fundamental solution in the transverse direction is

$$\langle v_{\perp} \rangle = 0. \quad (3.102)$$

But, in the direction of wave propagation we predict a drift velocity of

$$\langle v_z \rangle = c - \frac{\pi c}{2\mathbb{K}}(1 - \beta_z). \quad (3.103)$$

This is a nonlinear function of the laser beam's intensity. For small intensities the leading order drift velocity is

$$\langle v_z \rangle = c\beta_z \left(1 - \frac{1 - 2\varepsilon^2}{4(1 - \beta_z)^2} \eta^2 \right) + c \frac{1 - 2\varepsilon^2}{4(1 - \beta_z)^2} \eta^2 + \dots \quad (3.104)$$

Another new feature observed when comparing to the dipole-approximation is the appearance of higher harmonics in the particle's motion. This can be seen from the fundamental solution by using the Fourier series expansion of the Jacobian function [59, 60]. Using the formulas (C.17) one can rewrite the trajectory as

$$x(t) = \frac{4c\varepsilon}{\omega_L \sqrt{1 - 2\varepsilon^2}} \sum_{n=1}^{\infty} \frac{q^{n-1/2}}{(2n-1)(1 + q^{2n-1})} \sin(2n-1)\omega_P t, \quad (3.105)$$

$$y(t) = \frac{8c\sqrt{1 - \varepsilon^2}}{\omega_L} \sum_{n=1}^{\infty} \frac{q^{n-1/2}}{(2n-1)(1 - q^{2n-1})} \sin^2\left(n - \frac{1}{2}\right)\omega_P t, \quad (3.106)$$

$$z(t) = \langle v_z \rangle t - \frac{c}{\omega_L} \sum_{n=1}^{\infty} \frac{2q^n}{n(1 + q^{2n})} \sin 2n\omega_P t, \quad (3.107)$$

where q is called the *nome* parameter

$$q := \exp \left(-\pi \frac{\mathbb{K}'}{\mathbb{K}} \right). \quad (3.108)$$

Note that by using (C.18) the nome q can be written for small intensities as

$$q \approx \frac{1 - 2\varepsilon^2}{16(1 - \beta_z)^2} \eta^2 + O(\eta^4). \quad (3.109)$$

These higher harmonic terms are camouflaged in the usual parametric form of the relativistic solution [8,37–40], but are observed in the three dimensional trajectory [9].

When the intensity parameter is small one can perform a Galilean boost with the velocity $\mathbf{V} := -(0, 0, \langle v_z \rangle)$ to the *average rest frame* (ARF). In this frame the particle has zero drift velocity. Its motion is purely a superposition of all harmonic oscillations with frequency ω_P . For small intensities equations (3.105)-(3.107) in the ARF frame can be written as a series in η which, up to order η^2 , are

$$\begin{aligned} x_{\text{ARF}}(t) &= -\frac{c\varepsilon}{\omega'_L} \eta \sin \omega'_L t, \\ y_{\text{ARF}}(t) &= -\frac{2c\sqrt{1-\varepsilon^2}}{\omega'_L} \eta \sin^2 \left(\frac{\omega'_L t}{2} \right), \\ z_{\text{ARF}}(t) &= -\frac{c}{\omega'_L} \frac{1-2\varepsilon^2}{8(1-\beta_z)} \eta^2 \sin 2\omega'_L t, \end{aligned} \quad (3.110)$$

All of these features, the Doppler shift, the particle's oscillation frequency dependence on the laser beam intensity as well as the presence of higher harmonics in the particle's motion, leads to several important phenomena worthy of further study. Among them there is a non-linear modification to classical Thomson scattering and a charged particle's mass/energy shift in the electromagnetic background.

3.5 Concluding Remarks

The relativistic solution to a charged particle's motion in a laser plane wave electromagnetic background has previously been found [1, 7, 9, 36]. Non-relativistic solutions use the dipole approximation which leads to simple harmonic motion. The solution presented within the main body of this chapter is an improvement on the dipole approximated solution. First order relativistic effects have been included in the system, so the magnetic portion of the force is taken into account. For an elliptically polarised monochromatic plane wave the trajectory is written as a function of the Galilean time. The trajectory is described by the Jacobian elliptic functions, which for weak laser intensities reduce to trigonometric functions.

The method we used to obtain the solution involved parameterising the non-relativistic system. This enabled us to follow the same techniques which are familiar from the relativistic problem⁷. Once a specific monochromatic plane wave is introduced this parameter can be removed. Having obtained our solution we are now in a position to substitute it back into the Euler-Lagrange equations as a final check. For the plane wave (3.49), with $a(u) = a$, and the initial conditions

$$\mathbf{x}(0) = \mathbf{v}(0) = 0, \quad (3.111)$$

the equations of motion for system (3.7) are

$$\begin{aligned} \frac{d}{dt} \left[m\dot{x}(t) + \frac{ea\varepsilon}{c} \cos \omega_L \left(t - \frac{z(t)}{c} \right) \right] &= 0, \\ \frac{d}{dt} \left[m\dot{y}(t) + \frac{ea\sqrt{1-\varepsilon^2}}{c} \cos \omega_L \left(t - \frac{z(t)}{c} \right) \right] &= 0, \\ m\ddot{z}(t) &= \frac{ea\omega_L}{c^2} \left[\varepsilon\dot{x}(t) \sin \omega_L \left(t - \frac{z(t)}{c} \right) - \sqrt{1-\varepsilon^2} \dot{y}(t) \cos \omega_L \left(t - \frac{z(t)}{c} \right) \right]. \end{aligned} \quad (3.112)$$

⁷ In the following chapter the solution for the relativistic problem will be given. As we will see a similar method is employed to derive the non-relativistic and relativistic trajectories.

By inserting the z -component of our solution

$$z(t) = ct - \frac{c}{\omega_L} \text{am}(\omega_L t, \mu) , \quad (3.113)$$

where the parameter $0 \leq \mu^2 \leq 1$, into the equations of motion and by the using properties of the Jacobian functions (C.2) it can be seen that

$$\dot{x} = -c\varepsilon\eta \text{cn}(\omega_L t, \mu) , \quad (3.114)$$

$$\dot{y} = -c\sqrt{1 - \varepsilon^2}\eta \text{sn}(\omega_L t, \mu) . \quad (3.115)$$

Differentiating $z(t)$ the final equation of motion is satisfied upon recalling that $\mu^2 = (1 - 2\varepsilon^2)\eta^2$. Since the Jacobian function modulus is proportional to the intensity there is an interesting duality between high and low laser intensity which is discussed in section 3.3.2. The Jacobian functions take on a different form if $\mu^2 > 1$ and $\mu^2 < 0$.

An analysis of this solution enables us to predict a non-relativistic drift velocity, which has never been predicted by a non-relativistic treatment. It is possible to explore whether other relativistic features, such as the mass-shift, are expected non-relativistically. We observed that the period of the orbit depends upon the laser intensity η . Since our solution is not parametric it contains all harmonics. The Jacobian functions can be expanded as a Fourier series. Thus the higher harmonics are not a solely relativistic phenomenon.

Looking forward, the derivation of the canonical transformation between the free and interacting theories generating function will enable us to construct a quantum mechanical description. This is important for the study of laser atom interactions. The trajectory will enable us to derive a modification to Thomson/Compton scattering. Important effects such as electromagnetic dressing and a charged particle's acceleration due to a laser may be studied.

4. RELATIVISTIC CHARGE SUBJECTED TO THE BACKGROUND OF A LASER

In chapter 2 we introduced the idea of reparametrisation invariance and we saw that the system describing a free relativistic particle has this property. In chapter 3 we introduced a parameter into the system describing a non-relativistic charged particle interacting with a plane wave background. This makes the non-relativistic system more akin to the relativistic problem. The relativistic system has previously been solved and the methods used in chapter 3 for the non-relativistic parametric solution are virtually the same as those used for the relativistic solution in [7,8]. The only real difference comes about in the canonical transform, since for the relativistic theory it makes sense to transform to a free relativistic system. Since previous authors have studied this solution before, and the methods are familiar to us from the previous chapter, the parametric solution will only be sketched.

During this solution relativistic four-vector notation will be used and the metric is defined as $g^{\mu\nu} = \text{diag}(+1, -1)$. The derivation of the parametric solution in section 4.1 will closely follow the method employed by [7, 8]. Features of the parametric solution are presented as well as a discussion of some ‘missing’ features which are camouflaged in the parametric form. Sengupta [9] went beyond the parametric solution and derived the three dimensional trajectory. This work will be commented on and we shall find a new alternative method to derive the three dimensional trajectory in section 4.2. After studying the relativistic trajectory it is possible to further motivate the non-relativistic solution beyond the dipole approximation,

which we do in section 4.3.

4.1 Parametric Solution

A laser produces a Lorentz force on a particle within the laser's beam. This is described by the equation of motion

$$\frac{d\mathbf{p}}{dt} = e\mathbf{E} + \frac{e}{c}\mathbf{v} \times \mathbf{B}, \quad (4.1)$$

where $\mathbf{p} = m\gamma\mathbf{x}$ and $\gamma^2 = (1 - v^2/c^2)^{-1}$. The only difference between (3.6) and (4.1) is the relativistic γ factor. The Lagrangian from which (4.1) is derived is

$$\mathcal{L}_R\left(x^\mu(s), \frac{dx^\mu}{ds}\right) := -mc\sqrt{\frac{dx_\mu}{ds} \frac{dx^\mu}{ds}} - \frac{e}{c} \frac{dx^\mu}{ds} A_\mu(x(s)), \quad (4.2)$$

using the standard variational technique. Note that the first term in (4.2) is just the free kinetic energy term and the second term is equivalent to the interaction studied for the non-relativistic system. The laser beam is described in exactly the same way since the laws of electromagnetism are relativistic. The Lagrangian is a homogeneous function of degree one in the velocities so it is reparametrisation invariant and the canonical Hamiltonian vanishes. Note that the parameter $s \neq x^0$, s will later be interpreted as the light-cone time. The conjugate momenta to x^μ is

$$p^\mu = mc \frac{\dot{x}^\mu}{\sqrt{\dot{x}^2}} - \frac{e}{c} A^\mu, \quad (4.3)$$

and it is split into a free and interacting portion. The time evolution is described by the mass-shell constraint

$$\mathcal{H}_R = \left(p_\mu + \frac{e}{c} A_\mu\right) \left(p^\mu + \frac{e}{c} A^\mu\right) - (mc)^2 = 0. \quad (4.4)$$

This is the constrained Hamilton-Jacobi equation for the relativistic system.

The laser background is once again modelled by an arbitrary plane wave. The gauge potentials in (4.2) take on the form

$$A^\mu(\mathbf{x}, t) = A^\mu(\xi). \quad (4.5)$$

They are a function of only one dimensionless variable ξ where $\xi = n \cdot x$. The 4-vector, $n^\mu = (1, \hat{\mathbf{n}})/c$, where $\hat{\mathbf{n}}$ points in the direction of the plane wave's propagation and $n^2 = 0$. The Lorentz gauge is imposed on the vector potential which reduces to the condition that $n \cdot A(\xi) = 0$.

The process employed by [7, 8] to solve the equations of motion (4.1) will now be described and then carried out. A canonical transformation to the free relativistic system with variables (X^μ, Π^μ) will be derived using the constrained Hamilton-Jacobi technique described in section 2.4. A relationship between x^μ and X^μ exists due to the canonical transformation. After finding this relationship, a gauge fixing of the reparametrisation invariance will be done in the light cone gauge. As in chapter 3 the parametric trajectory will have been discovered.

The relativistic constraint (4.4) is used with the constrained Hamilton-Jacobi method (2.77). Let S_2 be the generating function of the canonical transform. Replace the canonical momentum in the Hamilton-Jacobi equation, (4.4) by

$$p^\mu = \frac{\partial S}{\partial x_\mu}. \quad (4.6)$$

From the definition $\xi = n \cdot x$ it can be seen the coordinates perpendicular to the plane wave's propagation direction are cyclic so the generating function may be separated into the form

$$S_2(x, \Pi) = -x \cdot \Pi + \mathcal{F}(\xi, \Pi). \quad (4.7)$$

Using this definition the Hamilton-Jacobi equation (4.4) becomes

$$mc^2 - \Pi^2 = \frac{e^2}{c^2} A_\mu A^\mu - 2n \cdot \Pi \frac{\partial \mathcal{F}}{\partial \xi} - 2\frac{e}{c} \Pi \cdot A. \quad (4.8)$$

The left hand side of this equation describes the free theory. If the right hand side is set equal to zero then the new coordinates will obey the free theory and its equations of motion can be solved as in equation (4.13). In order to absorb the laser field into the canonical transformation we find the generating function (4.7) must have the term

$$\mathcal{F}(\xi, \Pi) = \frac{1}{\Pi \cdot n} \int_0^\xi du \left[\frac{e^2}{2c^2} A_\mu A^\mu - \frac{e}{c} \Pi \cdot A \right]. \quad (4.9)$$

The Π 's are momenta from the free theory so they are constants of motion and may be taken outside the integral. This is somewhat less complex than the non-relativistic particle's solution because the trajectory will be real for all values. We have specified that the particle is initially at the origin at time $t = 0$ through the initial condition $\mathcal{F}(0, \Pi) = 0$. There is no inequality like (3.26) to concern us in the relativistic theory. From the theory of canonical transformations

$$X^\mu = \frac{\partial S}{\partial \Pi_\mu} = -x^\mu - \frac{1}{2} \frac{e}{c} \frac{n^\mu}{(\Pi \cdot n)^2} \int_0^\xi du \left[\frac{e}{c} (A_\mu A^\mu) - 2(\Pi \cdot A) \right] - \frac{1}{(\Pi \cdot n)} \frac{e}{c} \int_0^\xi du A^\mu, \quad (4.10)$$

$$p^\mu = \frac{\partial S}{\partial x_\mu} = -\Pi^\mu + \frac{1}{2} \frac{n^\mu}{\Pi \cdot n} \left[\frac{e}{c} (A_\mu A^\mu) - 2(\Pi \cdot A) \right]. \quad (4.11)$$

The total Hamiltonian for the new coordinates is

$$H = \frac{1}{2} \lambda(s) (\Pi^2 - (mc)^2), \quad (4.12)$$

here λ is a Lagrange multiplier function for the time evolution mass-shell constraint and reflects the reparametrisation invariance of the system. In the free relativistic

system the equations of motion can be solved

$$X^\mu(s) := X_{in}^\mu + \Pi^\mu \int_{-\infty}^s du \lambda(u). \quad (4.13)$$

The constants X_{in}^μ will be set equal to zero. The parameter s can now be gauge fixed in the light cone gauge, $s = \xi = x \cdot n$. By dotting n_μ into (4.10) it can be seen that $X \cdot n = x \cdot n$ and from (4.13) we find

$$\int_0^s du \lambda(s) = -\frac{s}{\Pi \cdot n}. \quad (4.14)$$

Therefore (4.13) becomes $X^\mu = -s\Pi^\mu/\Pi \cdot n$ and the gauge fixed parametric trajectory (4.10) reads

$$x^\mu(s) = \frac{\Pi^\mu}{(\Pi \cdot n)} s - \frac{1}{2} \frac{e}{c} \frac{n^\mu}{(\Pi \cdot n)^2} \int_0^s du \left[\frac{e}{c} (A_\mu A^\mu) - 2(\Pi \cdot A) \right] - \frac{1}{(\Pi \cdot n)} \frac{e}{c} \int_0^s du A^\mu. \quad (4.15)$$

This is the most general parametric solution describing the motion of a relativistic charge in a laser field. To derive the trajectory in terms of the proper time we note that the proper time is the arc length of the world-line

$$c\tau := \int_0^s du \sqrt{\frac{dx^\mu}{du} \frac{dx_\mu}{du}} = \frac{mc}{(\Pi \cdot n)} s. \quad (4.16)$$

To go further an explicit choice of plane wave must be made. Before studying the three dimensional solution some features of (4.15) will be discussed and we specialise the solution to the specific gauge choice (3.49).

Effective Mass

The time averaged 4-velocity may be calculated from (4.15) and (4.16). The 4-velocity

$$u^\mu = \frac{ds}{d\tau} \frac{dx^\mu}{ds} = \frac{1}{m} \left[\Pi^\mu - \frac{e}{c} A^\mu - \frac{n^\mu}{\Pi \cdot n} \left(\frac{e^2}{2c^2} A_\mu A^\mu - \frac{e}{c} \Pi \cdot A \right) \right], \quad (4.17)$$

can be averaged over one period of the plane wave

$$\langle u^\mu \rangle = \left\langle \frac{dx^\mu}{d\tau} \right\rangle = \frac{1}{m} \left[\Pi^\mu - \frac{n^\mu}{\Pi \cdot n} \frac{e^2}{2c^2} \langle A_\mu A^\mu \rangle \right]. \quad (4.18)$$

Define the *quasi-momentum*, $q^\mu := m \langle u^\mu \rangle$, it obeys a free mass-shell constraint, $q^2 := (m^* c)^2$ where m^* is the *effective mass*. The relativistic particle moving within a laser field is often described using these quantities. The averaged effect of the laser field is absorbed into these quantities. Using these quantities the system is effectively describing a free relativistic particle with mass m^* and 4-momenta q^μ . The effective mass is

$$m^{*2} = m^2 - \frac{e^2}{c^4} A_\mu A^\mu. \quad (4.19)$$

This is the same quantity which was discussed in the introduction (1.5). For non-relativistic theories there is no mass-shell constraint which makes the non-relativistic mass-shift harder to find.

Drift Velocity

The Lorentz gauge reduces to $n \cdot A = 0$. We now make the final gauge choice, $\phi = 0$. This gauge condition forces the gauge potential to be perpendicular to the laser beam. As discussed in section 2.1, $A_z = 0$ to avoid having a net electric field. An elliptically polarised laser beam travelling in the positive \hat{z} direction is modelled,

as in (3.49)

$$A^\mu(\xi) = a \left(0, \varepsilon \cos(\xi), \sqrt{1 - \varepsilon^2} \sin(\xi), 0 \right). \quad (4.20)$$

As mentioned after (3.49) the pulse function has been simplified $a(\xi) = a$. As we shall see, the form of the drift velocity is much more insightful if it is derived from a specific monochromatic plane wave.

Re-write the free theory's momentum by introducing the dimensionless velocity parameter β_z in the standard way

$$\Pi^\mu = \frac{mc}{\sqrt{1 - \beta_z^2}} (1, 0, 0, \beta_z). \quad (4.21)$$

It helps if we employ the notation from [36] and let

$$\alpha = \sqrt{\frac{1 - \beta_z}{1 + \beta_z}}. \quad (4.22)$$

The parametric trajectory for the specific gauge potential is found by substituting (4.20) into (4.15), in the new notation it is found that the parametric trajectory as a function of the proper time (4.16) is

$$\begin{aligned} x^\mu(\tau) = & c\tau \left(1, 0, 0, \frac{1 - \alpha^2}{1 + \alpha^2} \right) \frac{1 + \alpha^2}{2\alpha} \\ & + \frac{\eta^2}{2} \frac{c}{\omega_L} (1, 0, 0, 1) \frac{1}{\alpha^2} \left[\frac{1}{2} \omega_L \alpha \tau - \frac{1 - 2\varepsilon^2}{2} \left(\frac{1}{2} \sin(2\omega_L \alpha \tau) \right) \right] \\ & - \eta \frac{c}{\omega_L} \frac{1}{\alpha} \left(0, \varepsilon \sin(\omega_L \alpha \tau), 2\sqrt{1 - \varepsilon^2} \sin^2 \left(\frac{\omega_L \alpha \tau}{2} \right), 0 \right), \end{aligned} \quad (4.23)$$

with $\eta = ea/mc^2$, as derived in (3.50).

The average three velocity of a particle is defined as

$$\langle \mathbf{v} \rangle := \left\langle \frac{d\mathbf{x}}{d\tau} \right\rangle c / \left\langle \frac{dx^0}{d\tau} \right\rangle, \quad (4.24)$$

which for a particle with motion (4.23) gives

$$\langle \mathbf{v} \rangle = c(0, 0, 1) \left(\frac{1 - \alpha^2 + \frac{\eta^2}{2}}{1 + \alpha^2 + \frac{\eta^2}{2}} \right). \quad (4.25)$$

This is the *drift velocity* of the relativistic particle in a laser field. As before, the average rest frame (ARF) is the frame in which the drift velocity is equal to zero. For the specific choice in initial constant β_z which leads to

$$\alpha^2 = 1 + \frac{\eta^2}{2} \quad (4.26)$$

we have the initial velocity in the ARF,

$$\beta_{\text{ARF}} = -\frac{\eta^2}{4 + \eta^2}. \quad (4.27)$$

Since $\eta^2 \geq 0$ then $\alpha^2 \geq 1$, and the initial velocity $\beta_{\text{ARF}} \leq 0$ and dependent on the intensity. Before switching on the laser pulse the particle is moving in the negative \hat{z} direction, or towards the laser. The parametric trajectory in the ARF is plotted in figure 4.1, using (4.26) and (4.23), for a linearly polarised laser it can be seen that the particle moves through a figure of eight.

The proper time, which parameterises (4.23), can be very different from the reference frame time if the particle moves at relativistic velocities. The $\mu = 0$ component of (4.23) has not been inverted so the relationship describing τ as a function of the reference frame's time is unknown. It is of course possible to use (4.23) numerically, but this is not ideal. The higher harmonic oscillations, observed for the non-relativistic solution (3.105), are not apparent in (4.23). They are camouflaged by the parametric solution, but they will become apparent in the following section when we discuss the three dimensional relativistic trajectory.

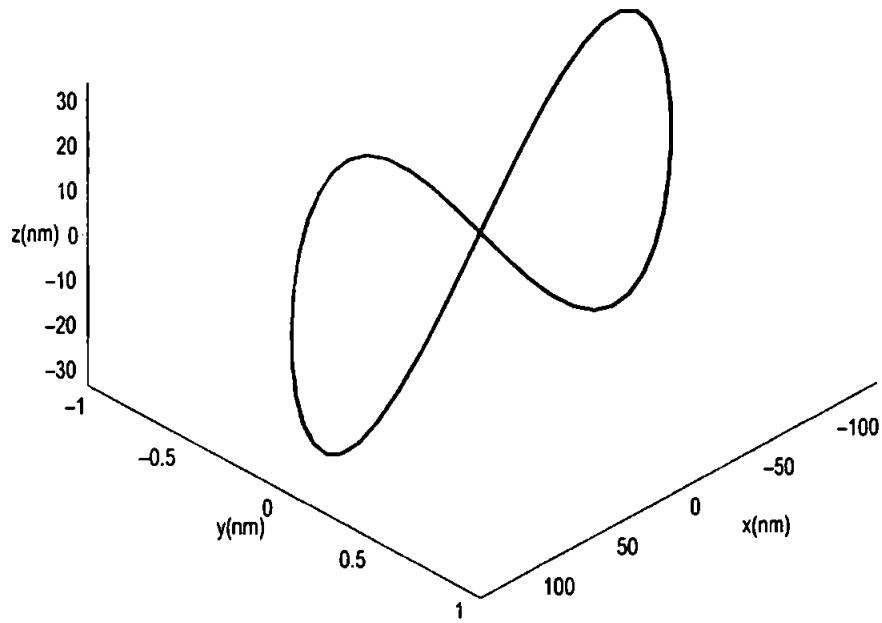


Fig. 4.1: Parametric relativistic trajectory for a linearly polarised ($\varepsilon = 1$) laser beam with optical wavelength $\lambda = 1000\text{nm}$ and intensity $\eta^2 = 1/2$. The orbit is the well know figure of eight.

4.2 Solution in terms of the Average Rest Frame's Time

Sengupta [9], after his equation (33) discusses an analogy between his equation and Kepler's equation [46]

$$t = \psi - e \sin \psi. \quad (4.28)$$

Kepler's equation is usually associated with a planet's elliptical orbit, with eccentricity e , about the sun. Inverting Kepler's equation, so that the trajectory of a planet can be written as a function of the time, attracted much research in the eighteenth and nineteenth centuries. Researchers have found over 100 methods to invert Kepler's equation. Sengupta merely comments on this analogy, but we have found a frame in which the $\mu = 0$ component of (4.23) is equal to Kepler's equation.

By studying the $\mu = 0$ component of (4.23) and letting the particle be in the ARF frame (4.26) Kepler's equation is found as

$$2\omega_L t = 2\alpha\omega_L \tau - \frac{1}{4} \frac{\eta^2(1 - 2\varepsilon^2)}{\alpha^2} \sin(2\alpha\omega_L \tau). \quad (4.29)$$

Only in the ARF is t the observable time because time is transformed under Lorentz boosts. The inversion of Kepler's equation will now be outlined. We will differentiate (4.29) with respect to $2\alpha\omega_L \tau$ then taking the reciprocal of the subsequent equation. Finally this will be expanded in terms of a Fourier cosine series [59, 63]. Let $\psi = 2\alpha\omega_L \tau$ and the 'eccentricity' is

$$e = \frac{1}{4} \frac{\eta^2(1 - 2\varepsilon^2)}{1 + \frac{\eta^2}{2}}. \quad (4.30)$$

Differentiating Kepler's equation with respect to ψ and inverting yields:

$$\frac{d\psi}{d(2\omega_L t)} = \frac{1}{1 - e \cos \psi} = f(\psi). \quad (4.31)$$

Here $f(\psi)$ can also be thought of as a function of $2\omega_L t$, since the aim of the analogy with Kepler's equation is to write τ as a function of t . Since $\eta^2 \geq 0$ the eccentricity $|e| < 1$ and the function, f is even, so a Fourier cosine series may be used to describe it.

$$f(2\omega_L t) = \frac{1}{2\pi} \int_0^{2\pi} \frac{d(2\omega_L t)}{1 - e \cos \psi} + \sum_{\nu=1}^{\infty} \frac{\cos(2\nu\omega_L t)}{\pi} \int_0^{2\pi} d(2\omega_L t) \frac{\cos(2\nu\omega_L t)}{1 - e \cos \psi}. \quad (4.32)$$

After a change of variables to ψ using (4.31) the integrals can be evaluated using identity (9.1.21) from reference [63]

$$\frac{1}{\pi} \int_0^{2\pi} dx \cos[\nu(2x - e \sin 2x)] = 2J_\nu(\nu e). \quad (4.33)$$

Here $J_\nu(\nu e)$ are Bessel functions [59, 63]. After integration (4.32) becomes

$$f(2\omega_L t) = 1 + 2 \sum_{\nu=1}^{\infty} \cos(2\nu\omega_L t) J_\nu(\nu e), \quad (4.34)$$

which may be inserted into (4.31) to obtain

$$2\alpha\omega_L \tau = 2\omega_L t + 2 \sum_{\nu=1}^{\infty} \frac{1}{\nu} J_\nu(\nu e) \sin(2\nu\omega_L t). \quad (4.35)$$

Equation (4.35) can be substituted into (4.23) to give the equation for the relativistic trajectory in the ARF in terms of the ARF time, we find

$$x = -\frac{c\varepsilon}{\omega_L} \left(\frac{\eta}{\sqrt{1 + \frac{\eta^2}{2}}} \right) \sin \left[\omega_L t + \sum_{\nu=1}^{\infty} \frac{1}{\nu} J_\nu(\nu e) \sin(2\nu\omega_L t) \right], \quad (4.36)$$

$$y = -\frac{2c\sqrt{1 - \varepsilon^2}}{\omega_L} \left(\frac{\eta}{\sqrt{1 + \frac{\eta^2}{2}}} \right) \sin \left[\frac{1}{2}\omega_L t + \frac{1}{2} \sum_{\nu=1}^{\infty} \frac{1}{\nu} J_\nu(\nu e) \sin(2\nu\omega_L t) \right], \quad (4.37)$$

$$z = -\frac{c}{\omega_L} \left(\frac{1 - 2\varepsilon^2}{2} \right) \left(\frac{\eta^2}{4 + 2\eta^2} \right) \sin \left[2\omega_L t + 2 \sum_{\nu=1}^{\infty} \frac{1}{\nu} J_\nu(\nu e) \sin(2\nu\omega_L t) \right]. \quad (4.38)$$

Therefore the equations of motion (4.1) have been solved as a function of the reference frame's time. Through the Bessel functions all harmonic oscillations are present, as was the case for the non-relativistic beyond dipole solution. This leads to the modification of Thomson scattering (see e.g., the basic references [8, 37–40] and for the recent direct experimental observation of the second harmonics [41]).

It is interesting to compare weak field expansions in the ARF for the relativistic and non-relativistic theories. This can be done by expanding the Bessel functions using identity (9.1.10) from reference [63]

$$J_\nu(\kappa) = \left(\frac{1}{2}\kappa\right)^\nu \sum_{n=0}^{\infty} \frac{1}{n!} \frac{\left(-\frac{1}{4}\kappa^2\right)^n}{\Gamma(\nu + n + 1)}. \quad (4.39)$$

Here Γ is the *gamma function* and $\Gamma(n + 1) = n!$ as can be seen in p161 of [64]. Expanding (4.35), using (4.39) to lowest order in the laser field strength gives

$$2\alpha\omega_L\tau = 2\omega_L t + \frac{1}{4} \frac{\eta^2}{\alpha^2} (1 - 2\varepsilon^2) \sin(2\omega_L t). \quad (4.40)$$

Using Taylor expansions we may calculate an expansion in the intensity η to any order. The trajectory in the ARF as a function of the ARF time, to order η^2 , is

$$\begin{aligned} x_{\text{ARF}}(t) &= -\frac{c\varepsilon}{\omega_L} \eta \sin \omega_L t, \\ y_{\text{ARF}}(t) &= -\frac{2c\sqrt{1-\varepsilon^2}}{\omega_L} \eta \sin^2 \left(\frac{\omega_L t}{2} \right), \\ z_{\text{ARF}}(t) &= -\frac{c}{\omega_L} \frac{1-2\varepsilon^2}{8} \eta^2 \sin 2\omega_L t. \end{aligned} \quad (4.41)$$

References [12, 24] indicate that the value of the intensity parameter $\eta^2 \approx 0.1$ is when we expect relativistic effects to become prominent. It is interesting to compare the

same expansion for the non-relativistic solution (3.110), which we repeat below

$$\begin{aligned} x_{\text{ARF}}(t) &= -\frac{c\varepsilon}{\omega'_L} \eta \sin \omega'_L t, \\ y_{\text{ARF}}(t) &= -\frac{2c\sqrt{1-\varepsilon^2}}{\omega'_L} \eta \sin^2 \left(\frac{\omega'_L t}{2} \right), \\ z_{\text{ARF}}(t) &= -\frac{c}{\omega'_L} \frac{1-2\varepsilon^2}{8(1-\beta_{\text{ARF}})} \eta^2 \sin 2\omega'_L t, \end{aligned} \quad (4.42)$$

and relativistic solution (4.41) since the two should coincide when the non-relativistic theory is valid. At first glance there appear to be differences. The non-relativistic solution (4.42) contains factors of the initial velocity β_{ARF} in the z component and through the Doppler shifted laser frequency $\omega'_L = (1 - \beta_{\text{ARF}})\omega_L$. However, we know that β_{ARF} is a function of η from (4.27) so (4.42) must be Taylor expanded. At order η^2 the relativistic and non-relativistic solutions describe an equivalent trajectory, but if we then go beyond this level it appears like deviations between the two theories appear.

The inversion (4.35) can only be done in the ARF, which has the specific relationship between the initial velocity and intensity $\alpha^2 = 1 + \frac{\eta^2}{2}$, because it is only in this frame that Kepler's equation (4.29) is produced. However, this may be generalised, since it is possible to conduct a boost into the ARF. Consider the system before the laser pulse is activated, i.e. at $t = -\infty$. Then (4.21) can be interpreted as the physical 4-momentum of the particle so β_z is the 3-velocity. We know that in order to be in the ARF the initial 3-velocity must be

$$\beta_{\text{ARF}} = -\frac{\eta^2}{4 + \eta^2}. \quad (4.43)$$

from (4.26). A Lorentz boost from a general frame with velocity, β_z to the ARF which has 'initial' velocity β_{ARF} may be constructed. Using the composition of velocities

formula, given on page 31 of [65], it is found that the boost velocity must be

$$\beta_{\text{boost}} = \frac{\beta_z(4 + \eta^2) + \eta^2}{(4 + \eta^2) + \beta_z(4 + \eta^2)}. \quad (4.44)$$

Therefore, using this boost parameter, we can solve the equations of motion (4.1) in terms of the reference frame's time, for all frames and laser intensities.

To conclude we have re-derived the relativistic parametric solution and observed effects such as the mass-shift and drift velocity. However, the parametric solution disguises the higher harmonics and complexity of the actual three dimensional trajectory. Solving the three dimensional trajectory in the ARF allows us to vastly simplify the derivation in [9] by using Kepler's equation.

4.3 Parameter Region between Dipole and Relativistic Solutions

It has been shown by H.R. Reiss [24] that there is a large domain where the particle can still be considered as non-relativistic but we must include the effect of the magnetic field i.e. go beyond the dipole approximation as in chapter 3.

It is well known that in the ARF the parametric solution for the relativistic theory (4.23) predicts that a linearly polarised laser beam causes a charge to move in a figure of eight, as displayed in figure 4.1. As the velocity induced by the laser decreases the figure of eight will narrow and eventually reduce approximately to simple harmonic motion predicted by the dipole approximation. The "small axis" is in the direction of the plane wave's propagation, chosen to be \hat{z} for solutions within this thesis. The size of the small axis of the figure of eight is a measure of the force applied by the magnetic field. If this dimension becomes as large as the size of an atom then the departure from the dipole approximation should have physical manifestations.

In the average rest frame of a relativistic particle, for a linearly polarised laser propagating in the z direction the parametric trajectory has been solved in (4.23),

the z -component of which is

$$z = \frac{c}{8\omega_L} \frac{\eta^2}{(1 + \eta^2/2)^2} \sin(2\omega_L \sqrt{1 + \eta^2/2} \tau). \quad (4.45)$$

Conduct an intensity expansion in η^2 , then study only the amplitude of (4.45), z_0 , which is

$$z_0 = \frac{c}{8\omega_L} \eta^2. \quad (4.46)$$

The magnetic field has physical manifestations if $z_0 \geq a_0$, the diameter of a Bohr atom [24]. Using the definition of the laser intensity parameter (3.5) the recorded intensity is equal to

$$I := \frac{\pi m^2 c^5 \eta^2}{2e^2 \lambda^2}. \quad (4.47)$$

It can be seen that the magnetic field has no physical manifestations when the intensity

$$I \leq \frac{8\pi a_0 c^5 m_e^2}{\lambda^3 e^2}. \quad (4.48)$$

Relativistic effects may be observed when $\eta^2 \geq 0.1$ (as motivated in [12, 24] and observed by comparing (3.110) and (4.41)). From (4.47) it can be seen the relativistic solution is needed when

$$I \geq \frac{\pi c^5 m^2}{20e^2 \lambda^2}. \quad (4.49)$$

From (4.49) and (4.48) it can be seen that there is an intermediate parameter region where one must go beyond the dipole approximation and incorporate the magnetic field but relativistic effects are not required. The non-relativistic solution beyond the dipole approximation is valid for a wider range of parameters than the dipole approximated solution, as displayed in figure 4.2. By comparing figures 1.1 and 4.2 we see that the particle is accurately described by the non-relativistic theory for lasers, which by today's standards, are strong.

Very short wavelength laser pulses lead to rapid oscillations with small magnitude.

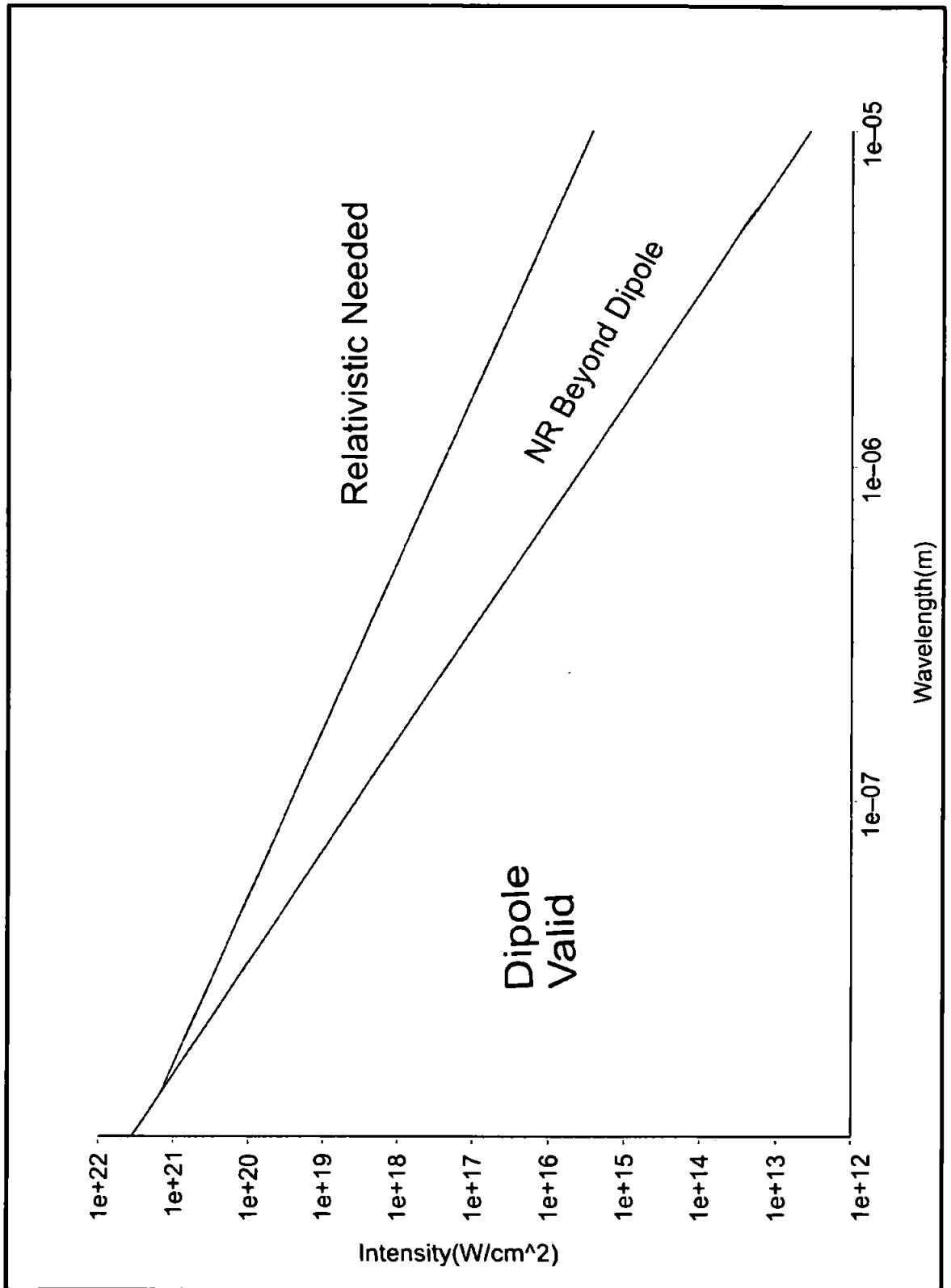


Fig. 4.2: Domains in which individual solutions are valid for a charge's motion in a linearly polarised laser's electromagnetic background, as found in [24]

The direction of the force applied by the magnetic field alternates frequently (4.1). The dipole approximation must be invalid to experimentally differentiate between the dipole approximation and the relativistic solution. This may be seen in figure 4.2 when λ becomes very small, approximately $\lambda \leq 1.05 \times 10^{-8}$.

It is now sensible to plot the previously unknown beyond dipole trajectory for a non-relativistic particle (3.67), since we now know what laser intensities this solution is valid. We also conduct a boost to the ARF to display graphs. The motion is essentially the same shape as that produced by the well known relativistic parametric solution. As discussed above, the charge's orbit appears as a figure of eight for a linearly polarised laser, which is displayed in figure 4.3(a). For circularly polarised laser beams, it is well known [20] that the motion is circular as shown in figure 4.3(b).

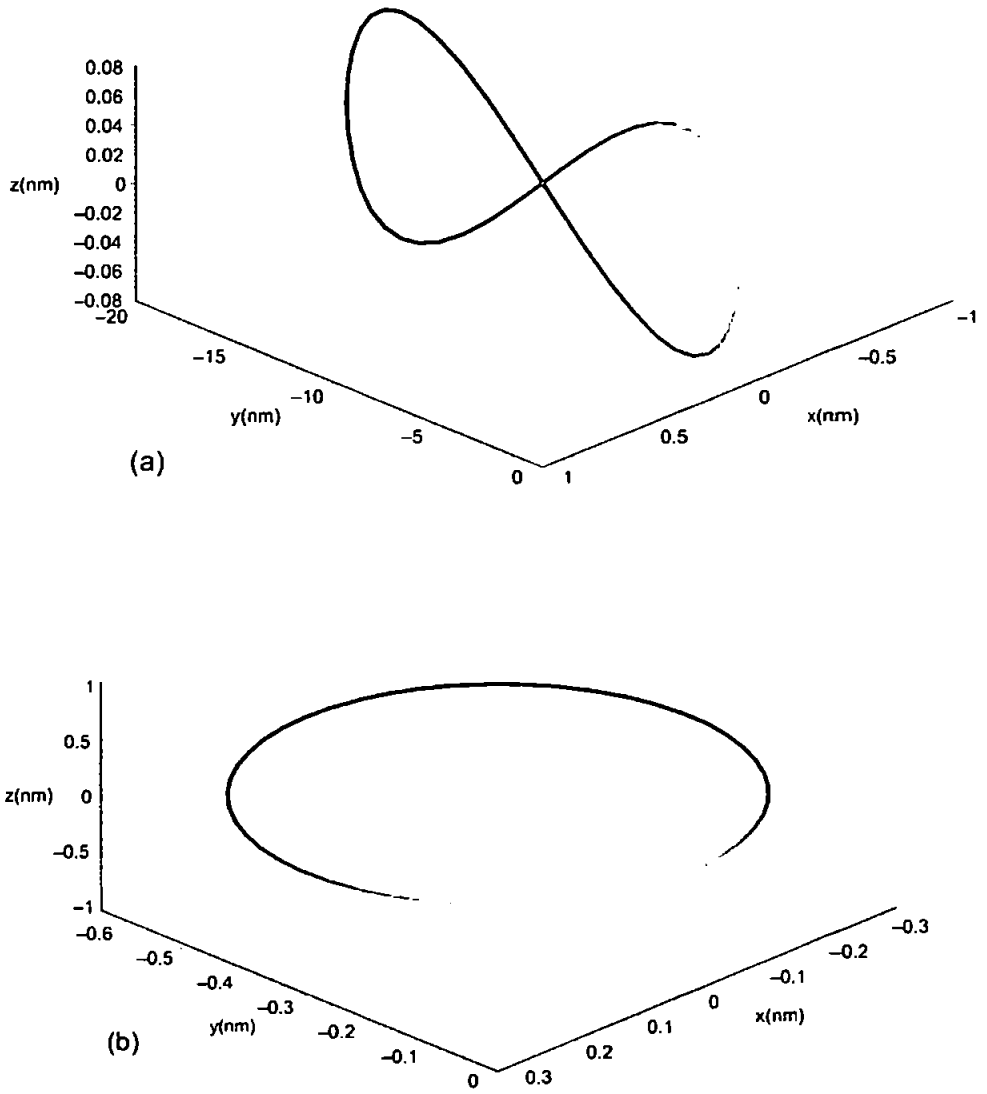


Fig. 4.3: Trajectory for a non-relativistic particle beyond the dipole approximation for a laser beam with intensity $I = 8.55 \times 10^{16} \text{ W/cm}^2$ and wavelength $\lambda = 10^{-6} \text{ m}$. In diagram (a) the beam is linearly polarised and in (b) circularly polarised. The non-relativistic particle is initially at rest at the origin before the laser pulse is switched on.

Part II

UNOBSERVED BACKGROUNDS AND INFRARED DIVERGENCES

1. INTRODUCTION

When considering the interaction between particles collided by a powerful accelerator it is necessary to go beyond the classical consideration of part I. Attempts made to combine relativity and quantum mechanics failed which led researchers to describe the interactions of fundamental particles using quantum field theory. Particle physicists describe the electromagnetic, weak and strong forces using gauge theories. In quantum electrodynamics (QED) interactions between electrically charged particles are mediated by massless spin one particles which are called photons. It is an abelian theory described by the unitary group $U(1)$. Particles with colour charge are described by quantum chromodynamics (QCD). Similarly this force is also mediated by massless spin one particles called gluons. However QCD is a non-abelian gauge theory described by the group $SU(3)$. This leads to there being more than one type of colour charge (red, green, blue and their anti-colours) and the gluons carry colour charge. This makes it possible for a gluon to interact with other gluons. It has been shown, through deep inelastic scattering experiments, that low energy gluons form a large proportion of the matter within a hadron [66]. The weak interaction is also described by a $SU(2)$ gauge theory, but in this case the gauge symmetry is broken (or hidden) and the gauge bosons W^\pm and Z acquire a mass. This model also unifies the weak and electromagnetic interactions into a single larger gauge theory called the electro-weak theory. The combination of the electro-weak and QCD theories is called the *standard model* of particle physics. Data gained from accelerator experiments matches the theoretical calculations for

observable quantities we can calculate¹. The LHC will be coming into operation during 2008 so there shall be a lot of new data available thereafter to compare with the predictions made by the standard model.

Experimentalists collide two particle beams together at high energies then observe the final state particles. Then this is compared to the theoretically calculated cross-section, which is a measure of the probability that a certain scattering process will occur. The first step in calculating the cross-section is to identify all the possible processes which have in common the same initial and final state particles. We may also include processes involving particles which the experiment cannot detect, which we refer to as *degenerate processes*. For example consider Coulomb scattering, the process where an electron is scattered electromagnetically off a nucleus. The initial and final states are the electron and nucleus. Feynman diagrams are drawn for the processes which contain these initial and final states. There are several different diagrams to consider, some of these processes are shown in figure 1.1. The contribution to the cross-section for each of the diagrams must be calculated using the Feynman rules. There are an infinite number of diagrams to consider but for perturbative theories the coupling constant is small so in practice we may stop considering new processes at some order of the coupling. The tree-level diagram, displayed in figure 1.1(a), is the simple scattering of an electron off the nucleus by the transfer of a virtual photon. This is the lowest order approximation in perturbation theory. Higher order corrections come in several degenerate forms, for example, bremsstrahlung displayed in figure 1.1(b) (the experiment is not sensitive enough to detect the emitted photon) and a virtual photon correction figure 1.1(c). However, these higher order diagrams are difficult to calculate because they contain infrared and ultraviolet singularities.

The ultraviolet divergences exist at small distance or large momentum scales.

¹ See [11] for a review of the precision tests which have taken place to confirm the predictions made by QED.

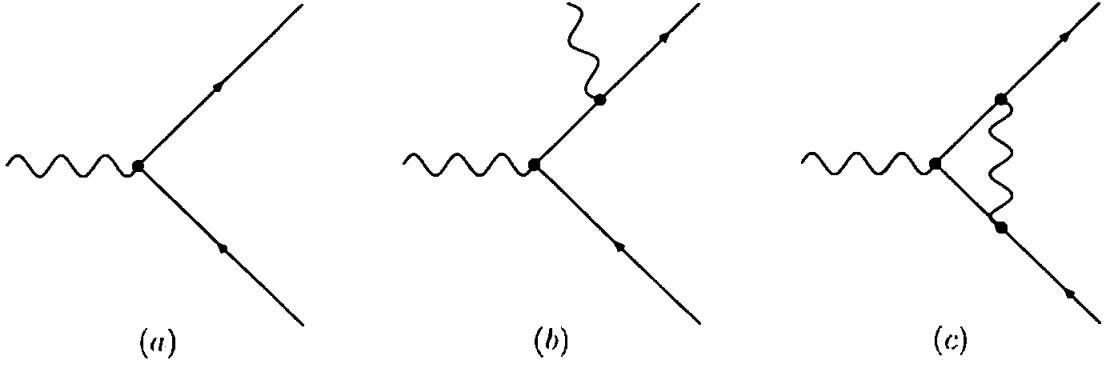


Fig. 1.1: Coulomb scattering of an electron off a static nucleus at tree-level (a) and some next to leading order effects: bremsstrahlung (b) and virtual (c). The photon on the left hand side of the diagrams is not external.

These divergences are well understood through the renormalisation group [67, 68]. The singularities are absorbed into the bare parameters and the field strength of the Lagrangian [68] as the large momentum degrees of freedom are removed. When calculating with renormalised perturbation theory the physical values of the mass, coupling strength and field strength must be used.

The infrared divergences have a dynamical origin. They arise because of the masslessness of the gauge bosons in QED and QCD. This means that the force can propagate over long ranges [3, 69, 70] which correspond to small momentum. There are two different types of infrared singularities called soft and collinear divergences. Consider the bremsstrahlung diagram in figure 1.1(b). Let the out-going electron have momentum² p'^μ and the emitted photon have momentum k'^μ . Both these momenta are on-shell, this means that $p'^2 = m^2$ and $k'^2 = 0$. The intermediate electron propagator has the denominator

$$\frac{1}{(p' + k')^2 - m^2} = \frac{1}{2p' \cdot k'} \quad (1.1)$$

If the photon momentum $k'^\mu \approx 0$ it is easy to see that the propagator diverges.

² The notation used to prime the final state particles momenta will be useful when considering more complex diagrams.

This is called a soft infrared singularity and it generates a divergence in an S -matrix element calculation. When the energy of a photon is referred to as soft it means that the photon has energy $0 \leq \omega' \leq \Delta$. Here Δ is some upper cut off, above which the photon would be detected in a particular experiment. Collinear divergences are present in scattering experiments where there are massless charged particles (e.g. gluons) or if the energy of the electron is much larger than its mass $E' \gg m$. For the latter case the electron is effectively massless so $|\mathbf{p}'| \approx E'$. Then the propagator may be written as

$$\frac{1}{2p' \cdot k'} \approx \frac{1}{E'\omega'(1 - \cos\theta)} \quad (1.2)$$

where θ is the angle between the electron and photon momenta 3-vectors \mathbf{p}' and \mathbf{k}' . If $\theta = 0$ then $(1 - \cos\theta)$ vanishes and we obtain a collinear divergence. Collinear divergences occur in massless and high-energy theories when particles are emitted or absorbed as they travel parallel to each other. We will use a small electron mass m to regulate collinear singularities. When calculating the contribution to the cross-section from a high energy process with collinear particles we obtain factors $\mathcal{O}(\ln m)$ which diverge as we let m return to zero. To summarise, we find that if the momentum of an internal line within a Feynman diagram is on-shell then the cross-section contribution for the process will be infrared divergent.

The soft infrared problem is much worse in asymptotically free theories such as QCD³. The coupling strength grows with the distance scale so the soft dynamics are much more important, because there is a much higher probability of emitting or absorbing soft particles. When calculating matrix elements from Feynman diagrams one usually makes the assumption that as $t \rightarrow \pm\infty$ the interactions are ‘switched off’ (see page 165 of [1] and [69]) and the particles become *free*. This is in direct conflict with the long range nature of QED and QCD. In QCD hadronisation shows that interactions occur far from the scattering centre. The dynamical origin of the

³ For a discussion on the problems cancelling soft divergences in QCD see [71, 72]

infrared problem will be discussed further in chapter 3.

In the particle physics community the consensus of opinion is that the S -matrix is infrared divergent but the cross-section is infrared safe. Papers have been written which explain that all the infrared divergences, produced by degenerate processes contributing to the cross-section, may be combined in such a way that the singularities cancel. There are two widely accepted ideas which deal with the cancellation of infrared divergences at the level of the cross-section. These are called the *Bloch-Nordsieck* theorem [2, 73, 74] and the *Lee-Nauenberg* theorem [5] which is sometimes referred to as the Kinoshita-Lee-Nauenberg theorem. It is widely believed that the combination of these two ideas removes both soft and collinear divergences. Bloch-Nordsieck is used to cancel soft divergences and, after this is complete, Lee-Nauenberg is used to remove collinear divergences. It is vital we fully understand the singularities appearing in physical theories and this thesis aims to provide a greater insight into the application of the underlying theories behind infrared divergence cancellation and expose some unknown complications.

The Bloch-Nordsieck paper was published in 1937, one of the earliest papers on QED. Lee and Nauenberg was published their work in 1964. Although several authors [10, 75–78] have revisited some aspects of the arguments used by Lee and Nauenberg, there has not been a systematic reappraisal of how their method should be applied to high-energy or massless gauge theories when there are both initial and final state degeneracies. Processes which have hadrons in the initial states obviously have both types of degeneracy. Given the relevance of precisely this type of process to the forthcoming LHC era in particle physics, such a reassessment of the role of the Lee-Nauenberg theorem is needed. This reassessment was started by Lavelle and McMullan [10] and during this thesis we will extend their work.

Bloch and Nordsieck recognised that in, for example, Coulombic scattering there is always the possibility to emit a soft photon off either the out-state,

displayed in figure 1.1(b), or in-state electron. The inclusive cross-section formed by summing over all possible soft final state photons and virtual processes is soft infrared finite. However, when one deals with high-energy or massless theories, there are also collinear divergences which are not removed in the same way. Lee and Nauenberg wanted to extend the Bloch-Nordsieck mechanism to include the collinear divergences. Building upon lessons learnt through explicit calculations by Kinoshita [4], they were able to prove a general quantum mechanical result. When applied to a field theory with massless fields, their argument concludes that cross-sections are free of both soft and collinear divergences if summed over both final (Bloch-Nordsieck processes) *and* initial degenerate states. By degenerate they mean degenerate in energy up to the resolving power of any given experiment. They do *not* explicitly investigate how soft divergences cancel but simply assume “*the infrared divergence has already been eliminated by including the contributions due to the emissions of soft photons*” (see the discussion following equation (20) in [5]). Lavelle and McMullan have shown that there is an inconsistency in this cancellation [10] which we will review in chapter 4. The authors of [78] claim the Lee-Nauenberg sum of initial and final state degenerate processes represents physical reality so further research is required.

The inconsistency discovered by Lavelle and McMullan could be interpreted to mean that the Lee-Nauenberg proposition fails. However, it is a fundamental quantum mechanical result and we may need to fully embrace the Lee-Nauenberg theorem for all infrared divergences. Using Coulomb scattering as an example we want to see how the Lee-Nauenberg theorem should be used in practice in field theory. From a modern point of view Lee-Nauenberg use some non-standard techniques that obscure a full understanding of their method and hide some important consequences of this approach to the infrared.

In chapter 2 a discussion of Yang Mills theory is presented which is specialised to

QED. QED is the simplest gauge theory in the standard model but it contains all the infrared problems. The asymptotic dynamics of QED is studied in chapter 3 to gain a greater insight into the physical reason behind this problem. In chapter 4 we move on to analyse the standard ways used to remove infrared singularities from the cross-section. The Bloch-Nordsieck theorem will be performed to all orders, we discuss how Lee-Nauenberg is used for collinear divergences and the inconsistency in cancelling soft and collinear divergences is presented. A new class of collinear divergences will be identified. In the final two chapters we embrace the Lee-Nauenberg proposition for all infrared divergences and study the simultaneous cancellation of soft and both types of collinear divergences for processes contributing to the Coulomb scattering cross-section at next to leading order in perturbation theory.

2. YANG MILLS THEORY

Here we review Yang-Mills theory [79] which is used to describe different fundamental forces. Some features of the Lagrangian for Yang-Mills theory will be presented and some specific properties of QED and QCD are covered.

In Yang-Mills theory the force is mediated by gauge bosons which are described by vector fields $A_\mu^a(x)$. The index a labels the internal degrees of freedom. The index μ refers to the space-time component of the vector. In four dimensions they appear to have four degrees of freedom (per space time point per internal degree of freedom) but we know spin one gauge bosons only have two. The gauge bosons can interact with other vector fields and matter with coupling strength g . The field strength $F_{\mu\nu}^a(x)$ is constructed from the vector fields by the formula

$$F_{\mu\nu}^a = \partial_\mu A_\nu^a - \partial_\nu A_\mu^a + gf^{abc}A_\mu^b A_\nu^c, \quad (2.1)$$

here f^{abc} are the structure constants which are totally antisymmetric. Yang-Mills theory with no matter present is given by the Lagrangian

$$\mathcal{L}_{\text{YM}} = -\frac{1}{4}F_{\mu\nu}^a F^{\mu\nu a}. \quad (2.2)$$

Even in the absence of matter it may be seen that this system is nontrivial and interacting because gauge bosons carry a charge for non-abelian groups. In Feynman diagram language this leads to three and four gauge boson vertices.

In physical theories matter is present and interacts with the gauge bosons. The

Dirac matter term of the Lagrangian is

$$\mathcal{L}_D = \bar{\psi} (i \not{D} - m) \psi, \quad (2.3)$$

where $D_\mu = \partial_\mu - ig A_\mu^a T^a$ and T^a are the representation matrices of the group used to construct the theory and obey a Lie algebra. The spinors ψ may have several different charges associated with it depending on the group. The full Yang-Mills theory is given by the Lagrangian

$$\mathcal{L} = \mathcal{L}_{\text{YM}} + \mathcal{L}_D + \mathcal{L}_{\text{G.F.}} + \mathcal{L}_{\text{Ghosts}}. \quad (2.4)$$

The gauge-fixing $\mathcal{L}_{\text{G.F.}}$ and ghost terms $\mathcal{L}_{\text{Ghosts}}$ are added to cancel the unphysical gauge boson degrees of freedom and the freedom associated with the gauge transformation (see page 63 & 152 of [80]).

The radiation and matter terms in (2.4) are gauge invariant. This means that if the fields undergo a transformation

$$\psi \rightarrow U^{-1} \psi \quad \text{and} \quad A_\mu \rightarrow U^{-1} A_\mu U + \frac{1}{g} U^{-1} \partial_\mu U, \quad (2.5)$$

where $A_\mu = A_\mu^a T^a$ and $U \in SU(N)$, the Lagrangian is invariant. With the gauge fixing and ghost terms the gauge symmetry of the Lagrangian is lost. It is replaced by BRST symmetry which is related to gauge invariance. However, for the topics studied in this thesis it is not important.

It is worth noting that if we looked at the Hamiltonian formulation of Yang-Mills theory the conjugate momenta to the A_0 variable is zero. The conjugate momenta constraint is interpreted to mean that A_0 is an unphysical degree of freedom in the system which must be removed through gauge fixing. Using the Dirac-Bergmann algorithm, which is discussed in part I section 2.3.1, to preserve the constraint for

all time leads to Gauss' law. Gauge fixing the constraint leads to the gauge fixing term in the Lagrangian. In QED Gupta and Bleuler (see page 87 in [81]) have shown that by using the positive frequency part of the Lorentz gauge the time-like and longitudinal photons cancel one another. This leaves only the two physical transverse photonic polarisations. For QCD, using Faddeev-Popov method and a Lorentz gauge condition one introduces 'ghosts'. These ghosts can be thought of as 'negative' degrees of freedom which cancel the unphysical gluon freedoms.

Renormalisation of ultraviolet divergences leads to a 'running' coupling constant [68]. In QED the coupling strength becomes weaker for less energetic particles. However, QCD is an asymptotically free theory (providing the number of fermion species in the representation is sufficiently small, $n_f \leq 16$), its coupling decreases as energy increases. Therefore the probability of a soft particle interacting is much more likely than an energetic particle. The matter in the theory are called quarks and they come in triplets

$$\psi = (\psi_r, \psi_g, \psi_b), \quad (2.6)$$

which corresponds to three colour charges (red, green and blue) and anti-colours. During QCD scattering experiments one never observes a free quark but we see jets of hadrons. Much experimental focus for over more than 30 years aimed to decipher the exact composition of a hadron. Deep inelastic scattering experiments have shown that a significant amount of material within a hadron is in the form of soft gluons [66]. This means that there are interacting massless charged particles in the final state of a scattering experiment. For LHC processes there are protons in the initial state, so it also contains massless charged particles. The presence of massless charged particles means that there will be soft and collinear infrared singularities present in cross-section calculations.

A much simpler theory which contains massless charged particles in the initial and final states is high-energy or massless QED (e.g. Compton scattering). The fermions

and photons are massless and will lead to both soft and collinear singularities. The infrared problem is a feature shared between QED and QCD although asymptotic freedom means the singularities associated with soft particles are much more severe in QCD. In order to explore infrared divergences in a simpler arena we study high-energy QED which is governed by the Lagrangian

$$\mathcal{L}_{QED} = -\frac{1}{4}F_{\mu\nu}F^{\mu\nu} + \bar{\psi}(i\not{D} - m)\psi + \mathcal{L}_{G.F.}, \quad (2.7)$$

as $m \rightarrow 0$. This is formed from the Yang-Mills Lagrangian using the $U(1)$ group. The Feynman rules used for calculating scattering amplitudes in QED are discussed in appendix D and can be derived from the Lagrangian as in [68]. The aim of the work in this thesis is to develop a sound understanding of the infrared problem in high-energy QED. We will not tackle the infrared problem in QCD or other Yang-Mills gauge theories.

3. THE INFRARED PROBLEM - ASYMPTOTIC DYNAMICS

Here a method introduced by Kulish and Faddeev to probe the soft dynamics of QED will be followed [3, 69]. By exploring the asymptotic dynamics of QED we can discover the physical reason for the infrared problem.

As noted in (2.5) neither the vector potential or matter fields are unique. The gauge transformation for QED may be written in infinitesimal form as

$$A^\mu(x) \rightarrow A^\mu(x) + \partial^\mu \chi(x), \quad \psi(x) \rightarrow e^{ie\chi} \psi(x). \quad (3.1)$$

This leads to the conclusion that only two of the four components of the vector potential are physical [44, 81] but, in contrast the gauge dependence of the matter field is not usually interpreted to mean that the matter fields are un-physical. This occurs because it is assumed in the LSZ formalism of QFT that the coupling $e \rightarrow 0$ at the asymptotic limit. Even in QED the $1/R$ fall-off (where R is the distance) in the interaction between two charges is too slow to be neglected at spatial infinity [3] so the non-interacting regime is never reached. This is much more obvious in an asymptotically free theory such as QCD where hadronisation shows that interactions still take place at large separations from the initial scattering site. It will be illustrated that the asymptotic interaction means it is possible to create an infinite number of particles.

The method used by Kulish and Faddeev will now be outlined. In the interaction picture (see [81] page 22-24 for a discussion on the Schrödinger, Heisenberg and interaction picture) the time evolution of an operator is given by the free Hamiltonian.

These fields are labelled as ‘free’ in the following calculations. The interaction Hamiltonian determines the evolution of physical states. The LSZ formalism of QFT assumes that the interaction Hamiltonian vanishes for early and late times so the Heisenberg and interaction pictures agree. The asymptotic dynamics are expected to be like that of a free theory. However if the interaction does not vanish it cannot be neglected.

In QED the interaction Hamiltonian [69] in the interaction picture is given by

$$H_{\text{int}}(t) = -e \int d^3x A_{\mu}^{\text{free}}(t, \mathbf{x}) J_{\text{free}}^{\mu}(t, \mathbf{x}), \quad (3.2)$$

where the current $J_{\text{free}}^{\mu}(t, \mathbf{x}) = \bar{\psi}^{\text{free}} \gamma^{\mu} \psi^{\text{free}}(t, \mathbf{x})$. The free fields can be expanded in terms of their creation and annihilation operators (see page 58 in [68]). Inserting these expansions into (3.2) results in 8 terms with time dependence of the form $e^{i\varphi t}$. Here φ involves different sums of energy terms from the fields contributing to the interaction Hamiltonian. These terms have been studied in the $t \rightarrow \pm\infty$ limit. The argument used by Kulish and Faddeev (see also [69, 82] and the discussion in supplement S4 of [83]) is that only if $\varphi \rightarrow 0$ can these terms contribute to the asymptotic interaction. If $\varphi \neq 0$ then, on average, $H_{\text{int}}(\pm\infty) = 0$. A more rigorous description of this is given in [84]. Denote the energy of the emitted/absorbed photon by ω_k and the ‘electrons’ energy before and after the interaction as E_p and E_{p+k} . When $\omega_k \approx 0$ the photon is soft. Two terms in (3.2) can meet the condition $\varphi \rightarrow 0$ when $\omega_k \rightarrow 0$, these are $\varphi = \pm(E_{p+k} - E_p \pm \omega_k)$ which meet the condition since $E_{p+k} \approx E_p$. This can only take place in a theory with massless exchange particles which can have zero energy¹. There is no infrared problem associated with weakly interacting particles because their gauge bosons are massive so $\omega_k > 0$. It can be shown [1, 3, 69] that the interacting Hamiltonian does not vanish asymptotically, it

¹ If a particle has a mass it has a minimum energy given by the famous formula, $E = mc^2$.

is given by

$$H_{\text{int}}^{\text{as}}(t) = -e \int d^3x A_{\mu}^{\text{free}}(t, \mathbf{x}) J_{\text{as}}^{\mu}(t, \mathbf{x}), \quad (3.3)$$

with

$$J_{\text{as}}^{\mu}(t, \mathbf{x}) = \int \frac{d^3p}{(2\pi)^3} \frac{p^{\mu}}{E} \left[\sum_s (b^{\dagger s}(p)b^s(p) - d^{\dagger s}(p)d^s(p)) \right] \delta^3\left(\mathbf{x} - \frac{t\mathbf{p}}{E}\right). \quad (3.4)$$

Here $b^{\dagger s}$ and $d^{\dagger s}$ create fermions and antifermions and b^s and d^s annihilation fermions and antifermions. The current is proportional to the velocity \mathbf{p}/E multiplied by the number operator of particles minus the number operator of antiparticles. QED's asymptotic dynamics are not free since $H_{\text{int}}^{\text{as}} \neq 0$. Therefore the coupling cannot be taken to zero in QED (or QCD). The fermion in the Lagrangian is not gauge invariant. This means it cannot be associated with anything physical such as the electron. Note that we have not discussed the collinear singularities at all here, an asymptotic discussion of these divergences is contained in [84, 85].

When studying the asymptotic limits of the matter field it is found that [69]

$$\psi^{\text{as}}(x) = \int \frac{d^3p}{(2\pi)^3} \frac{1}{\sqrt{2E}} D(p, t) [b^s(p)u^s(p)e^{-ip \cdot x} + d^{\dagger, s}(p)v^s(p)e^{ip \cdot x}], \quad (3.5)$$

where $D(p, t)$ is called a distorting factor. This distortion may be split into two terms, one is a phase factor which can be neglected [83], the other component depends on the soft dynamics of the system. Only the soft dynamics contribute to the asymptotic fields. This soft distortion operator modifies the creation and annihilation operators

$$b^s(p, t) = D_{\text{soft}}(p, t)b^s(p), \quad (3.6)$$

$$D_{\text{soft}} = \exp \left[-e \int_{\text{soft}} \frac{d^3k}{(2\pi)^3} \frac{1}{2\omega} \left(\frac{p \cdot a(k)}{p \cdot k} e^{-itk \cdot p/E} - \frac{p \cdot a^{\dagger}(k)}{p \cdot k} e^{itk \cdot p/E} \right) \right]. \quad (3.7)$$

The asymptotic limit of the matter fields are a coherent state of vector field operators

and matter. This operator no longer has a single particle interpretation, it does not even act in a Fock space. This is the infrared problem and has lead to the view amongst some theorists [3] that no relativistic particle description is possible for the electron. The view taken in references [69, 86, 87] is that the matter field ψ is unphysical therefore it should not be surprising if its asymptotic limit is also unphysical. We will not explore this approach here and instead move to analyse the more established method for dealing with infrared singularities in the remaining chapters.

4. FROM BLOCH-NORDSIECK TO LEE-NAUENBERG

During this chapter we will explore many degenerate processes contributing to the Coulomb scattering cross-section. Infrared singularities will be evaluated, and we will attempt to cancel all divergences using a combination of the Bloch-Nordsieck method and the Lee-Nauenberg proposition.

Tree-level Coulomb scattering is represented by the diagram drawn in figure 4.1. We will now evaluate the cross-section contribution to clarify the notation we use. The electron is scattered off a nucleus with charge = 1 and the four momentum of the electron before scattering is $p^\mu = (E, \mathbf{p})$ and after scattering is $p'^\mu = (E', \mathbf{p}')$. Using the Feynman rules for QED, given in appendix D, the tree-level cross-section is

$$\frac{d\sigma_0}{d\Omega} = \frac{e^2}{(4\pi)^2 |\mathbf{q}|^4} |\bar{u}' \gamma^0 u|^2, \quad (4.1)$$

where we introduce the shorthand notation $\bar{u}' = \bar{u}(p')$ and $u = u(p)$. The convention adopted for all diagrams is that out-going/final state particles are primed and incoming/initial state particles are not. Since the nucleus is static the energy of the in-state and out-state electrons is the same, $E = E'$. The exact form of the source is irrelevant, the only thing that matters is that it is static, so for simplicity we will drop factors in the denominator of (4.1) from now on. Other processes related to Coulomb scattering at the level of the cross-section will be considered in the following sections.

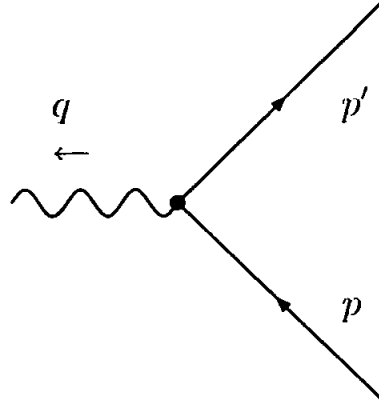


Fig. 4.1: Tree-level Coulomb scattering

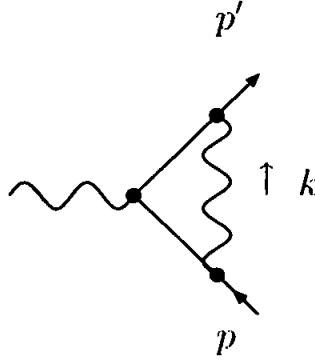


Fig. 4.2: Next to leading order virtual contribution to Coulomb scattering

4.1 The Virtual Process

A virtual photon with momentum k is emitted from the 'in' state electron and absorbed by the 'out' state. This diagram associated with this process is displayed in figure 4.2. At order e^4 this diagram contributes via interference with the tree-level process in the cross-section. Applying the Feynman rules in the Feynman gauge we find that this process is equal to

$$ie^3 \int \frac{d^D k}{(2\pi)^D} \frac{\gamma^\rho(\not{p}' - \not{k} + m)\gamma^0(\not{p} - \not{k} + m)\gamma_\rho}{[(p - k)^2 - m^2][(p' - k)^2 - m^2]k^2} \quad (4.2)$$

sandwiched between the tree-level spinors. These integrals will be regularised using dimensional regularisation [68] so D is the number of dimensions. By changing the number of dimensions, $D = 4 - 2\epsilon$, one can render the integral temporarily finite so it may be calculated. Please note that the external legs have been amputated in this discussion so S -matrix elements are being studied. After a little Dirac algebra the following integrals are found that must be solved

$$e^3 \left[4p \cdot p' \gamma^0 I_1 - 2(\not{p} \gamma_\alpha \gamma^0 + \gamma^0 \gamma_\alpha \not{p}') I_2^\alpha + (D - 2)(g_{\alpha\beta} \gamma^0 - 2\gamma_\alpha g_\beta^0) I_3^{\alpha\beta} \right], \quad (4.3)$$

where

$$I_1 = \int \frac{d^D k}{(2\pi)^D} \frac{1}{[(p - k)^2 - m^2][(p' - k)^2 - m^2]} k^2, \quad (4.4)$$

$$I_2^\alpha = \int \frac{d^D k}{(2\pi)^D} \frac{k^\alpha}{[(p - k)^2 - m^2][(p' - k)^2 - m^2]} k^2, \quad (4.5)$$

and

$$I_3^{\alpha\beta} = \int \frac{d^D k}{(2\pi)^D} \frac{k^\alpha k^\beta}{[(p - k)^2 - m^2][(p' - k)^2 - m^2]} k^2. \quad (4.6)$$

Through power counting of the momentum k it may be seen that some of these integrals diverge. The ultraviolet divergences are regulated by lowering the number of dimensions. To regulate the infrared divergences we increase the number of dimensions $\epsilon = -\epsilon_{\text{IR}}$. There is an ultraviolet divergence associated with $I_3^{\alpha\beta}$ and an infrared divergence associated with I_1 . The other integral, I_2^α , is finite.

The virtual process modifies the tree-level vertex so we must replace

$$\gamma^0 \rightarrow \left(\gamma^0 \{1 + F_1(q^2)\} + \frac{i\sigma^{0\nu} q_\nu}{2m} F_2(q^2) \right). \quad (4.7)$$

The integrals I_1 , I_2^α and $I_3^{\alpha\beta}$ are related to the form factors F_1 and F_2 . The anomalous magnetic moment $F_2(0)$ is infrared safe. Here F_1 is of order e^2 and $1 + F_1(0)$ is the

charge of an electron in units of e . Therefore $F_1(0) = 0$ to all orders, this is guaranteed by the Ward identity (see chapter 7 of [68]).

Calculations may be carried out in the Breit frame where the on-shell four momenta $p^\mu = m\gamma(1, v)$ and $p'^\mu = m\gamma(1, -v)$. The velocity in the Breit frame is related to the energy transferred to the nucleus, $Q^2 = -(p' - p)^2$ by $4v^2/(1 - v^2) = +Q^2/m^2$. Performing on-shell renormalisation to remove the ultraviolet divergence and neglecting any finite terms as either $\varepsilon_{\text{IR}} \rightarrow 0$ or $m \rightarrow 0$ we find

$$2F_1 = \frac{e^2}{4\pi^2} \left[-\frac{1}{\hat{\varepsilon}_{\text{IR}}} \left(\ln \left(\frac{Q^2}{m^2} \right) - 1 \right) + \frac{1}{2} \ln^2 \left(\frac{Q^2}{m^2} \right) + \frac{1}{2} \ln \left(\frac{Q^2}{m^2} \right) \left(1 - 2 \ln \left(\frac{Q^2}{\mu^2} \right) \right) \right], \quad (4.8)$$

where $1/\hat{\varepsilon}_{\text{IR}} = 1/\varepsilon_{\text{IR}} + \gamma - \ln(4\pi)$ and μ is the mass scale which enters dimensional regularisation. Here we have also multiplied by a factor of two since the virtual diagram can only contribute through interference terms at this level of the cross-section. The virtual diagram contains both soft and, when studying high-energy processes, collinear IR divergences which must be removed by combining $2F_1$ with other degenerate processes.

4.2 Soft Emission and the Eikonal Approximation

Soft emission, represented by figure 4.3, is degenerate with the tree-level process. The momenta p'_1 and k' are both on-shell and related to the tree-level electron momentum $p' = p'_1 + k'$ so that the total energy in the out-state is the same as the tree-level process. The spinor for an electron with momentum p'_1 is written in our shorthand notation as u'_1 . The photons have energy ω' which must be less than the out-state energy resolution of the detector, Δ_{out} , or the photon will be detected. Of course, if the photon is detected then it will not contribute to the Coulomb scattering cross-section.

First consider only the emission of a soft photon with momentum k' from the final

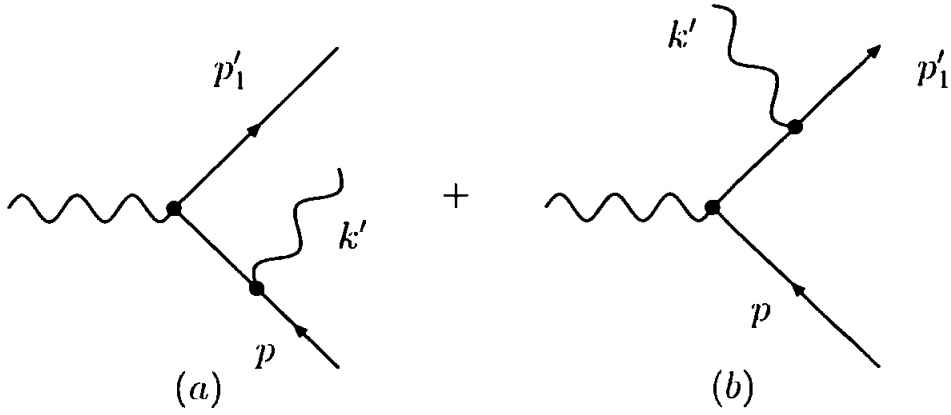


Fig. 4.3: Soft photon emission from (a) the initial state electron and (b) the final state electron

state fermion which is represented in figure 4.3(b). The amplitude is modified by an additional vertex and electron propagator. This leads to the following modification of a spinor in the amplitude

$$\bar{u}' \rightarrow \bar{u}'(ie\gamma^\mu)i\frac{\not{p}'_1 + \not{k} + m}{(p'_1 + k)^2 - m^2 + i\varepsilon}, \quad (4.9)$$

where ε is a small parameter. Here we have neglected the photon polarisation vector temporarily, it will be reinstated when we come to consider the cross-section. In the literature calculations involving soft photons are simplified through the *eikonal approximation* [88, 89] which tells us to let $k \rightarrow 0$ in numerators. Through on-shell power counting we can see that the dropped term is soft finite. Next commute the \not{p}'_1 past the gamma matrix and use the Dirac equation. Thus using the eikonal approximation (4.9) is simplified to

$$\bar{u}' \rightarrow -e\bar{u}'_1\frac{p_1^\mu}{p'_1 \cdot k + i\varepsilon}. \quad (4.10)$$

Note that here the Feynman rules for a spin 1/2 particle are used. Due to the eikonal approximation the emission of a soft photon modifies the amplitude for

charged particles with any spin in the same way [88]. The eikonal approximation removes the spin dependence from the calculation. Divergences correctly reproduced by the eikonal approximation are spin independent. Later we will see that this approximation does not correctly account for all collinear divergences, which are spin dependent divergences.

The emission S -matrix for both processes in figure 4.3 is

$$-ie^2 \bar{u}'_1 \left(\frac{2p'_1 \cdot \epsilon^{*\prime} + \not{\epsilon}^{*\prime} \not{k}'}{2p'_1 \cdot k'} \gamma_0 - \gamma_0 \frac{2p \cdot \epsilon^{*\prime} - \not{k}' \not{\epsilon}^{*\prime}}{2p \cdot k'} \right) u, \quad (4.11)$$

where $\epsilon^{*\prime} = \epsilon^*(k', \lambda')$ and λ' is the polarisation label for the photon. Using the eikonal approximation we drop $\mathcal{O}(\not{k}')$ in the numerator of (4.11). Also the spinor approximation $\bar{u}'_1 \sim \bar{u}'$ can be used (see appendix E), which removes some soft finite terms. After the emission process is squared up, so that it is a cross-section contribution, a sum over polarisations must be evaluated. The general identity for polarisation sums is

$$\sum_{\lambda'} \epsilon'_\mu \epsilon_{\nu'}^{*\prime} = -g_{\mu\nu} - \frac{k'_\mu k'_{\nu'}}{\omega'^2} + \frac{k'_\mu \eta_\nu + k'_\nu \eta_\mu}{\omega'}, \quad (4.12)$$

where the unit time-like vector $\eta_\mu = (1, \mathbf{0})$. However, after using the eikonal approximation in (4.11) only the first part of (4.12) needs to be used because gauge invariance is manifest. With the eikonal approximation the polarisation sum is multiplied by the conserved current associated with the classical change of momentum (see page 177-178 in [68]).

To find the final contribution to the cross-section an integral over a soft cone with maximum energy Δ_{out} will be performed, i.e.

$$e^2 \int_{\text{soft}} \frac{d^{D-1} k'}{(2\pi)^{D-1} 2\omega'} \left(\frac{2p' \cdot p}{p' \cdot k' p \cdot k'} - \frac{p'^2}{(p' \cdot k')^2} - \frac{p^2}{(p \cdot k')^2} \right). \quad (4.13)$$

To compare with the virtual process this is also evaluated in the Breit frame and gives

$$\frac{e^2}{4\pi^2} \left[\frac{1}{\hat{\epsilon}_{\text{IR}}} \left(\ln\left(\frac{Q^2}{m^2}\right) - 1 \right) - \frac{1}{2} \ln^2\left(\frac{Q^2}{m^2}\right) + \ln\left(\frac{Q^2}{m^2}\right) \left(1 + 2 \ln 2 + \ln\left(\frac{\tilde{\Delta}_{\text{out}}^2}{\mu^2}\right) \right) \right], \quad (4.14)$$

where $\tilde{\Delta}_{\text{out}}$ is the energy resolution in the Breit frame. Soft emission produces soft and collinear divergences which may be combined with the virtual process at NLO in the cross-section.

Block-Nordsieck Cancellation of Soft Divergences at NLO

The cross-section at $\mathcal{O}(e^4)$ is modified by the virtual and emission processes

$$\frac{d\sigma}{d\Omega} = e^2 |\bar{u}' \gamma^0 u|^2 (1 + 2 F_1 + \text{soft emission}). \quad (4.15)$$

Adding (4.8) and (4.14) in (4.15) leaves only collinearly divergent terms

$$\frac{e^4}{\pi^2} \ln\left(\frac{Q}{m}\right) \left[\frac{3}{4} + \ln 2 - \ln\left(\frac{Q}{\tilde{\Delta}_{\text{out}}}\right) \right] |\bar{u}' \gamma^0 u|^2. \quad (4.16)$$

Hence, soft divergences are removed by Bloch-Nordsieck but collinear divergences still remain. Later, we will prove that the soft singularities are removed for all orders in perturbation theory by the Bloch-Nordsieck method. The cancellation of all collinear divergences at one-loop level will be the main topic for the remaining sections.

It is simpler to work in the lab frame of the static nucleus when evaluating collinear singularities so now we will transform (4.16) into this frame. The momenta in the Breit frame may be re-written in terms of the Breit frame energy $\tilde{E} = m\gamma$. The energy transferred to the nucleus may be written as $Q^2 = 4m^2(\gamma^2 - 1)$. Pulling

out a factor of \tilde{E} it can be seen that

$$Q = 2\tilde{E}\sqrt{1 - \frac{m^2}{\tilde{E}^2}}, \quad (4.17)$$

where \tilde{E} is the electron's energy in the Breit frame. Since Q^2 is Lorentz invariant we can use it to relate energies in the two frames, we find

$$\frac{\tilde{E}}{\tilde{\Delta}_{\text{out}}} = \frac{E \sin^2(\frac{1}{2}\phi)}{\Delta_{\text{out}} \sin^2(\frac{1}{2}\phi)} = \frac{E}{\Delta_{\text{out}}}, \quad (4.18)$$

where ϕ is the scattering angle for the electrons in the lab frame, we see that the residual collinear divergence describe by (4.16) contributes to the cross-section as

$$\frac{e^4}{\pi^2} \ln\left(\frac{E}{m}\right) \left[\frac{3}{4} - \ln\left(\frac{E}{\Delta_{\text{out}}}\right) \right] |\bar{u}'\gamma^0 u|^2, \quad (4.19)$$

where we have dropped some collinear finite terms. Note that the cross-section is experimental detector resolution dependent.

To conclude, using informal notation, the Bloch-Nordsieck cancellation amounts to

$$2 \left(\text{diagram 1} + \text{diagram 2} \right) + \left| \text{diagram 3} + \text{diagram 4} \right|^2 = -\frac{1}{\epsilon_{\text{IR}}} + \frac{1}{\epsilon_{\text{IR}}}. \quad (4.20)$$

By including the virtual and eikonal approximated soft emission processes the NLO cross-section is soft finite. However, if we were to study high-energy QED the logarithm in (4.19) produces collinear singularities¹.

¹ We consider an electron with a very small mass as opposed to truly massless QED

4.3 Collinear Divergences and the Lee-Nauenberg Theorem

The processes considered by Bloch and Nordsieck are degenerate with Coulomb scattering in the final state but equivalent to Coulomb scattering in the initial state. We will now consider two other types of degeneracy which we call *collinear* and *initial state*. The inconsistency discovered by [10] in the simultaneous cancellation of soft and collinear singularities will be presented.

In the high-energy and/or massless limit(s) the initial and final state electrons move at the speed of light. If the photon is emitted parallel to the final state electron then both particles pass through the same point of a detector at the same time. Given that detectors have finite angular resolution δ , they can only measure the total outgoing energy of the pair of particles E . This collinear configuration provides another degenerate process to consider. Note that these photons may have any proportion of the energy in the electron leg $0 \leq \omega' \leq E$, however we have already included soft photons with energy $0 \leq \omega' \leq \Delta_{\text{out}}$ in the Bloch-Nordsieck cancellation. We can still include the collinear photons with energy $\Delta_{\text{out}} \leq \omega' \leq E$ in the cross-section for Coulomb scattering and we call these *semi-hard* collinear photons. Note that if a semi-hard photon is emitted collinearly to the initial state electron it would be detected in the final state and contribute to a different process.

In the final state we have collinear and soft degeneracies. It is possible to also have both these types of degeneracies in the initial state, this is obviously the case at the LHC since it has hadronic initial states. For the case of QED and LEP we could always have soft photons entering the experiment with the incoming electron. It is also possible to absorb semi-hard photons travelling collinearly to the initial electron beam. If an initial state semi-hard photon is not collinear to the initial state electron when it is absorbed it will be detected because its energy is greater than the experimental resolution. The experiment's ability to detect photons may not be the same in the initial and final state so we include different resolutions Δ_{in} and Δ_{out} for

initial and final state degeneracies. There may also be different angular resolutions for initial and final states, but we let $\delta_{\text{in}} = \delta_{\text{out}} = \delta$, since this will not modify our conclusions.

These extra degeneracies mean we must add several more S -matrix elements to the Coulomb scattering cross-section. We can consider semi-hard emission (from either electron) collinear with the final state electron or semi-hard absorption (on either electron) collinear with the initial state electron. Soft absorption may also be considered on either the initial or final state electron. These processes will produce additional infrared divergences so the question is whether the sum of these singularities cancel. According to the Lee-Nauenberg theorem the soft divergences have already been taken care of via the Bloch-Nordsieck method, so we are only interested in removing the remaining collinear divergences (4.19). Therefore we omit any soft photon effects other than those Bloch-Nordsieck consider because we do not want to re-introduce soft divergences. We only consider degenerate semi-hard collinear emission and absorption. It is important to note in what follows that emission, displayed in figure 4.4, is the complex conjugate of absorption, shown in figure 4.5. Therefore, at the level of the cross-section $|\text{emission}|^2 = |\text{absorption}|^2$. By recognising this we do not need to perform the same calculation twice.

A semi-hard photon may be emitted collinear with the final state electron off either electron line, but if the photon is emitted off the in-state electron (see figure 4.3(a)), it will not produce a divergent intermediate propagator. The propagator denominator $((p - k')^2 + i\varepsilon)^{-1} = (2p \cdot k')^{-1}$ and $p \cdot k' \neq 0$ since the three momenta are not collinear. The internal line within figure 4.3(a) is not on-shell. However, we do need to consider the semi-hard emission process shown in figure 4.4. As before the momentum $p' := p_1' + k'$, where p_1' and k' are on-shell but p' is not, unless the photon is collinear. Denote the energy in the out-going electron $E_1 = E - \omega'$. The

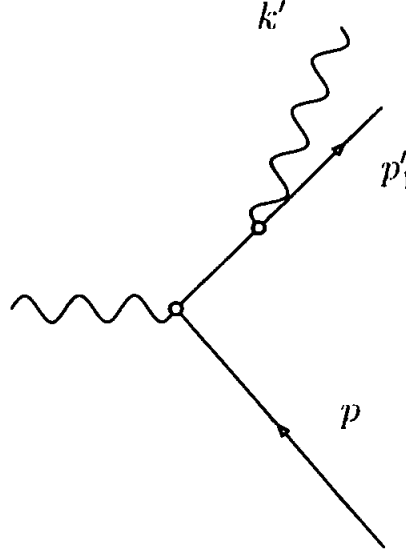


Fig. 4.4: Semi-hard collinear emission by the out-going electron

S -Matrix for this process is

$$-i \frac{e^2}{2p'_1 \cdot k'} \bar{u}'_1 (2p'_1 \cdot \epsilon'^* + \not{\epsilon}'^* \not{k}') \gamma^0 u, \quad (4.21)$$

where $\bar{u}'_1 = \bar{u}(p'_1)$. Once this is squared-up and the spin traces have been evaluated we find the cross-section contribution

$$\frac{e^4}{(p'_1 \cdot k')^2} \left[4(p'_1 \cdot \epsilon') (p'_1 \cdot \epsilon'^*) (p'_1 \cdot \tilde{p}) - 4(p'_1 \cdot \epsilon'^*) (\tilde{p} \cdot \epsilon') (p'_1 \cdot k') - 2(\epsilon' \cdot \epsilon'^*) (\tilde{p} \cdot k') (p'_1 \cdot k') \right], \quad (4.22)$$

where \tilde{p} is defined by $\tilde{p} = \gamma^0 \not{p}' \gamma_0$ so that $4\tilde{p} \cdot p' = |\bar{u}' \gamma^0 u|^2$. Prior to integrating over all the possible momentum of the semi-hard jet of photons, we need to sum over the photon polarisations. In contrast to the soft case, where we could simply replace $\epsilon'_\mu \epsilon'^*_\nu$ by $-g_{\mu\nu}$, we now need to use the full identity (4.12) because gauge invariance is not manifest in (4.22)

After summing over polarisations in (4.22), we find

$$\frac{e^4}{p'_1 \cdot k'} \left[\left(1 + \frac{2E_1}{\omega'}\right) 4(p'_1 \cdot \tilde{p}) + \left(1 + \frac{E_1}{\omega'}\right) 4(k' \cdot \tilde{p}) \right], \quad (4.23)$$

where we have dropped all collinear finite terms. As discussed in Appendix E for collinear photons and electrons we can write, up to collinear finite terms,

$$k' \cdot \tilde{p} = p' \cdot \tilde{p} \frac{\omega'}{E} \quad \text{and} \quad p'_1 \cdot \tilde{p} = p' \cdot \tilde{p} \frac{E_1}{E}. \quad (4.24)$$

Hence (4.23) becomes

$$e^4 |\bar{u}' \gamma_0 u|^2 \frac{E_1^2 + E^2}{(p'_1 \cdot k') E \omega'}. \quad (4.25)$$

We can now use this to build up the inclusive cross-section for the emission of collinear photons. Since the emitted photon we are considering is not soft, the in-coming and out-going electrons have different energies. We follow the lead set by Bethe-Heitler who say that for the cross-section we must include an *energy weighting* factor equal to the electron energy out divided by the electron energy in E_1/E (for references see section 5-2-4 in [1], page 499 of [90], page 244 of [49] and the original paper [91]. For an interpretation see page 309 [92]). The resulting cross-section is given by

$$e^4 |\bar{u}' \gamma_0 u|^2 \int_{\text{semi-hard cone}} \frac{d^3 k'}{(2\pi)^3 2\omega'} \frac{E_1^2 + E^2}{(p'_1 \cdot k') E \omega'} \frac{E_1}{E}. \quad (4.26)$$

The collinear divergences are contained in the $1/p'_1 \cdot k'$ term and take on an obviously singular form when integrated over the angle between the electron and photon. This can be seen by writing

$$p'_1 \cdot k' = E_1 \omega' - \omega' \cos \theta_1 \sqrt{E_1'^2 - m^2} = \frac{1}{2} \omega' E_1 \left(\theta_1^2 + \frac{m^2}{E_1^2} \right), \quad (4.27)$$

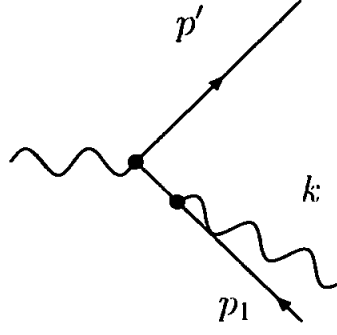


Fig. 4.5: Collinear absorption by the in-coming electron

here θ_1 is the (small) angle between the out-going electron and photon in the lab frame. The electron mass and angle θ_1 are small so we have Taylor expanded above.

Performing the angular integration over the cone with opening angle δ , the angular experimental resolution, we get

$$\frac{e^4}{4\pi^2} |\bar{u}' \gamma_0 u|^2 \ln \left(\frac{E_1 \delta}{m} \right) \frac{1}{E^2} \int_{\Delta_{\text{out}}}^E \frac{E_1^2 + E^2}{\omega'} d\omega', \quad (4.28)$$

collinear finite terms have been omitted. This final integral can be evaluated to yield the cross-section for semi-hard collinear emission:

$$-\frac{1}{2} \frac{e^4}{\pi^2} \ln \left(\frac{E_1 \delta}{m} \right) \left[\frac{3}{4} - \ln \left(\frac{E}{\Delta_{\text{out}}} \right) - \frac{\Delta_{\text{out}}}{E} + \frac{1}{4} \frac{\Delta_{\text{out}}^2}{E^2} \right] |\bar{u}' \gamma^0 u|^2. \quad (4.29)$$

In equation (20) of their original paper [5] Lee and Nauenberg do not write down the terms $\mathcal{O}(\Delta_{\text{out}}/E, \Delta_{\text{out}}^2/E^2)$.

Comparing this result with (4.19) we see that just including the out-going semi-hard collinear photons does not completely remove the residual collinear divergences since there is a factor of a half in (4.29) which obstructs the cancellation of the divergent terms found in (4.19). Lee-Nauenberg now include the in-coming degenerate process whereby a semi-hard photon is absorbed by the in-coming electron, displayed in figure 4.5, then we will get another contribution equal to (4.29)

and we see the cancellation of the mass logarithms in (4.19)

$$\frac{e^4}{\pi^2} \ln\left(\frac{E\delta}{m}\right) \left[\frac{\Delta_{\text{out}}}{E} - \frac{1}{4} \frac{\Delta_{\text{out}}^2}{E^2} \right] |\bar{u}' \gamma^0 u|^2. \quad (4.30)$$

There are several comments which must be made. The first and most obvious comment is that (4.30) is still collinearly infrared divergent. Lee and Nauenberg neglected these terms, which we call Δ divergences, but we observe from (4.30) that they must be considered. The ordinary $\ln(m)$ terms in (4.29) have been cancelled and from now on these are referred to as *regular* collinear divergences. The $\ln(\Delta_{\text{out}}) \ln(m)$ divergences have also cancelled but in order to achieve this cancellation we have insisted $\Delta_{\text{in}} = \Delta_{\text{out}}$. This was the conclusion reached by Lee and Nauenberg following their equation (21).

There are still collinear divergent terms in (4.30) that are linear and quadratic in Δ_{out}/E and these must be cancelled in order to get a collinear finite cross-section. To trace what is going on here, we note that these terms come from the semi-hard energy integral in (4.28) which may be split into two terms:

$$\ln(m) \int_{\Delta_{\text{out}}}^E \frac{E_1^2 + E^2}{\omega'} d\omega' = 2E^2 \ln(m) \int_{\Delta_{\text{out}}}^E \frac{d\omega'}{\omega'} + \ln(m) \int_{\Delta_{\text{out}}}^E (\omega' - 2E) d\omega'. \quad (4.31)$$

It is possible to remove all divergences above, but we must treat the integrals in an inconsistent manner. In the first term it is essential that the lower limit of Δ_{out} is kept otherwise we would reintroduce the soft divergences. Singularities originating from the first term are cancelled via the Lee-Nauenberg method in (4.30). However, the second term is finite as $\Delta_{\text{out}} \rightarrow 0$ so we are missing the collinear singularities produced by photons which are soft. The separation between soft and semi-hard photons is not a division between soft and collinear divergences.

The authors [10] traced where such terms were dropped in the Bloch-Nordsieck mechanism. In the discussion following equation (4.11) we used the eikonal

approximation and dropped factors of k' in the numerator. This has thrown away a relevant collinear term so we must go beyond the eikonal approximation for soft cross-section contributions. The corresponding term in (4.21) generates the divergent terms Lee-Nauenberg failed to cancel in (4.29). Reinstating this momentum in (4.13) and integrating the energy from 0 to Δ_{out} , we see that (4.19) should be replaced with

$$\frac{e^4}{\pi^2} \ln\left(\frac{E}{m}\right) \left[\frac{3}{4} - \ln\left(\frac{E}{\Delta_{\text{out}}}\right) - \frac{\Delta_{\text{out}}}{2E} + \frac{\Delta_{\text{out}}^2}{8E^2} \right] |\bar{u}' \gamma^0 u|^2. \quad (4.32)$$

This represents the Bloch-Nordsieck analysis with all collinear terms retained. Now we see that the Bloch-Nordsieck treatment beyond the eikonal approximation of a soft photon emission (4.32) with the emission of semi-hard collinear photons (4.29) results in the cross-section

$$\frac{1}{2} \frac{e^4}{\pi^2} \ln\left(\frac{E}{m}\right) \left[\frac{3}{4} - \ln\left(\frac{E}{\Delta_{\text{out}}}\right) \right] |\bar{u}' \gamma^0 u|^2. \quad (4.33)$$

To summarise, using diagrammatic notation, the Δ_{out} collinear divergences are removed via

$$\int_0^{\Delta_{\text{out}}} \left| \text{diagram} \right|^2 \Big|_{\text{beyond eikonal}} + \int_{\Delta_{\text{out}}}^E \left| \text{diagram} \right|^2. \quad (4.34)$$

In section 4.2 we saw that the eikonal approximation omits the spin dependence of the propagator, so the Δ divergences may be spin dependent.

It is important to note that here we are still only considering photons emitted collinear with the out-state electron. As mentioned, the cross-section contribution

$$\int_0^{\Delta_{\text{out}}} \left| \text{diagram} \right|^2 \Big|_{\text{beyond eikonal}}, \quad (4.35)$$

does not force an internal line to go on-shell. Therefore we do not get any additional

singularities. However, for the process in (4.35), we could consider soft emission parallel to the initial state electron. This will force the propagator to go on-shell and produce collinear divergences. This process is degenerate to tree-level since the photon is soft. The aim in this chapter is to discuss what is done within the literature, we will return to this diagram in chapter 6.

As expected, (4.33) is still collinearly divergent and we need to include the contribution from initial degenerate states. Now, though, we face a problem not addressed in [5]. Soft initial states are not included in the Bloch-Nordsieck analysis so there is no equivalent, consistent procedure similar to (4.34) for including initial soft photon contributions that are not infrared divergent. Hence we are forced to simply add the in-coming version of (4.29) to (4.33). This time we do not insist that $\Delta_{\text{in}} = \Delta_{\text{out}}$ and we find

$$\frac{1}{2} \frac{e^4}{\pi^2} \ln \left(\frac{E}{m} \right) \left[\ln \left(\frac{\Delta_{\text{out}}}{\Delta_{\text{in}}} \right) + \frac{\Delta_{\text{in}}}{E} - \frac{\Delta_{\text{in}}^2}{4E^2} \right] |\bar{u}' \gamma^0 u|^2. \quad (4.36)$$

Even by going beyond the eikonal approximation we cannot remove the Δ divergences. Regular collinear divergences are successfully removed by Lee-Nauenberg theorem since the eikonal approximation is not used for semi-hard processes.

The only way to remove the divergences in (4.36) is to consider soft absorption collinear with the initial state electron beyond the eikonal approximation. However, since $|\text{emission}|^2 = |\text{absorption}|^2$ we know the soft absorption cross-section contribution will reintroduce the soft divergences which Bloch-Nordsieck cancelled. Therefore there is no consistent way to remove both soft and collinear divergences² simultaneously.

Contrary to the procedure in [5], we must not treat the soft and collinear divergences using a mixture of Bloch-Nordsieck and Lee-Nauenberg arguments

² One could inconsistently remove all divergences by including only the collinear terms arising from soft absorption and neglecting the soft divergences. However, this clearly makes no physical sense.

separately. This does not necessarily mean that the general Lee-Nauenberg proposition is wrong. What it does mean is that we need to understand how to consistently deal with *both soft and collinear initial and final state degeneracies*. As we have seen, the naive inclusion of absorption from initial soft photons will double the soft infrared divergences that arise from real processes and hence lose the Bloch-Nordsieck soft cancellation. This suggests that the mechanism for infrared cancellations is more subtle than expected.

In chapters 5 and 6 we will embrace Lee-Nauenberg proposition for both soft and collinear infrared divergence and examine if all divergences may be cancelled for the Coulomb scattering process. Before moving on to this it will be interesting to discover if a mixture of Bloch-Nordsieck and Lee-Nauenberg theorem works for any processes, which we will cover in the following section. In section 4.4 we will consider the summation of soft divergences to all orders which will uncover vital information regarding the experimental energy resolution.

4.3.1 Processes with just Final State Degeneracies

Let us, for the sake of argument, assume there are no initial state soft degeneracies, $\Delta_{\text{in}} = 0$, and the initial state particles are massive³. This could be a LEP process $e^+e^- \rightarrow q\bar{q} \rightarrow \text{jets}$, represented in figure 4.6, where the quarks are very light. This assumption cannot be taken at the LHC because the hadronic initial states are messy but at LEP the initial states are cleaner than at the LHC so this unrealistic assumption is more plausible. This gives a counter example to the Coulomb scattering process where the Bloch-Nordsieck and Lee-Nauenberg cancellation takes place as expected.

Since the initial states are completely clean we do not consider absorption and

³ The experiment has been set up so that we are 100 percent certain what is in the initial state. This is of course an unrealistic assumption, but it leads to situations where the Lee-Nauenberg theorem works for all infrared divergences.

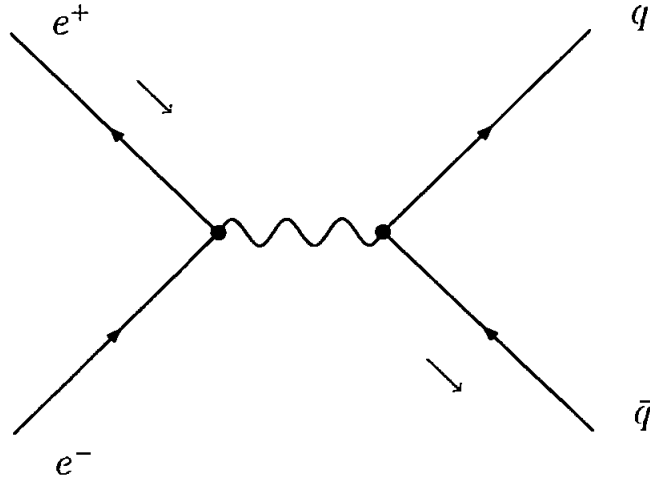


Fig. 4.6: LEP process $e^+e^- \rightarrow q\bar{q} \rightarrow \text{jets}$ where the quarks are taken to be very light

because the initial state particles are massive there can be no collinear degeneracies. Therefore we may only include soft emission and virtual processes for the initial states so the soft singularities are removed by the Bloch-Nordsieck method.

The final state particles are massless so there are also collinear divergences present. However, for the process in figure 4.6, a collinear emission off both the fermion or anti-fermion can be soft or semi-hard. Soft divergences can be removed using Bloch-Nordsieck so we only have collinear singularities to deal with. Regular collinear divergence may be removed by Lee-Nauenberg, in a similar way to the Coulomb scattering case, by considering semi-hard emission off both legs. Since the photons can be soft or semi-hard on both final state legs the resolution dependent Δ_{out} collinear divergences cancel if one goes beyond the eikonal approximation for the Bloch-Nordsieck calculation. Therefore we conclude that Lee-Nauenberg works for processes with clean initial states⁴ i.e. only final state degeneracies.

⁴ If $\Delta_{\text{in}} \neq 0$ this cancellation will be ruined by soft and collinear absorptions.

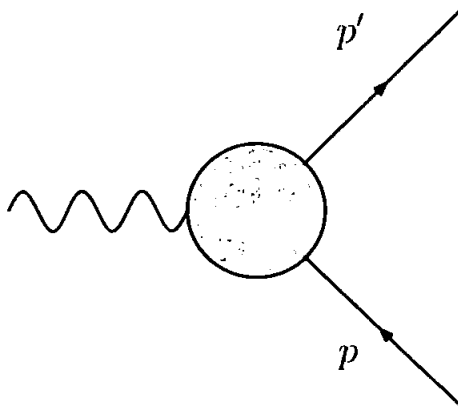


Fig. 4.7: Coulomb scattering including hard virtual processes

4.4 Summation of Soft Divergences to all Orders

The Δ_{out} collinear divergences are naively removed in (4.30) if the limit $\Delta_{\text{out}} \rightarrow 0$ is taken so in this section we will serve to reinforce why this cannot be done. By studying the summation of soft divergences to all orders we will uncover vital information regarding the experimental energy resolution. There are two reasons why $\Delta_{\text{out}} \neq 0$. Firstly, any real experiment has a non-zero resolution for both in-state and out-state. We would not be describing a physical scattering experiment if $\Delta_{\text{out}} = 0$. Another reason came in [88,93], as Yennie et al developed a method to sum up soft divergences from emission and virtual processes to all orders in perturbation theory.

Consider a Coulomb scattering process where we have included effects from hard virtual processes, figure 4.7. The following discussion can be extended to a more general process involving any number of initial and final state fermions [88], but for simplicity we only consider one electron in each state. The amplitude for this process we call $M^{(\Lambda)}$. The effect of n soft virtual and N real soft emitted photons on the amplitude will now be considered. The number, N , of soft photons emitted is related to the number of virtual soft photons by $N = 2n$.

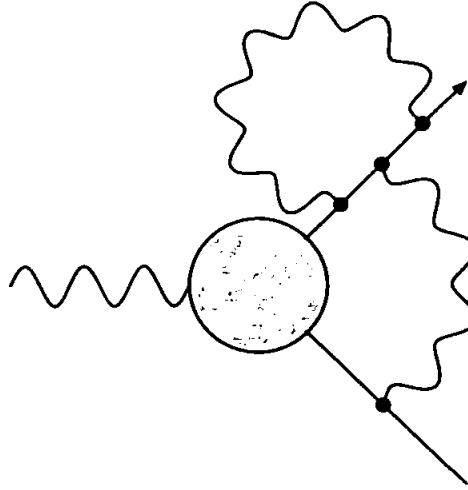


Fig. 4.8: Example virtual photon contribution

Soft Virtual Photons

Virtual soft photons also contribute to the amplitude, an example process is shown in figure 4.8. Let q be the momentum of each of the n virtual photons. Since loop momentum is integrated over there is no need to use a different symbol for each virtual momenta. The momenta in the virtual loops must be constrained because later in the calculation virtual and emission processes are going to be combined. Therefore it is necessary that the virtual momenta is not so large that the eikonal approximation (4.10) is invalid. This leads to an upper limit Λ for the virtual photon's momentum, Λ is arbitrary so observable quantities may not depend upon it. For the time being we regulate the infrared divergence with a small photon mass λ [88, 93], therefore $\lambda \leq q \leq \Lambda$. When the virtual and emission processes are combined the λ dependence will be removed so we can set the photon mass to be zero again.

For each virtual photon the amplitude is modified by a photon propagator factor

$$\frac{-ig_{\mu\nu}}{q^2 + i\varepsilon}, \quad (4.37)$$

and new electron propagators. At each order of perturbation theory there are many

different virtual processes that can contribute to the amplitude. Some combinatorics must be done to evaluate the number of ways we can link the $2n$ interaction vertices. There are $2n$ ways to choose the first vertex and $2n - 1$ ways to link it to another vertex, there are now $2n - 2$ remaining vertices to choose to link to another vertex, etc. A factor of $(2n)!$ is obtained. However, some of these factors reproduce equivalent diagrams, so we have over-counted. It does not matter which vertex we choose first, we still get the same diagram which leads to a $1/2^n$ factor. It also does not matter which way the lines are chosen. Swapping the photon propagator lines makes no difference and removing this over-counting give a factor of $1/n!$. This leaves

$$\frac{(2n)!}{2^n n!}. \quad (4.38)$$

different virtual diagrams. The $(2n)!$ factor is absorbed into the soft emission process. The total effect on the amplitude at all orders for n soft virtual photons is

$$M^{(\lambda)} = M^{(\Lambda)} \sum_{r=1}^n \frac{-ie^{2r}}{2^r r!} \left[\int_{\lambda}^{\Lambda} \frac{d^4 q}{q^2 + i\varepsilon} \left(\frac{p^\mu}{p \cdot q - i\varepsilon} - \frac{p'^\mu}{p' \cdot q + i\varepsilon} \right) \left(\frac{p_\mu}{-p \cdot q - i\varepsilon} - \frac{p'_\mu}{-p' \cdot q + i\varepsilon} \right) \right]^r. \quad (4.39)$$

Several comments are in order. The amplitude $M^{(\lambda)}$ includes soft and hard virtual photons and $M^{(\Lambda)}$ is the amplitude where soft virtual photons are neglected (i.e. figure 4.7). For electron self-energy diagrams the mass-shift effect is not being taken into account, since it is infrared finite in four dimensions, but the field strength renormalisation is included. This has the effect of replacing a $(p^2 - m^2)^{-1}$ propagator with an extra $(p \cdot q)^{-1}$ propagator. Therefore the fermion pole structure above is formed. In the second set of brackets there is a factor of $-p \cdot q$ because the photon is absorbed on this electron leg. Note that the effect of the virtual photons may be

exponentiated

$$M^{(\lambda)} = M^{(\Lambda)} \exp \left[+\frac{ie^2}{2} \int_{\lambda}^{\Lambda} \frac{d^4 q}{q^2 + i\varepsilon} \left(\frac{p^\mu}{p \cdot q - i\varepsilon} - \frac{p'^\mu}{p' \cdot q + i\varepsilon} \right) \right. \\ \left. \left(\frac{p_\mu}{-p \cdot q - i\varepsilon} - \frac{p'_\mu}{-p' \cdot q + i\varepsilon} \right) \right]. \quad (4.40)$$

These integrals in (4.40) may be evaluated, for q_0 the method of residues must be used. Details of this calculation can be found in [88] which finds the amplitude

$$M^{(\lambda)} = M^{(\Lambda)} \left(\frac{\lambda}{\Lambda} \right)^{\frac{A(p \rightarrow p')}{2}} \quad \text{where} \quad A(p \rightarrow p') = \frac{e^2}{4\pi^2} \left[\frac{1}{|\beta|} \ln \left(\frac{1 + |\beta|}{1 - |\beta|} \right) - 2 \right]. \quad (4.41)$$

Here β is the relative velocity between the in-state and out-state fermions and $0 \leq \beta \leq 1$. The function $A(p \rightarrow p')$ is positive for all $|\beta|$. This can be squared up so that at the level of the cross-section

$$\left(\frac{d\sigma}{d\Omega} \right)_{\text{virt}}^{(\lambda)} = \left(\frac{d\sigma}{d\Omega} \right)^{(\Lambda)} \left(\frac{\lambda}{\Lambda} \right)^{A(p \rightarrow p')}. \quad (4.42)$$

This formula is surprising because the NLO virtual processes cross-section (4.8) diverges, but at all orders as $\lambda \rightarrow 0$ the virtual contribution to the cross-section vanishes. The effect of the infrared on soft virtual particles at all orders is very different compared to the 1 loop calculation studied in section 4.2.

Soft Emission and Singularity Cancellation

As we saw in section 4.3 the eikonal approximation drops some next to leading order collinear divergences but reproduces all soft and regular $\ln^2(m)$ collinear divergences. It is an useful approximation if the theory we are studying only contains massive charges so that only soft singularities are present. As discussed soft divergences and leading order collinear divergences are spin independent but the $\ln(m)$ terms may be

spin dependent.

Consider the emission of a soft photon with momentum k from the final state electron. The amplitude is modified by an additional vertex and electron propagator. Using the eikonal approximation (4.10) the modification to a spinor in the amplitude due to a soft photon emitted from the out-state electron line is simplified to

$$\bar{u}' \rightarrow -e\bar{u}' \frac{p^{\mu'}}{p' \cdot k + i\varepsilon}. \quad (4.43)$$

Next, assume a soft photon is emitted from the 'in' state. The effect is similar but there is a sign difference in the propagator $(-p \cdot k + i\varepsilon)^{-1} = -(p \cdot k - i\varepsilon)^{-1}$. The amplitude, including all virtual processes, is modified for a single soft emission by

$$M^{(\lambda)\mu} \rightarrow eM^{(\lambda)} \left(\frac{p^\mu}{p \cdot k - i\varepsilon} - \frac{p^{\mu'}}{p' \cdot k + i\varepsilon} \right). \quad (4.44)$$

Here we have neglected the photon polarisation vector which will be reinstated later. This equation is spin independent and is manifestly gauge invariant. It can be shown [88], by induction, that the effect of adding more photons is to multiply the amplitude by a factor proportional to the object in brackets, i.e.

$$M^{(\lambda)\mu} \rightarrow M^{(\lambda)} e^N \prod_{r=1}^N \left(\frac{p^{\mu_r}}{p \cdot k_r - i\varepsilon} - \frac{p^{\mu'_r}}{p' \cdot k_r + i\varepsilon} \right), \quad (4.45)$$

is the amplitude at order N where $N \geq 0$. These must be summed up so that to all orders the amplitude is

$$M^{(\lambda)\mu} \rightarrow M^{(\lambda)} \sum_{N=0}^{\infty} e^N \prod_{r=1}^N \left(\frac{p^{\mu_r}}{p \cdot k_r - i\varepsilon} - \frac{p^{\mu'_r}}{p' \cdot k_r + i\varepsilon} \right). \quad (4.46)$$

The amplitude must be multiplied by the photon polarisation vector.

In (4.45) the photons emitted are soft since the eikonal approximation has

been used. However we did not discuss the experimental resolution required for this process to be degenerate with tree-level Coulomb scattering. There are two ways a photon could be detected by an experiment. The experiment could have photon detectors with resolution Δ_{out} . Therefore soft photons must have an energy $\omega_r \leq \Delta_{\text{out}} \forall r$. An experiment could also indirectly detect a photon through its measurement of the electron's energy. If the detector can measure a shift in the electron energy of $\Delta_{T_{\text{out}}}$ then this puts an upper limit on the total energy contained in soft photons $\sum_r \omega_r \leq \Delta_{T_{\text{out}}}$. To simplify this calculation we assume $\Delta_{\text{out}} = \Delta_{T_{\text{out}}}$; see [88] for the more general result⁵. These energy constraints must be incorporated into (4.46) at the level of the cross-section.

Contract each of the N real soft photons in (4.45) with their polarisation vector $\epsilon_\mu(k_i) = \epsilon_{\mu_i}$ and square up so we have a cross-section contribution

$$\left(\frac{d\sigma}{d\Omega}\right)^{(\lambda)} = \left(\frac{d\sigma}{d\Omega}\right)_{\text{virt}}^{(\lambda)} \sum_{N=0}^{\infty} e^{2N} \prod_{r,s=1}^N \left(\frac{p^{\mu_r}}{p \cdot k_r} - \frac{p'^{\mu_r}}{p' \cdot k_r} \right) \epsilon_{\mu_r} \left(\frac{p^{\nu_s}}{p \cdot k_s} - \frac{p'^{\nu_s}}{p' \cdot k_s} \right) \epsilon_{\nu_s}^* . \quad (4.47)$$

Here $(d\sigma/d\Omega)_{\text{virt}}^{(\lambda)}$ includes the tree-level process and all possible virtual effects, soft and hard. The remaining factors on the right hand side of (4.47) comprise the effect of the real soft photons. The polarisation sum may now be evaluated, (4.12) becomes $\sum_{\text{pols}} \epsilon_{\mu_i} \epsilon_{\nu_j}^* = -g_{\mu_i \nu_j}$, due to the manifest gauge invariance in (4.47). This leads to a factor of $(-1)^N$ in the cross-section depending on whether an even or odd number of polarisation sums are evaluated. The indexes r and s are just dummy variables and can be set equal to each other. Include a factor of $1/N!$ because we have counted permutations of N soft photons which we cannot distinguish between experimentally in the cross-section. Finally we integrate over all possible momenta for the emitted

⁵ During chapter 6 we will see that, for the cancellation of collinear singularities, it is important not to let $\Delta_{\text{out}} = \Delta_{T_{\text{out}}}$. Here we can let $\Delta_{\text{out}} = \Delta_{T_{\text{out}}}$ because it will not modify any conclusions we draw.

photons which yields

$$\left(\frac{d\sigma}{d\Omega}\right)^{(\lambda)} = \left(\frac{d\sigma}{d\Omega}\right)_{\text{virt}}^{(\lambda)} \sum_{N=0}^{\infty} \frac{(-1)^N e^{2N}}{N!} \prod_{r=1}^N \int \frac{d^3\mathbf{k}_r}{2\omega_r} \left(\frac{\mathbf{p}}{\mathbf{p} \cdot \mathbf{k}_r} - \frac{\mathbf{p}'}{\mathbf{p}' \cdot \mathbf{k}_r} \right)^2. \quad (4.48)$$

The angular integrals are the same as those encountered for soft virtual processes and may be evaluated (see [88] for details). We find that

$$\left(\frac{d\sigma}{d\Omega}\right)^{(\lambda)} = \left(\frac{d\sigma}{d\Omega}\right)_{\text{virt}}^{(\lambda)} \sum_{N=0}^{\infty} \frac{A(p \rightarrow p')^N}{N!} \int_{\lambda}^{\Delta_{\text{out}}} \prod_{r=1}^N \frac{d\omega_r}{\omega_r}, \quad (4.49)$$

so the logarithmic infrared divergence can be seen explicitly in each of the final integral products.

Each photon has been restricted to have energy less than Δ_{out} in (4.49), but $\sum_r \omega_r \leq \Delta_{\text{out}}$ has not been imposed. To incorporate this restriction we include a step function of the form

$$\theta\left(\Delta_{\text{out}} - \sum_r \omega_r\right) = \frac{1}{\pi} \int_{-\infty}^{\infty} du \frac{\sin(\Delta_{\text{out}} u)}{u} e^{iu \sum_r \omega_r}, \quad (4.50)$$

in (4.49). This gives us

$$\begin{aligned} \left(\frac{d\sigma}{d\Omega}\right)^{(\lambda)} &= \left(\frac{d\sigma}{d\Omega}\right)_{\text{virt}}^{(\lambda)} \left(\frac{1}{\pi} \int_{-\infty}^{\infty} du \frac{\sin(\Delta_{\text{out}} u)}{u} \right) \\ &\quad \times \left(\sum_{N=0}^{\infty} \frac{A(p \rightarrow p')^N}{N!} \int_{\lambda}^{\Delta_{\text{out}}} \prod_{r=1}^N \frac{d\omega_r}{\omega_r} e^{iu \sum_r \omega_r} \right), \end{aligned} \quad (4.51)$$

where the r index is a dummy variable so we replace ω_r with ω . The expression in the second set of brackets may be exponentiated

$$\left(\frac{d\sigma}{d\Omega}\right)^{(\lambda)} = \left(\frac{d\sigma}{d\Omega}\right)_{\text{virt}}^{(\lambda)} \left(\frac{1}{\pi} \int_{-\infty}^{\infty} du \frac{\sin(\Delta_{\text{out}} u)}{u} \right) \exp \left(A(p \rightarrow p') \int_{\lambda}^{\Delta_{\text{out}}} \frac{d\omega}{\omega} e^{iu\omega} \right). \quad (4.52)$$

Using a trick (see [88]) these integrals may be evaluated. The cross-section result,

for $\Delta_{\text{out}} = \Delta_{T_{\text{out}}}$ is

$$\left(\frac{d\sigma}{d\Omega}\right)^{(\lambda)} = \left(\frac{d\sigma}{d\Omega}\right)_{\text{virt}}^{(\lambda)} \left(\frac{\Delta_{\text{out}}}{\lambda}\right)^{A(p-p')}. \quad (4.53)$$

This formula has an infrared divergence as $\lambda \rightarrow 0$. Cancelling the infrared divergence with soft virtual photons (4.42) the λ dependence is removed and

$$\left(\frac{d\sigma}{d\Omega}\right)^{(\lambda)} = \left(\frac{d\sigma}{d\Omega}\right)^{(\Lambda)} \left(\frac{\Delta_{\text{out}}}{\Lambda}\right)^{A(p-p')}. \quad (4.54)$$

Taking $\Delta_{\text{out}} \rightarrow 0$ is equivalent to not allowing any processes with soft photons emitted to contribute to the total cross-section for Coulomb scattering which, as we can see from (4.54), vanishes. This is also true for a more general process with any number of initial and final state fermions [88, 93]. If you exclude the possibility of emitting any soft photons then there is zero probability of scattering occurring. Of course for any real experiment $\Delta_{\text{out}} \neq 0$. As required the right hand side of (4.54) is independent of Λ since $(d\sigma/d\Omega)^{(\Lambda)} \propto \Lambda^A$.

According to the LSZ formalism for scattering we measure the final state at time $t = +\infty$. For each period of time there is a finite probability of emitting a soft photon. During the infinite amount of time before the electron is theoretically measured an electron will always emit a soft particle. Therefore it seems physically intuitive that the theoretically predicted cross-section should vanish as $\Delta_{\text{out}} \rightarrow 0$. It has been shown that during the interaction of a charge with a classical current an infinite number of soft photons are produced [83, 94].

5. LEE-NAUENBERG FOR SOFT AND REGULAR COLLINEAR INFRARED DIVERGENCES

We return now to the stage in the argument reached at the end of section 4.3. Here we concluded that the failure to remove all divergences through a combination of Bloch-Nordsieck and Lee-Nauenberg did not mean that the Lee-Nauenberg proposition failed. It only means that the way in which we applied the theorem was not successful, therefore we will now use the theorem differently. The Lee-Nauenberg theorem claims that when one considers *all* degenerate processes all types of infrared divergences (soft, regular collinear and Δ) cancel. A process can be considered as degenerate with Coulomb scattering if it contains the tree-level scattering plus the emission/absorption of any number of soft or semi-hard collinear photons. Because any additional soft photon is degenerate to Coulomb scattering this will lead to some rather unfamiliar disconnected processes being considered. Disconnected processes are an essential part of the Lee-Nauenberg theorem [5] and have been considered by a variety of authors [10, 75–77, 95–97]. This leads to some success when combining the soft and collinear divergences but also raises some questions. Lavelle and McMullan presented an alternative approach for applying the Lee-Nauenberg proposition to Coulomb scattering and during the course of this chapter their approach will be reviewed [10].

Throughout this chapter the soft divergences will be evaluated at NLO in perturbation theory. The aim is to discover a way to cancel the soft divergences without spoiling the cancellation of the regular collinear divergences. Full calculations will

not be given here but may be found in [10]. The methods used for these calculations are also contained in chapter 6, but there the emphasis will be on the Δ collinear divergences rather than soft singularities. Here we will simply outline the method used to calculate soft divergences, the results obtained in [10] and then draw conclusions. This will further motivate the need to carefully study Δ divergences using the approach taken by Lavelle and McMullan.

First we summarise the state of the calculation at the end of section 4.3. We applied a combination of the Bloch-Nordsieck method and the Lee-Nauenberg proposition. We considered soft plus semi-hard emission, semi-hard absorption and virtual processes. In order to remove Δ and regular collinear singularities we saw we must also consider soft absorption. Therefore we find the soft divergences do not cancel

$$\begin{aligned}
 & 2 \left(\text{diagram 1} + \text{diagram 2} \right) + \left| \text{diagram 3} \right|^2 + \left| \text{diagram 4} \right|^2 - \left| \text{diagram 5} \right|^2 = -\frac{1}{\epsilon_{\text{IR}}} + \frac{1}{\epsilon_{\text{IR}}} + \frac{1}{\epsilon_{\text{IR}}}. \quad (5.1)
 \end{aligned}$$

Absorption has re-introduced a soft divergence. No consistent approach can be found which cancels all infrared divergences for these degenerate processes. We have gone beyond the eikonal approximation for emission collinear with the out-state and absorption collinear with the in-state. Since the soft divergences have not been removed by considering only these degenerate processes we must look for other degenerate processes which contribute to the cross-section. As noted, in the discussion following (4.35), we have yet to consider soft emission collinear with the in-state and absorption collinear with the out-state. This omission will not prove to be important when considering only the soft singularities. However, these are considered

in chapter 6 when our attention shifts back to the Δ collinear divergences.

At NLO, it is not obvious that there are any other processes which contribute to the cross-section. However, we have only considered processes with either initial or final state degeneracies. It is possible to consider a process with both types of degeneracies contributing. Consider the case when a photon is *both* emitted and absorbed displayed in figure 5.1. The unusual thing about this process is that to contribute to the cross-section at order e^4 , we need these emitting and absorbing processes (which are already at order e^3) to interfere with a process of order e . Following [5], we consider the *disconnected* process shown in figure 5.2 where the in-coming electron is accompanied by a photon that does *not* interact with it

In order to contribute to the Coulomb scattering cross-section the disconnected photon must also be degenerate with the tree-level process. It cannot be collinear with both the initial and final state particle. Therefore it must be a soft photon so that its momentum is less than the experimental resolution.

The Feynman rule associated with the disconnected process is also given in figure 5.2. The interference effect between the processes displayed in figures 5.1 and 5.2 leads to a soft infrared divergence which may be calculated by using the eikonal approximation (4.10). The technical details of this calculation may be found in [10] where it is shown that

$$2 \left(\text{diagram 1} + \dots \cdot \text{diagram 2} \right) = -\frac{2}{\epsilon_{\text{IR}}}. \quad (5.2)$$

Since these are interference terms we multiply by a factor of 2. Label this contribution to the cross-section $P_{1,1}$. We define $P_{n,m}$ as the cross-section contribution to Coulomb scattering from a degenerate processes which is accompanied by n degenerate photons in the initial state and m degenerate photons in the final state.

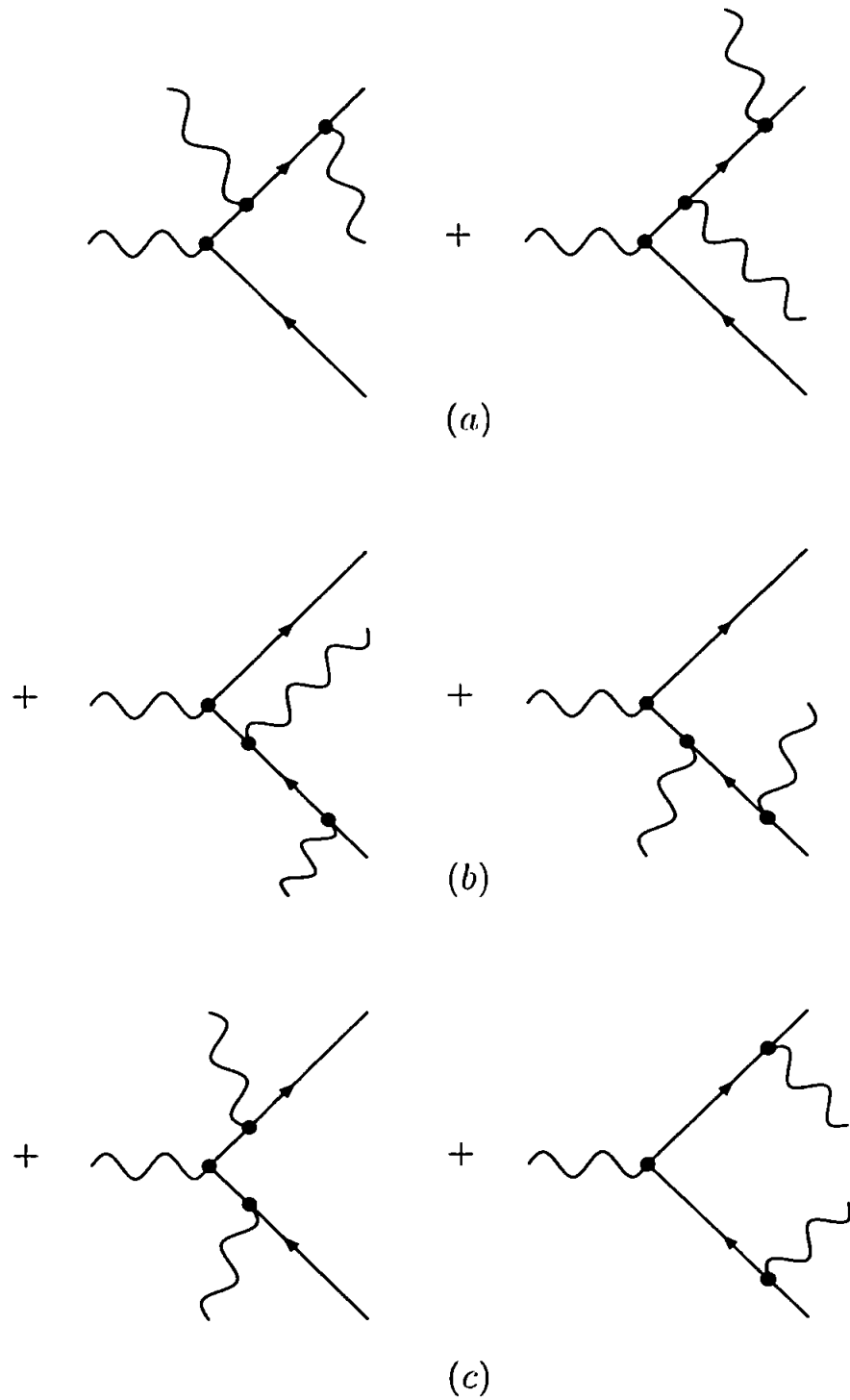


Fig. 5.1: Emission and absorption processes which we call $P_{1,1}$. Diagrams (a) represent emission and absorption on the final state electron, (b) on the initial state electron and (c) emission off one electron and absorption on the other.

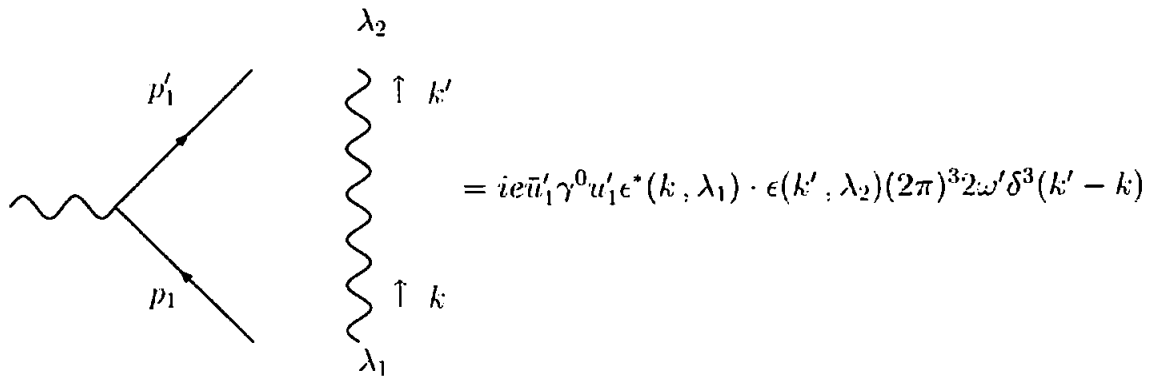
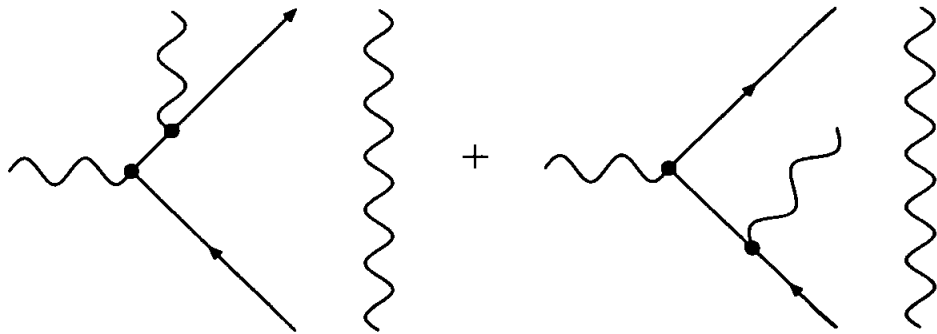


Fig. 5.2: Disconnected process and its associated Feynman rule


 Fig. 5.3: Emission combined with a disconnected photon – $P_{1,2}$

When we consider virtual ($P_{0,0}$), emission ($P_{0,1}$), absorption ($P_{1,0}$) and $P_{1,1}$ processes there remains an overall infrared singularity, $-1/\epsilon_{\text{IR}}$. Therefore we must look for another degenerate process. Now that we have begun including disconnected processes there is no reason not to consider the disconnected and emission process which is displayed in figure 5.3. There is one photon in the initial state and two in the final state, so the cross-section contribution is labelled $P_{1,2}$. Once again the disconnected photon must be soft because it cannot be collinear with both the initial and final state particles. By squaring up this diagram we get a cross-section contribution at NLO. The calculation details may be found in [10] and chapter 6, the result for the soft divergence is

$$\left| \begin{array}{c} \text{Diagram 1} \\ \text{Diagram 2} \end{array} \right|^2 = + \frac{1}{\epsilon_{\text{IR}}} . \quad (5.3)$$

It is important to note that we only consider fully connected diagrams¹. Using all these processes soft infrared divergences can be removed.

Thus we have seen it is possible to remove soft divergences when considering the combination of $P_{0,0}$, $P_{0,1}$, $P_{1,0}$, $P_{1,1}$ and $P_{1,2}$. However, we have not considered the collinear divergences – regular or Δ types. We will now consider the regular collinear divergences and leave the Δ collinear singularities for the next chapter. We have argued that disconnected photons must be soft. We will see, in the following chapter, that since only the fully connected diagrams are considered all the photons contained in the $P_{1,1}$ and $P_{1,2}$ processes must be soft. Therefore they will not produce any regular collinear divergences. We obtain semi-hard collinear divergences from Bloch-Nordsieck processes (4.32), semi-hard emission (4.29) and

¹ We follow the lead set by Lee-Nauenberg who omit vacuum bubble contributions to the cross-section once the photons have been contracted to one another. Further discussion on connecting diagrams is contained within chapter 6 and [10].

semi-hard absorption also contributes a factor of (4.29). During the section 4.3 we concluded that the regular collinear divergences are removed via this combination. The Lee-Nauenberg proposition can successfully remove soft singularities and regular collinear divergences when considering the processes discussed in this chapter. This is more consistent than the approach taken within [5]. Specifically we do not only have to consider semi-hard absorption which, as we saw in section 4.3, leads to overall Δ collinear divergences at the level of the cross-section. Lavelle and McMullan's approach has yielded some success. We have found a better approach to the infrared but there are many questions which still remain. During the remainder of this chapter the questions raised by the disconnected photons and the Δ collinear divergences are discussed.

We included the emission + disconnected process $P_{1,2}$ represented in figure 5.3 but we did not take into account an absorption + disconnected, $P_{2,1}$ process which is displayed in figure 5.4. The $P_{2,1}$ process is the complex conjugate of the $P_{1,2}$ diagrams so it will have the same probability of occurring. Without this process our cancellation is unbalanced between emission and absorption which conflicts with our intuition. However, $P_{2,1}$ is not included in the discussion because it would re-introduce soft divergences. But, $P_{2,1}$ is degenerate with tree-level Coulomb scattering if all the photons are soft, so according to the Lee-Nauenberg theorem (which states we should include *all* degenerate processes) this process should be considered and we will obtain an overall infrared divergence. By following this path onto its logical conclusion we can go on to argue that if we allow one disconnected photon, why not allow two, three or n ? The disconnected photons do not add additional vertices to Feynman diagrams so these are all valid processes at NLO in perturbation theory. The introduction of disconnected processes leads to an infinite number of diagrams at each order of perturbation theory. Usually disconnected diagrams are not considered. However, as we have seen without them there is no way to consistently remove

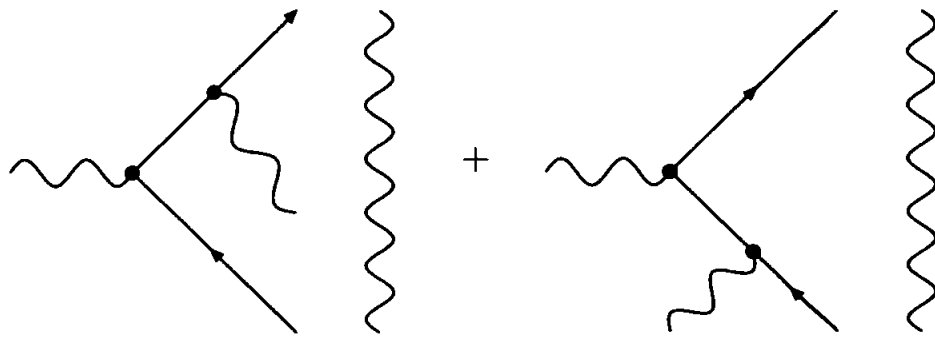


Fig. 5.4: Absorption combined with a disconnected photon – $P_{2,1}$

soft and collinear divergences for processes with initial and final state degeneracies, so they are an essential part of the Lee-Nauenberg theorem. Therefore we must accept this infinitely long divergent series at each order of perturbation theory. Lee-Nauenberg state that they do not address the convergence of this series but a discussion of this can be found in [10, 95]. In practice when we do calculations we simply stop at a finite point. We add degenerate processes until the overall result is infrared finite then stop – as we did in this chapter. To go any further would re-introduce soft divergences. If the cross-section is infrared finite the regular and Δ collinear divergence must cancel in the same way as soft singularities.

By adding more and more disconnected photons a pattern emerges for the cancellation of soft divergences. Our discussion involving one disconnected photon shows that the virtual process $P_{0,0}$ is cancelled by the emission process $P_{0,1}$ through the Bloch-Nordsieck mechanism and the absorption process $P_{1,0}$ is cancelled by the processes $P_{1,1}$ and $P_{1,2}$. That is,

$$0 = -1 + 1 + 1 - 2 + 1 = \underbrace{-1 + 1}_{\text{Bloch-Nordsieck}} + \underbrace{1 - 2 + 1}_{\text{Lee-Nauenberg}} . \quad (5.4)$$

The Lee-Nauenberg proposition requires us to sum over *all* degeneracies. It will be shown in chapter 6 that as far as the soft infrared poles are concerned, we have the

identities:

$$P_{n,n+1} = P_{0,1} \quad P_{n+1,n+1} = P_{1,1} \quad \text{and} \quad P_{n+1,n} = P_{1,0}. \quad (5.5)$$

Here the number of disconnected photons, $n \geq 0$, and we omit vacuum bubble diagrams. The generalisation of (5.4) to an arbitrary number of disconnected photons is then

$$P_{0,0} + P_{0,1} + \sum_{a=1}^{\infty} (P_{a,a-1} + P_{a,a} + P_{a,a+1}). \quad (5.6)$$

It can be seen that there are several points in this series where soft divergences are removed. No factor is present which suppresses processes with more than one disconnected photon in (5.5) so the series in (5.6) does not converge. This was the conclusion reached by Lavelle and McMullan in [10].

We have not discussed the Δ collinear divergences. These did not get removed via the approach taken by Lee and Nauenberg discussed in section 4.3. Here, following the approach taken by Lavelle and McMullan, we have included many more processes with disconnected photons that can only be soft. If these soft photons are also collinear then they will produce Δ divergences. There cannot be any corresponding semi-hard disconnected processes which are degenerate with Coulomb scattering. If the cross-section is to be infrared finite these divergences must also cancel at the same point as the soft and regular collinear divergences in the series (5.6). If they cancel at a different point then the cross-section would be soft divergent again. Lavelle and McMullan did not consider the Δ divergences. In the following chapter they will be considered using the processes contained in the series (5.6). Our aim is to discover whether the cross-section is simultaneously soft and collinear finite.

6. Δ COLLINEAR DIVERGENCES AND LEE-NAUENBERG THEOREM

Throughout part II of this thesis we have examined how soft and collinear infrared divergences are dealt with. This material will now be summarised. We have shown that interactions with photons which are *both* soft and collinear generate a class of collinear divergences of the form $\Delta^n \ln(m)$ and $\ln(\Delta) \ln(m)$. Here Δ is the experimental energy resolution and $n > 0$. This class of singularities are referred to as Δ divergences. For a real experiment, the detector's energy resolution will not necessarily be the same for both 'in' and 'out' state particles. This leads to two resolutions Δ_{in} and Δ_{out} .

There are various responses to soft and collinear divergences. However, an often used approach – going at least as far back as the initial paper by Lee and Nauenberg [5] – is to add sufficient degenerate processes so that one obtains a finite answer. It is not generally clear why one should not include further degenerate processes and questions of convergence are rarely addressed (see, e.g. [10]).

In their original paper [5] Lee and Nauenberg *assume* that all soft divergences are removed by summing over soft emission, i.e. they follow Bloch-Nordsieck. To remove the residual collinear divergences they sum over the emission of a semi-hard photon which is collinear with the out-going electron. Semi-hard photons possess energy in between the detector resolution Δ_{out} and the total energy experimentally observed E . Soft photons are not added again as this would be double counting.

Only half of the regular collinear divergences¹ are eliminated so the absorption of semi-hard photons are also considered. However, we saw in section 4.3 that the Δ collinear divergences lead to an inconsistency in the infrared cancellation. If one only includes semi-hard absorption, which has the minimum energy Δ_{in} , we are left with Δ_{in} collinear divergences. To eliminate these we must also account for the possibility of soft photon absorption. However, by removing the energy cut off Δ_{in} , we re-introduce the soft divergence. By involving just these degenerate processes the cross-section for Coulomb scattering is divergent.

We came to the conclusion that we must be using the Lee-Nauenberg theorem in the wrong way. Therefore we changed our approach and applied Lee-Nauenberg to all infrared divergences, not just collinear. In chapter 5 this approach led to some success. Soft and regular collinear infrared divergences can be removed in a consistent manner. However, in order to achieve this success we must introduce disconnected degenerate processes and we have not considered the Δ collinear divergences. We have argued that, in order to obtain a finite cross-section, the Δ divergences must cancel through the same degenerate processes required for the removal of soft and regular collinear divergences. During this chapter we will check whether the cross-section is in fact an infrared safe quantity or whether it will always contain some sort of infrared divergence irrespective of how many degenerate processes are taken into account.

We will continue using Coulomb scattering as our concrete example to display the Lee-Nauenberg proposition in action. We will show that there are more Δ divergences which come from the processes considered in figures 5.1, 5.2 and equation (5.1). We will check to see if they cancel by calculating the Δ divergences for emission, absorption, $P_{1,1}$ and processes with more disconnected photons, $P_{n,m}$. Virtual loops do not include the energy cut-off Δ so they cannot generate Δ

¹ We remind the reader that we use the term *regular collinear divergence* to mean terms $\mathcal{O}(\ln m)$ but not proportional to Δ .

divergences. If all infrared divergences cancel then we have found a finite point where it is mathematically appealing to stop considering additional degenerate processes. However, if they do not cancel through the same processes as the soft singularities then the Coulomb scattering cross-section is infrared divergent.

6.1 Collinear Emission – $P_{0,1}$

Collinear with the out-state electron

A photon can be emitted collinear with the out-state electron off either the initial state or final state electron. We have argued, in section 4.3, that emission from the initial state electron collinear with the final state electron is not infrared divergent because it does not force an internal line of the Feynman diagram to be on-shell. Therefore we only consider the diagram represented by figure 4.4. This process has previously been evaluated and we found that it contributes a factor of (4.28). Note that in (4.28) we only allowed the photon to be semi-hard and this led to Δ divergences in (4.29). These delta divergences are easily removed in the current calculation because soft photon emission is also considered. The photon's energy integration limits for soft emission can be combined with the limits in (4.28) to give

$$\int_{\Delta_{\text{out}}}^E d\omega' + \int_0^{\Delta_{\text{out}}} d\omega' = \int_0^E d\omega'. \quad (6.1)$$

This removes all delta dependence from this process. The upper integral limit is the electron's energy E and this produces regular collinear divergences. The eikonal approximation (4.10) throws away Δ collinear divergences so we do not use this for all photons considered in this chapter. We have seen that processes in which the photons can be both soft and semi-hard do not produce Δ divergences.

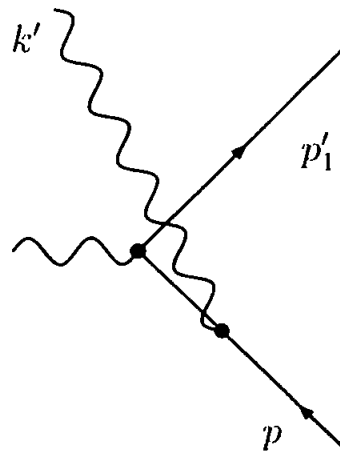


Fig. 6.1: Emission of a photon by the in-state electron which is collinear with the in-state electron

Collinear with the in-state electron

Consider the process displayed in figure 6.1 where a photon is emitted from the in-state collinear with the in-state. One could also consider an emission process from the out-state collinear with the in-state. However, this would not cause a collinear divergence since it does not force an internal propagator to go on-shell. The emitted photon is not collinear with the final state electron so, unless it is soft, it will be detected. Therefore, to contribute to Coulomb scattering, the photon must be soft. In the cross-section we can only integrate over the photon's energy up to Δ_{out} therefore we will discover Δ_{out} divergences which, until now, have never been considered.

Retaining only singular terms the cross-section contribution for the process displayed in figure 6.1 will now be evaluated. The S -matrix element is

$$+i \frac{e^2}{2p \cdot k'} \bar{u}'_1 \gamma^0 (2p \cdot \epsilon^{*'} - \not{k}' \not{\epsilon}^{*'}) u, \quad (6.2)$$

where the Dirac equation has already been used. Squaring up and evaluating spin

traces we find

$$\frac{e^4}{(p \cdot k')^2} \left[4(p \cdot \epsilon')(p \cdot \epsilon^*)(\tilde{p}'_1 \cdot p - \tilde{p}'_1 \cdot k') + 2(p \cdot k')\{(p \cdot \epsilon')(\tilde{p}'_1 \cdot \epsilon^*) + (p \cdot \epsilon^*)(\tilde{p}'_1 \cdot \epsilon')\} - 2(\epsilon' \cdot \epsilon^*)(\tilde{p}'_1 \cdot k')(p'_1 \cdot k') \right]. \quad (6.3)$$

It is important to note that we have omitted $\mathcal{O}(k' \cdot \epsilon')$ in (6.3). This is because when k' is dotted into the polarisation sum (4.12) it vanishes. Photon polarisations must be summed over which yields

$$\frac{e^4}{p \cdot k'} |\bar{u}'_1 \gamma^0 u|^2 \left(\frac{2E}{\omega'} - 2 + \frac{\omega'}{E} \right). \quad (6.4)$$

Here we have used the collinear approximations, discussed in appendix E, to write the collinear finite term

$$k' \cdot \tilde{p}'_1 = p \cdot \tilde{p}'_1 \frac{\omega'}{E}. \quad (6.5)$$

The same energy weighting factor used for equation (4.26) is applied which multiplies the cross-section by the factor of E'_1/E . The spinors may be re-expressed as

$$|\bar{u}'_1 \gamma^0 u|^2 = \frac{E'_1}{E} |\bar{u}' \gamma^0 u|^2. \quad (6.6)$$

Overall the Bethe-Heitler energy weighted cross-section may be written as

$$\frac{e^4}{p \cdot k'} |\bar{u}' \gamma^0 u|^2 \frac{E'^2_1}{E^3 \omega'} (E^2 + E^2_1). \quad (6.7)$$

This contribution to the cross-section, after integrating over a soft cone, will produce soft divergences and the new Δ_{out} collinear divergences. For the process of collinear emission off an in-coming electron the Δ divergences are *not* artifacts of an unphysical decomposition of the integration region but rather Δ_{out} plays the role of a physical cutoff which, as shown in section 4.4, is non-zero for any experiment. This integral

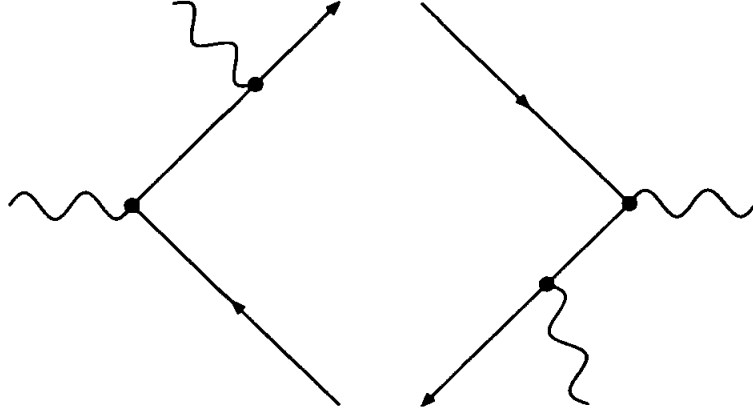


Fig. 6.2: Interference between emission by the in-state and out-state electrons

will be performed in section 6.6 after evaluating all other possible Δ divergences.

It is important for what follows to observe that interference between emission off the in-coming and out-going fermions, displayed in figure 6.2, does not generate these new collinear divergent structures. This comment also holds for absorption (since it is just the complex conjugate of emission) and indeed for all other processes discussed in the remainder of this chapter. Cross-terms contain purely soft divergent contributions to the cross-section, which can be seen from the first term in brackets in (4.13). As we will see this difference between the production of soft and Δ divergences will be important when we form our conclusions.

6.2 Collinear Absorption – $P_{1,0}$

Collinear absorption on the in-coming electron leg as displayed in figure 4.5 can be soft or semi-hard and be degenerate to tree-level Coulomb scattering. It will not produce Δ divergences but, as seen in section 4.3, eliminates the regular collinear divergences from the cross-section. However, absorption collinear with the out-going electron, represented by figure 6.3, will produce new collinear divergences. The momentum associated with the in-coming electron in figure 6.3 is defined as $p_1 =$

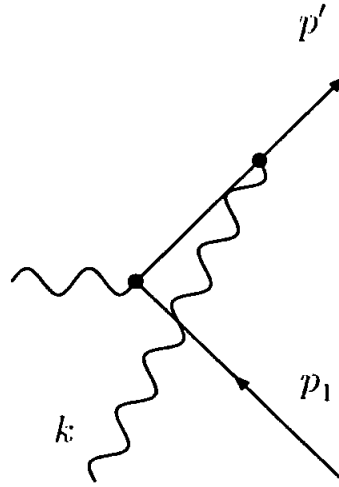


Fig. 6.3: Absorption collinear with the out-going electron

$p - k$. The absorbed photon must be soft otherwise it would be detected in the initial state and this process would not be degenerate with Coulomb scattering. Since this is an initial state degeneracy the energy cutoff is Δ_{in} .

The S -matrix element for the process of absorption on the in-coming electron leg is:

$$+i \frac{e^2}{2p' \cdot k} \bar{u}' (2p' \cdot \epsilon' - \not{\epsilon}' \not{k}') \gamma^0 u_1, \quad (6.8)$$

Comparing (6.8) with (6.2) it can be seen that the cross-section calculation will be almost equivalent because emission* = absorption. The final result can be derived following the same method (evaluating spin traces and polarisation sums) to find the cross-section contribution

$$\frac{e^4}{p' \cdot k} |\bar{u}' \gamma^0 u_1|^2 \left(\frac{2E'}{\omega} - 2 + \frac{\omega}{E'} \right). \quad (6.9)$$

If one were to exchange $E \leftrightarrow E'$, $\omega \leftrightarrow \omega'$ and the spinors then this is the same as (6.4). We are scattering off a heavy, static nucleus which takes away no energy so $E = E'$. The photon is soft and its energy is integrated over so ω' is a dummy variable and can easily be redefined as ω providing we still integrate up to energy

Δ_{in} . So (6.9) is actually equivalent to (6.4).

We must discuss the energy weighting that we apply for absorption. In the original derivation of the energy weighting Bethe and Heitler only consider the emission process [91]. They conclude that the cross-section should be multiplied by a factor of the energy in the out-going electron and divided by the energy in the in-coming electron. Their work, to the best of my knowledge, has never been extended to include absorption processes. However, we assume that the probability of an electron emitting or absorbing a photon should be the same². Therefore after the cross-section is energy weighted we should obtain the same contribution from emission and absorption. In order to achieve this we must apply an *inverted energy weighting* for absorption which is defined as electron energy in divided by electron energy out. For $P_{1,0}$ this yields a factor of:

$$\frac{E_1}{E'} . \quad (6.10)$$

Note that the energy weighting in equation (4.26) did not modify the soft or $\ln \Delta$ collinear divergences, but it does modify the Δ^n terms. Since Δ divergences are not usually considered in the literature this issue has not received a great deal of attention, but it is discussed in [78, 98]. The spinors are related by

$$|\bar{u}' \gamma^0 u_1|^2 = \frac{E_1}{E} |\bar{u}' \gamma^0 u|^2 , \quad (6.11)$$

and the inverted energy weighting will lead to the same contribution as (6.7):

$$\frac{e^4}{p' \cdot k} |\bar{u}' \gamma^0 u|^2 \frac{E_1^2}{E'^3 \omega} (E'^2 + E_1^2) . \quad (6.12)$$

The only difference between emission and absorption is that here we must integrate

² In the literature it is always assumed that the background is in equilibrium.

over a soft cone which has the upper limit Δ_{in} instead of Δ_{out} .

An alternative energy weighting would make it impossible to remove Δ^n divergences. If, for instance, we applied the same energy weighting as we did for the case of emission we would obtain a factor of E/E_1 . Instead of (6.12) we would find

$$\frac{e^4}{p' \cdot k} |\bar{u}' \gamma^0 u|^2 \frac{1}{E' \omega} (E'^2 + E_1^2) . \quad (6.13)$$

This is a linear expression in ω but (6.7) is a cubic equation for ω' . Therefore, after doing an integral over the photon energies we would have different powers for Δ^n and no cancellation would be possible.

Now we will proceed by calculating the Δ divergences for all the other $P_{n,m}$ processes in order to attempt to cancel them.

6.3 Collinear Emission and Absorption – $P_{1,1}$

We consider the $P_{1,1}$ process which is an interference effect between figures 5.1 and 5.2. We have previously argued that, since the disconnected photon cannot be collinear with both the initial and final state particle, it must be a soft photon. For the time being all we can say about the disconnected photon's upper energy limit is that it is soft, but we will return to this point later.

Initially we consider only the (b)-type emission and absorption diagrams displayed in figure 5.1 and label the momenta for these processes as in figure 6.4. However, we will show that the diagrams in figure 5.1(a) produce similar Δ divergences. As mentioned in section 6.1, it can also be shown that the diagrams in figure 5.1(c) do not produce any Δ divergences but this will not be proven here. Contract the diagrams in figure 6.4 with the complex conjugate of the disconnected process which is displayed in figure 5.2 along with the associated Feynman rule. The cross-section

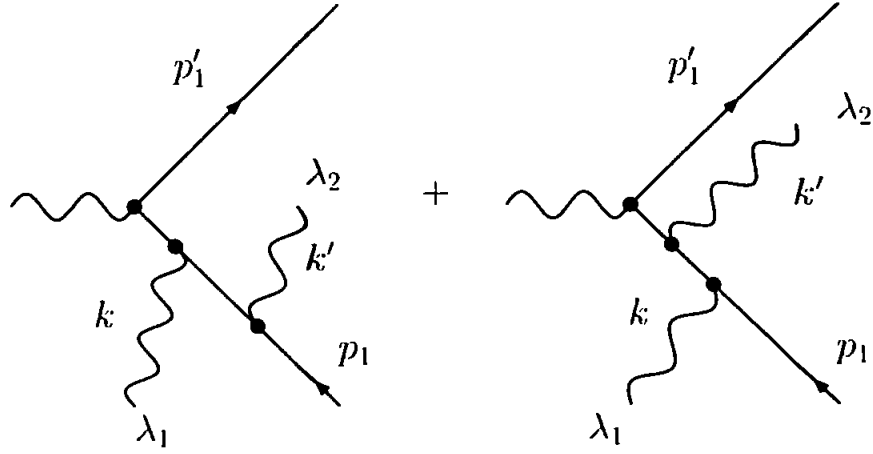


Fig. 6.4: Emission and absorption by the in-state electron

contribution is

$$\begin{aligned}
 & 2 \frac{(2\pi)^3 (2\omega') e^4 \epsilon_1 \cdot \epsilon_2^* \delta^3(k - k')}{8[p_1 \cdot (k - k')](p_1 \cdot k)(p_1 \cdot k')} \bar{u}_1' \gamma^0 (\not{p}_1 + \not{k} - \not{k}') \\
 & \times \left\{ 2(p_1 \cdot k') \not{\epsilon}_2' (2p_1 \cdot \epsilon_1^* + \not{k} \not{\epsilon}_1^*) - 2(p_1 \cdot k) \not{\epsilon}_1^* (2p_1 \cdot \epsilon_2' + \not{k}' \not{\epsilon}_2') \right\} u_1 \bar{u}_1 \gamma_0 u_1'.
 \end{aligned} \tag{6.14}$$

Here we have simplified by using the Dirac equation. The shorthand notation $\epsilon_2^* = \epsilon^*(k', \lambda_2)$ is also introduced. It is important to keep track of the individual polarisations of the photons when we come to evaluate the polarisation sums. Terms with an odd number of gamma matrices will be dropped because they vanish when spin traces are evaluated.

The same calculatory steps as executed for $P_{0,1}$ and $P_{1,0}$ must be performed in order to calculate the final form of the cross-section. However, here it is considerably more difficult due to the extra complexity of (6.14) which may be seen by studying the possible divergences in (6.14). There are collinear divergences of the form $1/p_1 \cdot k$ and $1/p_1 \cdot k'$. A different divergence $1/p_1 \cdot (k - k')$ which has not been met until now prevents us from using the delta function in (6.14). We are only interested in collinear divergences, therefore we aim to extract the $1/p_1 \cdot (k - k')$ divergence from

the cross-section. This gives us a strategy with which to tackle the calculation of (6.14). To remove the $1/p_1 \cdot (k - k')$ divergence it helps to separate the calculation into two parts by splitting the $(\not{p}_1 + \not{k} - \not{k}')$ into \not{p}_1 and $(\not{k} - \not{k}')$ terms.

First consider the \not{p}_1 term which is proportional to:

$$\bar{u}_1' \gamma^0 \not{p}_1 \left\{ 2(p_1 \cdot k') \not{\epsilon}_2' \left(2p_1 \cdot \epsilon_1^* + \not{k} \not{\epsilon}_1^* \right) - 2(p_1 \cdot k) \not{\epsilon}_1^* \left(2p_1 \cdot \epsilon_2' + \not{k}' \not{\epsilon}_2' \right) \right\} u_1. \quad (6.15)$$

The \not{p}_1 can be commuted through the brackets in order to use the Dirac equation $\not{p}_1 u_1 = 0$. Then take \not{k} and \not{k}' terms to the right hand side of $\not{\epsilon}_1^*$ or $\not{\epsilon}_2'$ terms, neglecting terms $\mathcal{O}(k \cdot \epsilon_1^*)$ and $\mathcal{O}(k' \cdot \epsilon_2')$ because they will vanish when polarisation sums are evaluated. Then (6.15) becomes

$$\begin{aligned} \bar{u}_1' \gamma^0 \left[-8p_1 \cdot (k - k') (p_1 \cdot \epsilon_2') (p_1 \cdot \epsilon_1^*) - 8(p_1 \cdot k) (p_1 \cdot k') \epsilon_1^* \cdot \epsilon_2' \right. \\ \left. + 4p_1 \cdot (k - k') \left\{ p_1 \cdot \epsilon_2' \not{\epsilon}_1^* - p_1 \cdot \epsilon_1^* \not{\epsilon}_2' \right\} \not{k}' - 4p_1 \cdot k' \left\{ p_1 \cdot \epsilon_2' \not{\epsilon}_1^* - p_1 \cdot \epsilon_1^* \not{\epsilon}_2' \right\} (\not{k} - \not{k}') \right] u_1. \end{aligned} \quad (6.16)$$

Notice that for the first and third terms of (6.16) the $1/p_1 \cdot (k - k')$ divergence in (6.14) will be removed. In the second term both collinear divergent denominators have been removed by the $(p_1 \cdot k)(p_1 \cdot k')$ factor and we are just left with the $1/p_1 \cdot (k - k')$ divergence. Since we are only interested in collinear divergences we will drop the second term in (6.16) because it will not provide any of the Δ divergences. The final term is of the form $(\not{k} - \not{k}')$ so we combine it with the remaining terms in the cross-section (6.14).

Now move on to the second part of the cross-section and combine it with the

additional $(\not{k} - \not{k}')$ term from (6.16). This is

$$\begin{aligned} & \bar{u}'_1 \gamma^0 (\not{k} - \not{k}') \left\{ 2(p_1 \cdot k') \not{\epsilon}'_2 \left(2p_1 \cdot \epsilon_1^* + \not{k} \not{\epsilon}_1^* \right) - 2(p_1 \cdot k) \not{\epsilon}_1^* \left(2p_1 \cdot \epsilon'_2 + \not{k}' \not{\epsilon}'_2 \right) \right. \\ & \quad \left. + 4p_1 \cdot k' (p_1 \cdot \epsilon'_2 \not{\epsilon}_1^* - p_1 \cdot \epsilon_1^* \not{\epsilon}'_2) \right\} u_1 \\ & = \bar{u}'_1 \gamma^0 (\not{k} - \not{k}') \left\{ -4p_1 \cdot (k - k') p_1 \cdot \epsilon'_2 \not{\epsilon}_1^* + 2p_1 \cdot k' \not{\epsilon}'_2 \not{k} \not{\epsilon}_1^* + 2p_1 \cdot k \not{\epsilon}_1^* \not{k}' \not{\epsilon}'_2 \right\} u_1. \end{aligned} \quad (6.17)$$

In the first term the unexpected divergence has been removed. When the delta function in (6.14) sets $k = k'$ this term will vanish so we may neglect it from now on. Some terms which vanish under the photon polarisation sum have been dropped. It is now much more convenient to evaluate electron spin traces than at the initial stage (6.14). From (6.16) the trace from the third term yields

$$16p_1 \cdot (k - k') (p_1 \cdot k) \{ p_1 \cdot \epsilon'_2 \bar{p}'_1 \cdot \epsilon_1^* - p_1 \cdot \epsilon_1^* \bar{p}'_1 \cdot \epsilon'_2 \}. \quad (6.18)$$

The trace in the second and third term of (6.17) can be made easier by re-writing it as

$$2(p_1 \cdot k) \text{Tr} \left\{ \not{p}_1 \not{p}'_1 (\not{k} - \not{k}') \left(\not{\epsilon}'_2 \not{k} \not{\epsilon}_1^* - \not{\epsilon}_1^* \not{k}' \not{\epsilon}'_2 \right) \right\} - 2p_1 \cdot (k - k') \text{Tr} \left\{ \not{p}_1 \not{p}'_1 (\not{k} - \not{k}') \not{\epsilon}'_2 \not{k} \not{\epsilon}_1^* \right\}. \quad (6.19)$$

Here the second trace extracts the $1/p_1 \cdot (k - k')$ term and it also vanishes when we use the delta function to set $k = k'$ so we neglect it. The first trace may now be evaluated to give:

$$16(p_1 \cdot k) \left[p_1 \cdot (k - k') \bar{p}'_1 \cdot k \epsilon_1^* \cdot \epsilon'_2 + \bar{p}_1 \cdot (k - k') \left\{ p_1 \cdot \epsilon_1^* k' \cdot \epsilon'_2 + p_1 \cdot \epsilon'_2 k' \cdot \epsilon_1^* - p_1 \cdot k' \epsilon_1^* \cdot \epsilon'_2 \right\} \right]. \quad (6.20)$$

Once again, in the first term, we have extracted the $1/p_1 \cdot (k - k')$ term. Note that in the second term this divergence is not removed. However, by looking inside the curly brackets the first two terms vanish when we evaluate the photon polarisation

sums and the final term does not contain any collinear divergence so we neglect it for the moment.

After this derivation we may write the collinear divergent terms in (6.14) as

$$2 \frac{(2\pi)^3 (2\omega') e^4 \epsilon_1 \cdot \epsilon_2^* \delta^3(k - k')}{(p_1 \cdot k)(p_1 \cdot k')} \left[- (p_1 \cdot \epsilon_2')(p_1 \cdot \epsilon_1^*) |\bar{u}_1' \gamma^0 u_1|^2 \right. \\ \left. + 2(p_1 \cdot k) \left\{ p_1 \cdot \epsilon_2' \tilde{p}_1' \cdot \epsilon_1^* - p_1 \cdot \epsilon_1^* \tilde{p}_1' \cdot \epsilon_2' + 2p_1 \cdot k \tilde{p}_1' \cdot k' \epsilon_2' \cdot \epsilon_1^* \right\} \right]. \quad (6.21)$$

The $1/p \cdot (k - k')$ divergence has been cancelled. There are two final state photons which we have to integrate over their momenta. First integrate over k' and then use the delta function to leave

$$2 \frac{e^4 \epsilon_1 \cdot \epsilon_2^*}{(p_1 \cdot k)^2} \left[- (p_1 \cdot \epsilon_2)(p_1 \cdot \epsilon_1^*) |\bar{u}_1' \gamma^0 u_1|^2 \right. \\ \left. + 2(p_1 \cdot k) \left\{ p_1 \cdot \epsilon_2 \tilde{p}_1' \cdot \epsilon_1^* - p_1 \cdot \epsilon_1^* \tilde{p}_1' \cdot \epsilon_2 + 2p_1 \cdot k \tilde{p}_1' \cdot k \epsilon_2 \cdot \epsilon_1^* \right\} \right]. \quad (6.22)$$

Now we must sum over the polarisations λ_1 and λ_2 using (4.12) to find

$$- \frac{e^4}{p_1 \cdot k} |\bar{u}_1' \gamma^0 u_1|^2 2 \left(\frac{\omega}{E_1} + \frac{2E_1}{\omega} \right). \quad (6.23)$$

Some collinear finite terms have been dropped here.

Some technical details have been omitted in the above calculation which we will now consider. In figure 6.4 the absorbed photon can be either soft or semi-hard so $0 \leq \omega \leq E$. In order to generate a collinear divergence the emitted photon must be collinear with the initial electron, so it is soft $0 \leq \omega' \leq \Delta_{\text{out}}$. In the previous paragraph we integrated over the external photon momentum k' , but did not take into account the detector resolution. We find

$$\int_0^E d^3k \int_0^{\Delta_{\text{out}}} d^3k' \delta^3(k - k') = \int_0^{\Delta_{\text{out}}} d^3k. \quad (6.24)$$

This means that the disconnected photon in figure 5.2 forces k to be soft in figure 6.4, so $0 \leq \omega \leq \Delta_{\text{out}}$. Since ω is set equal to ω' by the delta function the energy weighting (energy-in divided by energy-out or the inverted version) is zero. The spinors generate a factor of $(E_1/E)^2$ and the collinear approximations, discussed in appendix E, gives another factor of (E_1/E) . The overall contribution to the cross-section is thus

$$-2 \frac{e^4}{p \cdot k'} |\bar{u}' \gamma^0 u|^2 \frac{E_1^2}{E^3 \omega} (2E_1^2 + \omega^2) . \quad (6.25)$$

The diagrams in figure 5.1(a) are very similar to the process we have just calculated. Naively one would simply multiply (6.25) by a factor of two. However, this would not take into account the difference in the integration limits that will arise in (6.24). In figure 5.1(a) it is the absorbed photon which must be soft and this leads to an upper integration limit of Δ_{in} .

Note that, as indicated above, processes with a photon emitted by the incoming/out-going electron and absorbed on the other line, displayed in figure 5.1(c), do not generate these Δ divergences.

Now we return to discuss the non-collinear divergences which arose in the above calculation. From the second term in (6.16) and the final term in (6.20) we obtain the cross-section contribution

$$2 \frac{(2\pi)^3 (2\omega) e^4 \delta^3(k - k') \epsilon_1 \cdot \epsilon_2^* \epsilon_1^* \cdot \epsilon_2'}{p_1 \cdot (k - k')} \left(|\bar{u}'_1 \gamma^0 u_1|^2 + 2\tilde{p} \cdot (k - k') \right) . \quad (6.26)$$

In the limit $k \rightarrow k'$ we can re-write

$$\frac{1}{p_1 \cdot (k - k')} = \frac{1}{p_1^2 - m^2} . \quad (6.27)$$

The momentum p_1 is on-shell and we can see that this term should be interpreted as a mass-shift and can be removed by a counter term. Remember that in part I of this

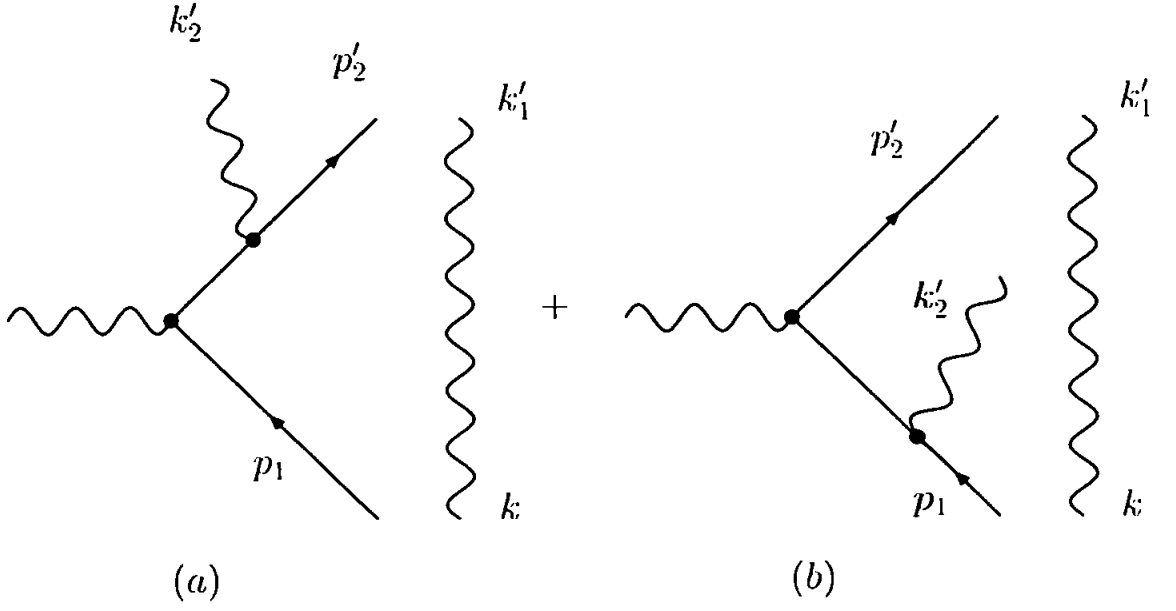


Fig. 6.5: Emission combined with a disconnected process, $P_{1,2}$, with momenta labels

thesis we observed a mass-shift for a classical charge when it is subjected to a laser's electromagnetic background. This unobserved background containing disconnected photons leads to a similar effect.

6.4 Collinear Emission + Disconnected - $P_{1,2}$

The process described by figure 6.5 can only be degenerate with Coulomb scattering if the disconnected photon's momentum is soft. However, we don't know if the disconnected photon is collinear with the initial or final state electron in either diagram so we cannot assign a maximum energy to it. In order to generate a collinear divergence the photon emitted in figure 6.5 diagram (a) must be collinear with the final state electron. Therefore technically the emitted photon can be soft or semi-hard. However, we will see that this photon must be soft in order to contribute to the fully connected³ cross-section. Therefore diagram (a) will produce Δ divergences.

³ See the discussion on connected diagrams in the following paragraph.

The emitted photon in figure 6.5 diagram (b) must be soft if it is to produce a collinear divergence. Note that we define the electron momenta in figure 6.5 as $p = p_1 + k$ and $p' = p'_2 + k'_1 + k'_2$ and the photon polarisations are λ, λ_1 and λ_2 respectively (the subscript refers to the photon's momentum).

Throughout this thesis we have insisted that we are studying the *fully connected cross-section*. With the aid of figure 6.6, which shows the possible cross-section contributions for the process in 6.5(a), we will now explain what it means to be “fully connected”. This $P_{1,2}$ process can contribute to the cross-section at order e^4 in two possible ways. In figure 6.6 the contraction of photon lines are represented by a dashed line. By connecting our photons to the dashed lines then either the disconnected photon lines are contracted together to yield a disconnected contribution, displayed in figure 6.6(a), or one obtains the fully connected contribution described by figure 6.6(b). We will follow Lee-Nauenberg's lead and ignore the vacuum bubble diagrams. We will see that the fully connected contribution is straightforward to calculate because the ‘loop’ of photons can be unwound. Let k'_2 be emitted from the left hand side of figure 6.6(b). Following the direction of momentum flow round the ‘loop’ it can be seen that, since the disconnected processes conserve momentum, k'_2 is finally absorbed by the complex conjugate $P_{1,2}$ process.

The diagrams in figure 6.5 have a symmetry factor of $1/2$ (from normalisation), but this factor is removed by combinatorial factors associated with having two photons in the out-state. Let us consider the diagram in figure 6.5(b) and calculate its cross-section contribution. The S -matrix element for this process is a mixture between an emission $P_{0,1}$ process and the disconnected diagram (see figure 5.2). We find

$$\frac{ie^2}{2p_1 \cdot k'_2} \bar{u}'_2 \gamma_0 (\not{p}_2 + \not{k}'_2) \not{\epsilon}'_2(\lambda_2) u_1 \epsilon'_1(\lambda_1) \cdot \epsilon(\lambda) (2\pi)^3 2\omega'_1 \delta^3(k'_1 - k). \quad (6.28)$$

When squaring this up it is important to remember that the momentum k'_2 is now

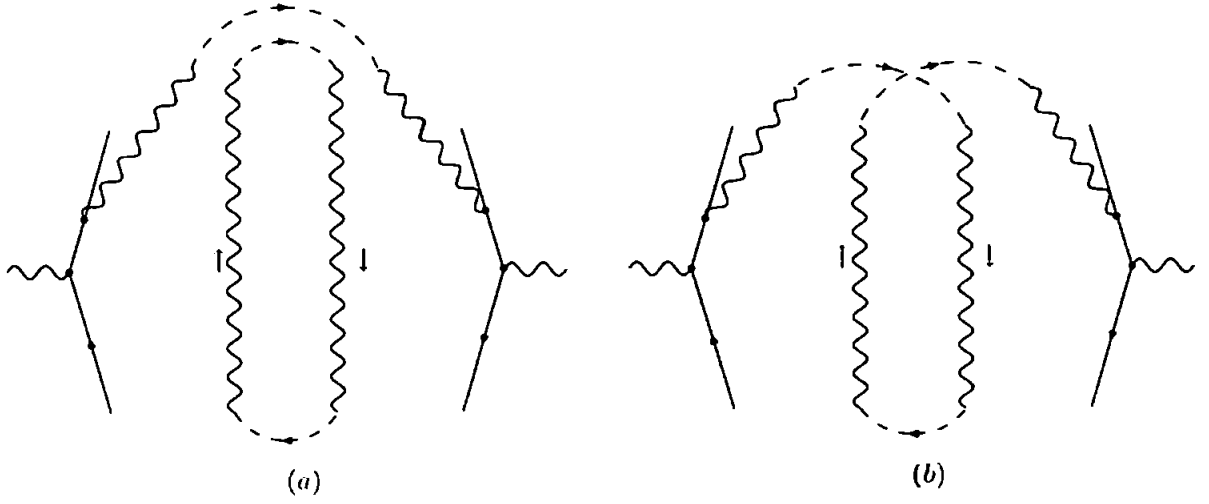


Fig. 6.6: The two possible contractions of photon lines for a $P_{1,2}$ process: (a) disconnected contribution (b) fully connected

flowing through the disconnected photon. The cross-section contribution is

$$\frac{e^4}{4p_1 \cdot k'_1 p_1 \cdot k'_2} \bar{u}'_2 \gamma_0 (\not{p}_1 + \not{k}'_2) \not{\epsilon}'_2(\lambda_2) u_1 \bar{u}_1 \not{\epsilon}_1(\lambda_1) (\not{p}_1 + \not{k}'_1) \gamma_0 u'_2 \quad (6.29)$$

$$(\epsilon'_1(\lambda_1) \cdot \epsilon(\lambda)) (\epsilon^*(\lambda) \cdot \epsilon'_2(\lambda_2)) (2\pi)^6 (2\omega'_1)(2\omega'_2) \delta^3(k'_1 - k) \delta^3(k'_2 - k).$$

The $\delta^3(k'_2 - k)$ factor shows us that the disconnected photon is parallel to the initial state electron. This restricts the photon energies to $0 \leq \omega \leq E$ since k can be semi-hard and $0 \leq \omega'_1 \leq \Delta_{\text{out}}$ since k'_1 can only be soft. It is now convenient to perform a sum over photon polarisations λ_1 and λ_2 . When the delta functions are used any terms of the form $k \cdot \epsilon$ vanish,

$$\frac{e^4}{4p_1 \cdot k'_1 p_1 \cdot k'_2} \bar{u}'_2 \gamma_0 (\not{p}_1 + \not{k}'_2) \not{\epsilon}^* u_1 \bar{u}_1 \not{\epsilon} (\not{p}_1 + \not{k}'_1) \gamma_0 u'_2 (2\pi)^6 (2\omega'_1)(2\omega'_2) \delta^3(k'_1 - k) \delta^3(k'_2 - k). \quad (6.30)$$

The integral over the out-going photon momenta k'_1 and k'_2 yields

$$\frac{e^4}{4(p_1 \cdot k)^2} \bar{u}'_2 \gamma_0 (\not{p}_1 + \not{k}) \not{\epsilon}^* u_1 \bar{u}_1 \not{\epsilon} (\not{p}_1 + \not{k}) \gamma_0 u'_2. \quad (6.31)$$

Careful examination of equation (6.31) shows us that we have reduced this process to figure 6.1, albeit with different electron momenta. Therefore the contribution from this process is virtually identical to the basic emission process. The only difference being the initial-state and final-state electron momenta which is now $p_1 = p - \omega$ and $p'_2 = p' - 2\omega$.

Earlier, in section 4.4, we discussed the Bloch-Nordsieck cancellation of soft divergences to all orders. In the paragraph following (4.46) we saw that there are two possible ways to detect soft photons experimentally. Firstly, they can be directly observed via photon detectors, which lead to the resolutions Δ_{in} and Δ_{out} . When we integrate over the out-going photon momenta in (6.30), remembering that the disconnected photon is collinear with the initial state electron, we see that

$$\int_0^E d^3k \int_0^{\Delta_{\text{out}}} d^3k'_1 \int_0^{\Delta_{\text{out}}} d^3k'_2 \delta^3(k - k'_1) \delta^3(k - k'_2) = \int_0^{\Delta_{\text{out}}} d^3k. \quad (6.32)$$

The $P_{1,2}$ process reduces to basic emission of a photon with maximum energy Δ_{out} . We will obtain Δ divergences. An experiment can also indirectly detect a soft photon through measurements of the electron's energy [88]. This leads to the requirement that $\omega'_1 + \omega'_2 \leq \Delta_{\text{T}_{\text{out}}}$ in the out-going state for this process. Here $\Delta_{\text{T}_{\text{out}}}$ is the experimental resolution for the electron detector, $\Delta_{\text{T}_{\text{out}}} \geq \Delta_{\text{out}}$ for a real detector⁴. The delta functions have acted in (6.31) to set $\omega'_1 = \omega'_2 = \omega$, so we have two conditions for the photon energy in (6.31):

1. $\omega \leq \Delta_{\text{out}} \leq \Delta_{\text{T}_{\text{out}}}$;
2. $2\omega \leq \Delta_{\text{T}_{\text{out}}}$.

The integration limits in (6.32) will be modified if the second condition is stronger than the first. For instance, if the photon is indirectly detected in the electron leg

⁴ If $\Delta_{\text{T}_{\text{out}}} \leq \Delta_{\text{out}}$ then there would be no point in installing a soft photon detector in the experiment.

then $\Delta_{\text{out}} \leq \Delta_{T_{\text{out}}} \leq 2\Delta_{\text{out}}$ and the second condition is stronger. If the photon is directly observed we know $\Delta_{T_{\text{out}}} \geq 2\Delta_{\text{out}}$ and the maximum photon energy is Δ_{out} because the first condition is stronger. If the second condition is stronger then we must incorporate this into (6.32) by taking the photon energy integration limits to be

$$0 \leq \omega \leq \min \left(\frac{1}{2}\Delta_{T_{\text{out}}}, \Delta_{\text{out}} \right). \quad (6.33)$$

If we were to consider a process with more than one disconnected photon this discussion should be modified since the second condition would no longer be strong enough. For instance, if there were two disconnected photons which are not detected via some ‘missing’ electron energy then $\omega'_1 + \omega'_2 + \omega'_3 \leq \Delta_{T_{\text{out}}}$. After the delta functions have been used we would find that the second condition is replaced by the stronger constraint on the photon energy $3\omega \leq \Delta_{T_{\text{out}}}$. For a real experiment we would have different electron detector resolutions in the initial and final states $\Delta_{T_{\text{out}}}$ and $\Delta_{T_{\text{in}}}$.

We have ‘unwound’ the $P_{1,2}$ process so that it is equivalent (up to electron energies and photons integration limits) to a $P_{0,1}$ process. The final result for the cross-section before approximations and weightings may be obtained from (6.4):

$$\frac{e^4}{p_1 \cdot k} |\bar{u}'_2 \gamma^0 u_1|^2 \frac{1}{E_1 \omega} (E_1^2 + E_2'^2). \quad (6.34)$$

The electron energies have been modified from those in (6.4) to account for the different momentum in the initial and final state electrons. Similarly figure 6.5(a) gives a contribution comparable to (4.25),

$$\frac{e^4}{p'_2 \cdot k} |\bar{u}'_2 \gamma^0 u_1|^2 \frac{1}{E'_2 \omega} (E_1^2 + E_2'^2). \quad (6.35)$$

For this case the disconnected photon is collinear with the out-state electron which

leads to the energy restriction

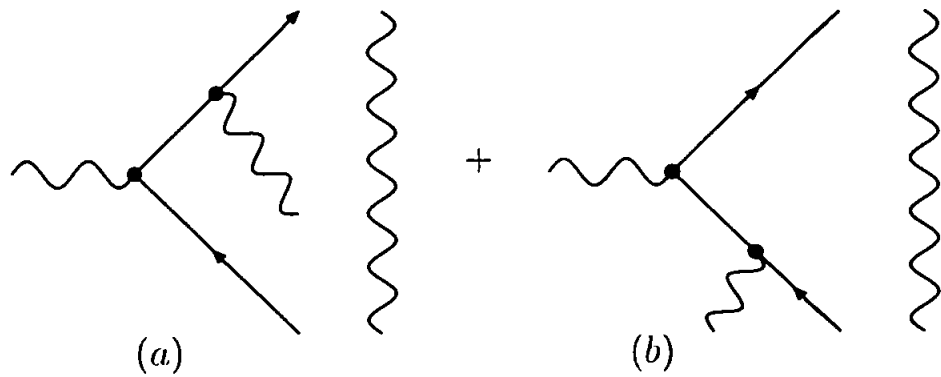
$$\int_0^{\Delta_{\text{in}}} d^3 k' \int_0^{E'} d^3 k'_1 \int_0^{E'} d^3 k'_2 \delta^3(k - k'_1) \delta^3(k - k'_2) = \int_0^{\Delta_{\text{in}}} d^3 k'. \quad (6.36)$$

Here there is only one Δ_{in} upper limit which means that there is only one chance to detect the soft particle. In (6.32) there are two Δ_{out} upper limits which leads to the photon energy modification (6.33). There shall be no similar condition to the second condition discussed above for the process displayed in 6.5(a). Note that the only difference is through the integration limits for the cross-section contributions from the two processes in figure 6.5. Using the collinear approximations discussed in appendix E we find that each of these processes contributes

$$\frac{e^4}{p \cdot k} |\bar{u}' \gamma^0 u|^2 \frac{E'_2 E_1}{E^3 \omega} (E_1^2 + E_2'^2). \quad (6.37)$$

Note that the energy weighting has not been considered here. This will be left until we come to consider the sum of all processes.

To summarise we have found that the photon emitted in the diagram displayed by figure 6.5(b) has energy $0 \leq \omega' \leq \min(\Delta_{\text{Tout}}/2, \Delta_{\text{out}})$. The electron's energy detector modifies the upper limit for diagram 6.5(b) because this process has two soft photons in the final state. For the second diagram, since we have only one photon in the initial state, the electron's energy detector will not modify results, so $0 \leq \omega' \leq \Delta_{\text{in}}$. For processes with more than one soft photon in the initial or final state the upper limits of integrals over the photon's energy will be modified.

Fig. 6.7: Absorption and disconnected - $P_{2,1}$

6.5 Further $P_{n,m}$ Processes which Contribute to the Cross-Section at NLO

We have now considered all the processes which we saw in chapter 5 may be used to cancel soft and regular collinear singularities at the level of the cross-section. We also observed that there are other combinations of processes, which fall into a pattern involving more disconnected photons (5.6), that lead to a soft and regular collinear finite cross-section. During the following section we want to see if the Δ collinear divergences are also eliminated in the same way found for soft and regular collinear divergences. Therefore, we must consider processes with more disconnected photons at NLO in perturbation theory.

Having evaluated the emission and disconnected process $P_{1,2}$ in the last section it is straightforward to calculate an absorption and disconnected process $P_{2,1}$ as displayed in figure 6.7. We have seen, in sections 6.1 and 6.2, that the only difference between emission and absorption is the upper energy integration limit. This was because emission = absorption* and in a similar way $P_{1,2} = P_{2,1}^*$. Therefore we obtain, up to differences in the photon energy integration limits, another two factors of (6.37) since there are two $P_{2,1}$ diagrams to consider. Absorption on the final state electron which is displayed in figure 6.7(a) has two soft photons in the initial state.

This will lead to a similar modification to the photon energy upper integration limit as we found for the process described by figure 6.5(b). However, process 6.7(a) has two soft photons in the initial state whereas 6.5(b) has two soft photons in the final state. Therefore Δ_{Tout} will be replaced by Δ_{Tin} . Absorption on the initial state electron shown in figure 6.7(b) needs to be integrated over ω up to energy Δ_{out} and on the final state displayed in figure 6.7 (a) up to energy $\omega = \min(\Delta_{\text{Tin}}/2, \Delta_{\text{in}})$.

In section 6.4 we described how to unwrap a $P_{1,2}$ process so that it becomes the fundamental $P_{0,1}$ emission process. This method, applied to $P_{2,1}$ unwraps it to become the fundamental $P_{1,0}$ absorption process. By performing the necessary polarisation sums and integrating over the new disconnected photon momentum a $P_{2,2}$ process may also be unwound into the fundamental emission plus absorption $P_{1,1}$ process. All diagrams contributing to the cross-section at NLO in perturbation theory come in the form of $P_{n+1,n}$, $P_{n,n+1}$ and $P_{n+1,n+1}$ processes, where n is the number of disconnected photons. They can all be unwound into the fundamental $P_{0,1}$, $P_{1,0}$ and $P_{1,1}$ processes. In section 6.4 we saw that the electrons for $P_{1,2}$ processes carry energy $E_1 = E - \omega$ or $E_2 = E - 2\omega$ and from section 6.1 the electrons for $P_{0,1}$ processes carry energy $E_0 = E$ or E_1 . By comparing the cross-section contributions (6.37) and, after removing the energy weighting (4.11), one can observe that the sole difference comes in the subscript of the electrons' energy in the numerator, $E_0 \leftrightarrow E_1$ and $E_1 \leftrightarrow E_2$. When switching the formulas between cross-section contributions $P_{0,1} \leftrightarrow P_{1,2}$ we can let $E_\kappa \leftrightarrow E_{\kappa+1}$, where $\kappa = 0, 1$. There are two $P_{0,1}$ diagrams so the process has two photon energy integration limits⁵ E and Δ_{out} , and the $P_{1,2}$ process has limits Δ_{in} and $\min(\Delta_{\text{Tin}}/2, \Delta_{\text{in}})$. By comparing the diagrams for $P_{0,1}$ and $P_{1,2}$ it can be seen that integration limits swap between $E \leftrightarrow \Delta_{\text{in}}$ and $\Delta_{\text{out}} \leftrightarrow \min(\Delta_{\text{Tout}}/2, \Delta_{\text{out}})$.

The next challenge is to discover how to modify the fundamental processes

⁵ A process with upper photon energy integration limit E can be soft or semi-hard. For the case of $P_{0,1}$ this is displayed in figure 4.4.

cross-section contributions (6.7), (6.12) and (6.25) to describe a general NLO process with n disconnected photons. After unwinding disconnected 'loops' there are only two differences between the fundamental processes $P_{0,1}, P_{1,0}, P_{1,1}$ and the $P_{n,n+1}, P_{n+1,n}, P_{n+1,n+1}$ processes cross-section contribution. The energy carried by the initial and final state electrons and the upper photon energy integration limits are not the same but in all other respects the contributions are equivalent. To modify the cross-section contributions of the fundamental process to become the contribution of the processes with n disconnected photons $P_{n+1,n}, P_{n,n+1}, P_{n+1,n+1}$ we let

$$E_\kappa \rightarrow E_{\kappa+n} = E - (\kappa + n)\omega, \quad (6.38)$$

in the numerator of (6.7), (6.12) and (6.25). The photon energy integration limits applied to the cross-section contributions must also be modified from the limits obtained for the fundamental processes to describe n disconnected photons. If the energy of more disconnected photons is 'missing' from the electron via equation (6.38) then the electron energy detector becomes an increasingly useful experimental tool when compared to the photon detector. This will lead to a stronger condition than the one we applied in section 6.4. For n disconnected photons we find

1. $\omega \leq \Delta_{\text{out}} \leq \Delta_{T_{\text{out}}}$ or $\omega \leq \Delta_{\text{in}} \leq \Delta_{T_{\text{in}}}$;
2. $n\omega \leq \Delta_{T_{\text{out}}}$ or $n\omega \leq \Delta_{T_{\text{in}}}$.

The integration limits for the fundamental processes are proportional to either $\Delta_{\text{in}}, \Delta_{\text{out}}$ or E which will be modified due to the stronger second condition for the $P_{n+1,n}, P_{n,n+1}$ and $P_{n+1,n+1}$ processes. Here E stands for the integration limit of the $P_{0,1}$ and $P_{1,0}$ diagrams which can be both soft and semi-hard. These diagrams eliminate the virtual processes regular collinear divergences but they do not produce Δ divergences. If the fundamental processes integration limits are proportional to

Δ_{in} , Δ_{out} or E it will be converted for $n \geq 1$ according to

$$\Delta_{\text{in}} \rightarrow \min \left(\frac{\Delta_{T_{\text{in}}}}{n+1}, \Delta_{\text{in}} \right), \quad \Delta_{\text{out}} \rightarrow \min \left(\frac{\Delta_{T_{\text{out}}}}{n+1}, \Delta_{\text{out}} \right), \quad (6.39)$$

$$P_{0,1} : \text{ for } n = 1, E \rightarrow \Delta_{\text{in}} \quad \text{and for } n > 1, E \rightarrow \min \left(\frac{\Delta_{T_{\text{in}}}}{n}, \Delta_{\text{in}} \right), \quad (6.40)$$

$$P_{1,0} : \text{ for } n = 1, E \rightarrow \Delta_{\text{out}} \quad \text{and for } n > 1, E \rightarrow \min \left(\frac{\Delta_{T_{\text{out}}}}{n}, \Delta_{\text{out}} \right).$$

Equation (5.5) holds for the soft pole but for the Δ singularities we need to modify (5.5) using (6.38), (6.39) and (6.40).

To summarise, we have evaluated the cross-section contributions for the fundamental $P_{0,1}$, $P_{1,0}$ and $P_{1,1}$ processes. In section 6.4 we saw that processes with disconnected photons may be un-wound to become similar cross-section contributions to the fundamental processes. During this section we have found how to relate any NLO $P_{n,m}$ processes contribution to the cross-section with one of the fundamental processes contributions. This is done by modifying the fundamental processes cross-sections by (6.38) and using either (6.39) or (6.40) depending on the process in question. Now we are ready to discover if the Δ collinear divergences are eliminated when considering only the same processes as the soft and regular collinear singularities.

6.6 Cancelling Collinear Divergences and Energy Weighting

We have shown that there is a new class of collinear singularities of the form $\Delta^n \ln(m)$ and $\ln(\Delta) \ln(m)$ which have not previously been considered. These have been evaluated for all the degenerate processes which contribute to the consistent cancellation of soft and regular collinear divergences in the cross-section at NLO in perturbation theory. These divergences must be summed up to see if they are

removed at the level of the cross-section. If the Δ divergences are removed in the same way as the soft divergence (5.6), which we recall is given by

$$P_{0,0} + P_{0,1} + \sum_{a=1}^{\infty} (P_{a,a-1} + P_{a,a} + P_{a,a+1}), \quad (6.41)$$

then we have found that the cross-section is infrared finite. However, if they are not removed, then the only possible conclusion is that the Lee-Nauenberg proposition fails and the cross-section is divergent. If Δ divergences are removed by some other combination of degenerate process than that displayed in (6.41) we will re-introduce soft divergences.

Our results for all the processes which contribute to the NLO Coulomb scattering cross-section will be combined. Before doing this consider the regular Bethe-Heitler energy weighted $P_{0,1}$ emission process. In equation (6.7) we found the cross-section contribution is

$$\underbrace{\frac{e^4}{p \cdot k'} |\bar{u}' \gamma^0 u|^2}_{\text{angular term}} \underbrace{\frac{E_1'^2}{E^3 \omega'} (E^2 + E_1'^2)}_{\text{energy term}}. \quad (6.42)$$

Here we have labelled the term which contains all the angular dependence and the terms which depend on the photon's energy ω . We must integrate each process over the photon momentum and combine the results. The generic integration measure being

$$\int \frac{d^3 k}{(2\pi)^3} \frac{1}{2\omega} = -\frac{1}{4(2\pi)^2} \int_0^\Delta \omega d\omega \int_0^{\delta^2} d\theta^2 \frac{d\sigma}{d\Omega}. \quad (6.43)$$

Here Δ stands for the experimental energy resolution for the process under consideration. As we have seen different processes have different resolutions. First perform the angular integral, using a similar expansion to (4.27). The angular integral is the same for all $P_{n,m}$ processes because we have used the second type

of collinear approximation discussed in appendix E. We find

$$-\frac{e^4}{(2\pi)^2} |\bar{u}' \gamma^0 u|^2 \ln \left(\frac{E\delta}{m} \right) \frac{1}{E} \int_0^\Delta \sum_{\text{all processes}} (\text{energy terms}) d\omega. \quad (6.44)$$

This equation is singular as $m \rightarrow 0$, the collinear divergences are all contained in the angular integration. Since the collinear divergences have been extracted the remaining integral is either finite or contains soft singularities. Each processes' energy terms may be substituted into (6.44). By specifying the correct integration limit and performing the integral the cross-section contribution shall be evaluated.

Table 6.1 serves to summarise all the results presented within this chapter and shows the energy terms and photon energy integration limits for some of the $P_{n,m}$ processes. In the literature the Bethe-Heitler energy weighting has only been evaluated for the $P_{0,1}$ process. In section 6.2 we argued for the need to use an *inverted* energy weighting for absorption, so that an electron has the same probability to absorb a photon as to emit one. The energy weightings for processes with disconnected photons has never been discussed so we use a trial and error method and apply three different types of energy weighting:

- no weighting;
- regular energy weighting which comprises of a factor equal to the electron energy out divided by energy in;
- a factor equal to the electron energy in divided by energy out which we call an inverted weighting.

For each of the processes contained in table 6.1 we must evaluate the remaining integral in (6.44). All these integrals are going to produce Δ divergences but we need to see if they cancel for some summation of processes and then check if this complies with (6.41). Table 6.1 has been extended indefinitely to include n disconnected

photons using the rules in equations (6.38), (6.39) and (6.40). It is important to realise that each process given in the table has two contributions to the cross-section – one from each integration limit.

Process	No Weighting	Regular Weighting	Inverted Weighting	Integration Limit(s) Δ
$P_{0,1}$	unphysical	$\frac{E_1^2}{E^3\omega} (E_0^2 + E_1^2)$	unphysical	$\Delta_{\text{out}} \ \& \ E$
$P_{1,0}$	unphysical	unphysical	$\frac{E_1^2}{E^3\omega} (E_0^2 + E_1^2)$	$E \ \& \ \Delta_{\text{in}}$
$P_{1,1}$	$-2 \frac{E_1^2}{E^3\omega} (2E_1^2 + \omega^2)$	no effect	no effect	$\Delta_{\text{out}} \ \& \ \Delta_{\text{in}}$
$P_{1,2}$	$\frac{E_2 E_1}{E^3\omega} (E_1^2 + E_2^2)$	$\frac{E_2^2}{E^3\omega} (E_1^2 + E_2^2)$	$\frac{E_2^2}{E^3\omega} (E_1^2 + E_2^2)$	$\min(\frac{1}{2}\Delta_{\text{T}_{\text{out}}}, \Delta_{\text{out}}) \ \& \ \Delta_{\text{in}}$
$P_{2,1}$	$\frac{E_2 E_1}{E^3\omega} (E_1^2 + E_2^2)$	$\frac{E_1^2}{E^3\omega} (E_1^2 + E_2^2)$	$\frac{E_2^2}{E^3\omega} (E_1^2 + E_2^2)$	$\Delta_{\text{out}} \ \& \ \min(\frac{1}{2}\Delta_{\text{T}_{\text{in}}}, \Delta_{\text{in}})$
$P_{2,2}$	$-2 \frac{E_2^2}{E^3\omega} (2E_2^2 + \omega^2)$	no effect	no effect	$\min(\frac{1}{2}\Delta_{\text{T}_{\text{out}}}, \Delta_{\text{out}}) \ \& \ \min(\frac{1}{2}\Delta_{\text{T}_{\text{in}}}, \Delta_{\text{in}})$
$P_{2,3}$	$\frac{E_3 E_2}{E^3\omega} (E_2^2 + E_3^2)$	$\frac{E_3^2}{E^3\omega} (E_2^2 + E_3^2)$	$\frac{E_2^2}{E^3\omega} (E_2^2 + E_3^2)$	$\min(\frac{1}{3}\Delta_{\text{T}_{\text{out}}}, \Delta_{\text{out}}) \ \& \ \min(\frac{1}{2}\Delta_{\text{T}_{\text{in}}}, \Delta_{\text{in}})$
$P_{3,2}$	$\frac{E_3 E_2}{E^3\omega} (E_2^2 + E_3^2)$	$\frac{E_2^2}{E^3\omega} (E_2^2 + E_3^2)$	$\frac{E_3^2}{E^3\omega} (E_2^2 + E_3^2)$	$\min(\frac{1}{2}\Delta_{\text{T}_{\text{out}}}, \Delta_{\text{out}}) \ \& \ \min(\frac{1}{3}\Delta_{\text{T}_{\text{in}}}, \Delta_{\text{in}})$
$P_{3,3}$	$-2 \frac{E_3^2}{E^3\omega} (2E_3^2 + \omega^2)$	no effect	no effect	$\min(\frac{1}{3}\Delta_{\text{T}_{\text{out}}}, \Delta_{\text{out}}) \ \& \ \min(\frac{1}{3}\Delta_{\text{T}_{\text{in}}}, \Delta_{\text{in}})$
\vdots	\vdots	\vdots	\vdots	\vdots
$P_{n,n+1}$	$\frac{E_n E_{n+1}}{E^3\omega} (E_n^2 + E_{n+1}^2)$	$\frac{E_{n+1}^2}{E^3\omega} (E_n^2 + E_{n+1}^2)$	$\frac{E_n^2}{E^3\omega} (E_n^2 + E_{n+1}^2)$	$\min(\frac{1}{n+1}\Delta_{\text{T}_{\text{out}}}, \Delta_{\text{out}}) \ \& \ \min(\frac{1}{n}\Delta_{\text{T}_{\text{in}}}, \Delta_{\text{in}})$
$P_{n+1,n}$	$\frac{E_n E_{n+1}}{E^3\omega} (E_n^2 + E_{n+1}^2)$	$\frac{E_n^2}{E^3\omega} (E_n^2 + E_{n+1}^2)$	$\frac{E_{n+1}^2}{E^3\omega} (E_n^2 + E_{n+1}^2)$	$\min(\frac{1}{n}\Delta_{\text{T}_{\text{out}}}, \Delta_{\text{out}}) \ \& \ \min(\frac{1}{n+1}\Delta_{\text{T}_{\text{in}}}, \Delta_{\text{in}})$
$P_{n+1,n+1}$	$-2 \frac{E_{n+1}^2}{E^3\omega} (2E_{n+1}^2 + \omega^2)$	no effect	no effect	$\min(\frac{1}{n+1}\Delta_{\text{T}_{\text{out}}}, \Delta_{\text{out}}) \ \& \ \min(\frac{1}{n+1}\Delta_{\text{T}_{\text{in}}}, \Delta_{\text{in}})$

Tab. 6.1: Cross-section contribution for all processes contributing at NLO to Coulomb scattering. Three different energy weightings are applied to the cross-section: (i) no weighting, (ii) regular and (iii) inverted. The different integration limits relate which diagram(s) the cross-section contribution comes from.

The remaining integral in (6.44) must be performed for each of the $P_{n,m}$ processes. Before doing this integral it is interesting to consider the sum of energies $\{E_{a-1}^2 + E_a^2\} - 2\{2E_a^2 + \omega^2\} + \{E_a^2 + E_{a+1}^2\}$, where $a = 0, 1, 2 \dots$ and $E_a = E - a\omega$. It can be proven algebraically that

$$\{E_{a-1}^2 + E_a^2\} - 2\{2E_a^2 + \omega^2\} + \{E_a^2 + E_{a+1}^2\} = 0. \quad (6.45)$$

If the energy terms of the degenerate processes discussed in table 6.1 can be combined as in (6.45) then the collinear divergences will be removed⁶. For $a = 1$ (6.45) reads

$$\{E_0^2 + E_1^2\} - 2\{2E_1^2 + \omega^2\} + \{E_1^2 + E_2^2\} = 0. \quad (6.46)$$

Using table 6.1, it can be seen that $P_{0,1}$ is proportional to the first set of brackets, $P_{1,1}$ is proportional to the second set of brackets and $P_{2,1}$ is proportional to the final set of brackets. However, in order to produce something that is proportional to the whole of equation (6.46), we must choose the energy weighting from table 6.1 carefully.

By applying two different energy weighting methods we will see that there are two different ways of clustering the processes which eliminate the collinear divergences from the cross-section. The first cancellation we consider is symmetric between emission and absorption processes and the energy weighting seems natural. However, the soft singularities are not cancelled by taking this approach so the cross-section is divergent. The second cancellation uses the same processes required to eliminate soft divergences and leads to a finite cross-section. Unfortunately we must make some questionable assumptions to achieve infrared finiteness. Both these approaches will now be explained.

⁶ Reservations regarding the convergence of the series (6.41) are not addressed here.

Symmetric Collinear Cancellation

Using a regular energy weighting for $P_{0,1}$ and $P_{2,1}$ allows us to combine $P_{0,1} + P_{1,1} + P_{2,1}$ in such a way that they are equal to $E_1^2/E^3\omega$ times (6.46)⁷. As explained previously all the terms in table 6.1 must be integrated over the photon energy (6.44) with their respective maximum integration limits. Simply combining terms so that they are proportional to (6.45) is not sufficient because if the integration limits for the processes in question are different the cancellation in (6.45) cannot take place. From the table it can be seen that the processes $P_{0,1} + P_{1,1} + P_{2,1}$ have a common integration limit Δ_{out} . By combining these processes the integral in (6.44) can be written as

$$\frac{1}{E} \int_0^{\Delta_{\text{out}}} d\omega' \frac{E_1^2}{E^3\omega'} \left(\{E_0^2 + E_1^2\} - 2\{2E_1^2 + \omega^2\} + \{E_1^2 + E_2^2\} \right) = 0. \quad (6.47)$$

It can be seen from table 6.1 that these are the only processes with upper integration limit Δ_{out} , so all Δ_{out} collinear divergences have been completely removed. In a similar way an inverted energy weighting applied to $P_{1,0}$ and $P_{1,2}$ allows us to remove all Δ_{in} divergences.

Through a careful examination of the energy terms and integration limits in table 6.1 a pattern for the cancellation of all Δ divergences for n collinear photons emerges. For all *final state* contributions, by which we mean they have an integration limit proportional to Δ_{out} or Δ_{Tout} , we apply a regular energy weighting. We do the opposite for all *initial state* contributions and apply an inverted energy weighting. By carefully selecting the three processes which can have the same integration limit and applying the energy weighting as described we obtain the general cancellation

⁷ Note that we also could produce something proportional to (6.46) using the $(P_{1,0} + P_{1,1} + P_{1,2})$ processes or an alternative mixture.

of collinear divergences valid for any number of disconnected photons

$$\begin{aligned}
& \frac{1}{E} \int_0^{\Delta_{\text{out}}} d\omega' \frac{E_1^2}{E^3 \omega'} \left(\{E_0^2 + E_1^2\} - 2\{2E_1^2 + \omega^2\} + \{E_1^2 + E_2^2\} \right) \\
& + \frac{1}{E} \int_0^{\Delta_{\text{in}}} d\omega' \frac{E_1^2}{E^3 \omega'} \left(\{E_0^2 + E_1^2\} - 2\{2E_1^2 + \omega^2\} + \{E_1^2 + E_2^2\} \right) \\
& + \frac{1}{E} \sum_{a=2}^{\infty} \int_0^{\Delta_{\text{out}}^{\min}} d\omega \frac{E_a^2}{E^3 \omega} \left(\{E_{a-1}^2 + E_a^2\} - 2\{2E_a^2 + \omega^2\} + \{E_a^2 + E_{a+1}^2\} \right) \\
& + \frac{1}{E} \sum_{a=2}^{\infty} \int_0^{\Delta_{\text{in}}^{\min}} d\omega \frac{E_a^2}{E^3 \omega} \left(\{E_{a-1}^2 + E_a^2\} - 2\{2E_a^2 + \omega^2\} + \{E_a^2 + E_{a+1}^2\} \right) = 0.
\end{aligned} \tag{6.48}$$

Here the shorthand notation $\Delta_{\text{out}}^{\min} = \min(\Delta_{T_{\text{out}}}/a, \Delta_{\text{out}})$ and $\Delta_{\text{in}}^{\min} = \min(\Delta_{T_{\text{in}}}/a, \Delta_{\text{in}})$ has been introduced. We have discovered a way to remove all Δ collinear divergences but we must still consider whether the soft singularities are removed by this combination of processes. Written in terms of the processes involved (6.48) is

$$\begin{aligned}
& \frac{1}{E} \int_0^{\Delta_{\text{out}}} d\omega' \left(P_{0,1} + P_{1,1} + P_{2,1} \right) \Big|_{\text{regular weighting}} \\
& + \frac{1}{E} \int_0^{\Delta_{\text{in}}} d\omega' \left(P_{1,0} + P_{1,1} + P_{1,2} \right) \Big|_{\text{inverted weighting}} \\
& + \frac{1}{E} \sum_{a=2}^{\infty} \int_0^{\Delta_{\text{out}}^{\min}} d\omega \left(P_{a-1,a} + P_{a,a} + P_{a+1,a} \right) \Big|_{\text{regular weighting}} \\
& + \frac{1}{E} \sum_{a=2}^{\infty} \int_0^{\Delta_{\text{in}}^{\min}} d\omega \left(P_{a,a-1} + P_{a,a} + P_{a,a+1} \right) \Big|_{\text{inverted weighting}} = 0.
\end{aligned} \tag{6.49}$$

Each collinear cancellation contains one process which can be reduced to emission and one process which can be reduced to absorption. Therefore (6.49) is symmetric between emission and absorption. From an initial inspection of (6.49) it appears that some processes are being counted twice. By studying figure 6.8 it can be seen that processes are not double counted but there are in fact different diagrams contributing to the same process with different integration limits.

The energy weighting used in the cancellation in (6.49) is interesting. On the first

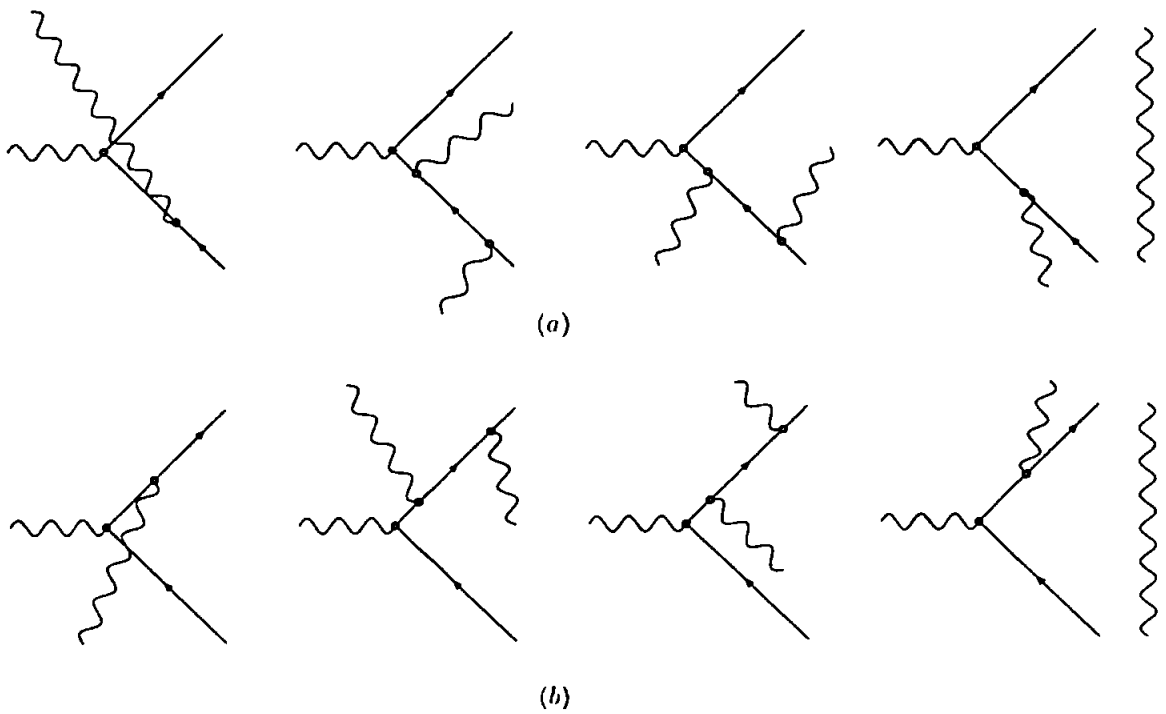


Fig. 6.8: Processes contributing to the first cancellation of Δ divergences discovered in (6.49). Diagrams (a) represent the Δ_{out} cancellation. The first and final diagram contribute these divergences when squared up, and the $P_{1,1}$ diagrams contribute when interfering with a disconnected process. Similarly diagrams (b) represent the Δ_{in} cancellation.

line of (6.49) for a $P_{2,1}$ diagram we used a regular energy weighting. However, on the final line an inverted energy weighting is used for the other $P_{2,1}$ diagram. If one applied the same energy weighting to both $P_{2,1}$ diagram and combined the processes as in (6.49) the collinear divergences will not be eliminated because the Δ divergences are sensitive to the weighting. Both $P_{1,0}$ processes require the same energy weighting to cancel the regular collinear divergences. This suggests that further research is needed to fully understand the energy weighting. It is important to stress that, we can see from table 6.1 and (6.45) that an energy weighting scheme is required to remove Δ divergences.

In figure 6.8 we have displayed all the processes which are used to cancel the Δ_{in} and Δ_{out} singularities in the first two lines of (6.49). This method of combining

processes will now be compared to the version discussed for soft divergences (6.41). To remove soft divergences we require both $P_{0,1}$ diagrams displayed in figure 4.3. We can see from (4.13) that the interference effect (figure 6.2) between the two diagrams produces a soft divergence, but interference effects do not produce any Δ_{out} divergences. However, it is possible to add the extra $P_{0,1}$ process in figure 4.3 and the interference effects without destroying the Δ_{out} cancellation because this process can be integrated up to the full electron energy E . The same conclusions may be reached for $P_{1,0}$ and Δ_{in} divergences. Turning our attention to the $P_{1,1}$ processes it can be seen that the diagrams in figure 5.1(c) are not present in figure 6.8. The diagrams in figure 5.1(c) are essential to the soft divergence cancellation. They do not produce Δ divergences so it will not harm the collinear cancellation to add these to the diagrams in figure 6.8. In figure 6.8 we have just one diagram of each of the $P_{1,2}$ and $P_{2,1}$ processes and these diagrams cannot interfere with each other. For the soft cancellation we required both of the $P_{1,2}$ (or $P_{2,1}$) diagrams and again interference effects are essential because these diagrams can be unwound to give a similar factor to (4.13). With just one of each of the $P_{1,2}$ and $P_{2,1}$ diagrams we cannot produce this essential interference effect. By attempting to add the additional $P_{1,2}$ or $P_{2,1}$ diagram we would reintroduce the Δ divergences⁸. Therefore we must conclude that this cancellation of collinear divergences does not use the same processes as the soft cancellation (6.41). Put bluntly, the Lee-Nauenberg theorem fails to produce a finite cross-section if the processes are combined as in (6.49). It is interesting to observe that the cancellation of collinear divergences is symmetric between emission and absorption type processes. This is in contrast with the soft cancellation (6.41). Intuitively we should expect symmetry between emission and absorption and this gives (6.49) a somewhat more 'natural feel' compared to (6.41).

⁸ Cancellation of both types of divergence could be arranged if we only add the interference effect between the extra diagrams, but it would be extremely unnatural to allow a physical process to take place only as an interference effect.

Collinear and Soft Cancellation

Another careful study of table 6.1 shows us that it is possible to obtain *both* a soft and collinear infrared finite cross-section. To do this we must alter the cancellation which takes place in (6.49) and the symmetry between emission and absorption is ruined. Take the same processes considered at the first finite point of the soft singularity cancellation ($P_{0,1}$, $P_{1,0}$, $P_{1,1}$ and $P_{1,2}$) and apply a regular energy weighting to $P_{0,1}$ and an inverted weighting to all other processes. Note that we apply an inverted weighting to a process which can be unwound into emission. The cancellation of the Δ_{in} divergences in (6.49) proceeds as before but we are left with the following final state Δ divergences

$$\frac{E_1^2}{E^4 \omega} \left[\int_0^{\Delta_{\text{out}}} d\omega \left(\{E_0^2 + E_1^2\} - 2\{2E_1^2 + \omega^2\} \right) + \int_0^{\Delta_{\text{out}}^{\text{min}}} d\omega \{E_1^2 + E_2^2\} \right], \quad (6.50)$$

where $\Delta_{\text{in}}^{\text{min}} = \min(\Delta_{\text{T}_{\text{out}}}/2, \Delta_{\text{out}})$. If $\Delta_{\text{out}}^{\text{min}} = \Delta_{\text{out}}$ it can be seen that the Δ_{out} collinear singularities will cancel. However, by insisting $\Delta_{\text{out}}^{\text{min}} = \Delta_{\text{out}}$ we are physically saying that the photon is always directly observed through the photon detector and never observed indirectly by the electrons' energy detector. This is not necessarily true for a given experiment. To produce an infrared finite cross-section we have put a constraint on the way experiments are carried out. Consider the soft cancellation series (6.41) and now include the next cluster of processes which are soft finite ($a = 2$). Apply an inverted energy weighting to each of these processes ($P_{2,1}$, $P_{2,2}$ and $P_{2,3}$). All these process share a common integration limit $\Delta_{\text{T}_{\text{in}}}/2$ and the cancellation of these divergences proceeds as in (6.49). For the final state

degeneracies we are left with the Δ divergences

$$\begin{aligned} \frac{E_2^2}{E^4\omega} \left[\int_0^{\Delta_{\text{out}}} d\omega \left(E_1^2 + E_2^2 \right) - 2 \int_0^{\min(\frac{1}{2}\Delta_{\text{Tout}}, \Delta_{\text{out}})} d\omega \left(2E_2^2 + \omega^2 \right) \right. \\ \left. + \int_0^{\min(\frac{1}{3}\Delta_{\text{Tout}}, \Delta_{\text{out}})} d\omega \left(E_2^2 + E_3^2 \right) \right]. \end{aligned} \quad (6.51)$$

These divergences are removed if the photon is observed directly so $\Delta_{\text{Tout}} \geq 3\Delta_{\text{out}}$.

This discussion may be extended for any value of a and the collinear divergences cancel in the same way as the soft divergences providing $\Delta_{\text{Tout}} \geq (a+1)\Delta_{\text{out}}$:

$$\begin{aligned} \frac{E_a^2}{E^4\omega} \left[\int_0^{\min(\frac{1}{(a-1)}\Delta_{\text{Tout}}, \Delta_{\text{out}})} d\omega \left(E_{a-1}^2 + E_a^2 \right) \right. \\ - 2 \int_0^{\min(\frac{1}{a}\Delta_{\text{Tout}}, \Delta_{\text{out}})} d\omega \left(2E_a^2 + \omega^2 \right) \\ \left. + \int_0^{\min(\frac{1}{(a+1)}\Delta_{\text{Tout}}, \Delta_{\text{out}})} d\omega \left(E_a^2 + E_{a+1}^2 \right) \right]. \end{aligned} \quad (6.52)$$

Therefore collinear divergences may be cancelled in exactly the same way as soft divergences. However a constraint is placed upon the way experiments are conducted.

Concluding remarks

We have calculated all possible Δ divergences for all the processes which contribute at NLO to the Coulomb scattering cross-section and displayed them in table 6.1. Through a careful examination of this table we found two ways of combining degenerate processes to cancel collinear divergences.

The first cancellation we observed is given in equation (6.49), it is symmetric between emission and absorption processes. Soft divergences are produced from interference effects (displayed in figure 6.2) as can be seen from (4.13). These interference effects are missing in (6.49) and this puts the cancellation of Δ divergences in conflict with the soft singularities (6.41) cancellation. Therefore,

combining collinear divergences as in (6.49) means that the Lee-Nauenberg theorem fails because the cross-section is not simultaneously both soft and collinear finite.

By insisting that an inverted energy weighting is applied to all processes other than $P_{0,1}$ another collinear singularity cancellation is possible. This takes place using the same processes required for the soft cancellation (6.41). Degenerate processes can be combined in a way which leads to an infrared finite cross-section through (6.41). There is no physical motivation to apply the energy weighting in such a way, but it does allow us to preserve the Lee-Nauenberg proposition. Bethe-Heitler energy weighting has not been considered for many of the processes under consideration, so a trial and error method was employed here. More research must be done to discover if this energy weighting is physical. In order to achieve the cancellation in (6.41) for collinear divergences and preserve the Lee-Nauenberg proposition we have to place an unpleasant constraint on experiments. We insist that experiments detect a photon through a photon detector. If an experimentalist detected a photon indirectly through energy which is 'missing' in the electron then the delicate infrared cancellation we have achieved in (6.41) is ruined.

Through systematically applying the Lee-Nauenberg proposition we have discovered that it makes an assumption regarding how experiments are conducted. There are problems to do with the convergence of series containing soft and collinear singularities. We have recognised that further research is required to understand the energy weighting and this research could disprove the Lee-Nauenberg theorem.

CONCLUSION

In this thesis new results on the motion of a charged particle within the electromagnetic background of a laser and on the summation and cancellation of infrared divergences have been presented. The main new results will now be summarised. More detailed/technical conclusions may be found at the end of the corresponding chapters and sections contained within this thesis.

The Dynamics of a Particle in a Laser Background

The motion of a particle in a laser background has previously been solved for a relativistic charged particle [8], but the three dimensional trajectory where the motion is described as a function of a reference frame's time is complicated to solve [9]. For a non-relativistic charge the state-of-the-art solution used the dipole approximation (see section 3.1) where terms $\mathcal{O}(v/c)$ and higher are neglected. This disregards the influence of the magnetic field produced by the laser on the trajectory. Work done by Reiss [24] has shown that there is an interesting intermediate region where the fully relativistic theory is not needed but the magnetic field is.

The previously unknown trajectory for a non-relativistic particle under the influence of the electromagnetic background produced by a laser has been found (without using the dipole approximation). The method used to discover this trajectory involved introducing a parameter into the non-relativistic system and thus making time a proper canonical variable. When parameterised in this way the non-relativistic theory has been shown to mimic the relativistic problem and similar techniques may be applied. An interesting duality between high and low intensity regimes has been discussed.

The non-relativistic trajectory we derived is very similar to the well known parametric relativistic solution [8] and the lesser known three dimensional solution [9]. Traditionally trajectories are considered in frames in which the particle is on-average at rest. Here the motion of the particle for a circularly polarised laser is

circular and for a linear polarisation we find a figure of eight. Both of these orbits are expected from the solution to the relativistic problem. By expanding the non-relativistic and relativistic trajectories as functions of the intensity parameter (1.4) we saw that to order η^2 these two models agree. We observed that many of the relativistic phenomena such as the drift velocity and higher harmonic oscillations are also predicted by the non-relativistic theory.

We found an improvement to the method used to derive the three dimensional relativistic trajectory originally discovered by Sengupta [9]. Often the relativistic solution is presented in a parametric form [8] and the evolution is described by the proper time parameter. Using Kepler's equation, the proper time parameter can be removed in the frame in which the particle is, on average, at rest. By finding this analogy to Kepler's equation we made the derivation of the three dimensional relativistic trajectory much more efficient.

The mathematical model we used to describe the laser assumed that the laser pulse is infinitely long. This could be improved upon by including a more realistic pulse function. For instance the constant pulse function chosen in (4.20) could be replaced with a Gaussian. Looking forward, we could examine the non-relativistic modification to Thomson scattering and the effect of the particle's spin on the non-relativistic trajectory. Other potentially fruitful directions we may take are to look into solving the Schrödinger equation using this method or to consider the motion of two non-relativistic charged particles in the background of a laser which are bound together by some potential.

Infrared Divergences

The Lee-Nauenberg theorem has been carefully applied to the Coulomb scattering process. A fundamental aspect of this theorem is the need for unobservable particles in both the final *and* initial state. The Bloch-Nordsieck mechanism only allows for

degeneracies in the final state of a process. A particular emphasis has been placed on the class of divergences omitted by Lee and Nauenberg but noted by Lavelle and McMullan. We call these singularities Δ divergences, where the quantity Δ is the detectors experimental energy resolution i.e. the minimum energy a particle must have for the experiment to detect it. These singularities are associated with the emission and/or absorption of massless charged particles which are *both* soft and collinear. In the bulk of the literature the Bloch-Nordsieck method [2] is used to remove soft divergences and then the Lee-Nauenberg theorem [5] is applied to cancel the remaining collinear divergences in the cross-section. By calculating the Δ divergences we have shown that this infrared cancellation cannot be done for processes with both initial and final state degeneracies.

Lavelle and McMullan [10] were the first to systematically apply the Lee-Nauenberg proposition to all infrared divergences. They showed that, using Coulomb scattering as an example, there are several sums of degenerate processes, different from those used by Bloch and Nordsieck, which remove soft divergences. To achieve this cancellation they needed to incorporate processes involving disconnected photons which provide interference contributions to the cross-section. A careful examination of [5] shows that disconnected processes are an essential part of the Lee-Nauenberg proposition. Each different sum of processes that led to the cancellation of soft divergences involves a different number of disconnected photons.

The aim of this part of the thesis was to give a thorough description of the Lee-Nauenberg theorem and its implications. We have extended the work of Lee and Nauenberg to incorporate the Δ divergences and to see if they can be removed in the same way that Lavelle and McMullan removed the soft divergences. We conclude that, even with the new Δ class of divergences, the cross-section may be rendered infrared finite. Therefore, the Lee-Nauenberg proposition may be preserved, but only if it is systematically applied to soft as well as collinear divergences. However, to

achieve this some questionable assumptions must be made which we describe below.

Recently Weinberg has made his reservations concerning the Lee-Nauenberg theorem clear when he wrote on page 552 of [88]: *"The sum over initial states is more problematic. Presumably one may argue that truly massless particles are always produced as jets accompanied by an ensemble of soft quanta that is uniform within some volume of momentum space. However, to the best of my knowledge no one has given a complete demonstration that the sums of transition rates that are free of infrared divergences are the only ones that are experimentally measurable."* By carefully studying the Lee-Nauenberg proposition when applied to Coulomb scattering we have seen that we must make two questionable assumptions in order to mathematically preserve the Lee-Nauenberg proposition. One of these assumptions places a constraint on experiments. Experimentalists must observe photons directly through a photon detector i.e. they are not allowed to indirectly observe a photon through some 'missing' electron energy. This shows that Weinberg's concerns are in fact well founded. An inverted Bethe-Heitler energy weighting must be introduced for all processes other than the basic emission of a photon. Currently there is no physical motivation to modify the cross-section in this way so further research is required.

There are many topics which may be possible avenues for future work. There has been no attempt made to extend this analysis to QCD, where due to asymptotic freedom and its non-abelian nature, the infrared problem is much more severe [71]. J.C. Taylor has raised an interesting question regarding the fine tuning of the initial state within Lee-Nauenberg theorem and its applicability to real experiments [98]. The infrared problem in QED is also much worse if one lowers the number of dimensions and this could prove to be another important test for the Lee-Nauenberg proposition.

APPENDIX

A. NON-RELATIVISTIC SYMMETRIES

Here we discuss the gauge symmetry and implementing Galilean boosts for a classical charged “non-relativistic” particle travelling in an electromagnetic background.

A.1 Gauge Transformations

In three dimensional notation the gauge potential, $A^\mu = (\phi, \mathbf{A})$ and the coordinates, $x^\mu = (ct, \mathbf{x})$, are transformed under a gauge transformation as

$$\mathbf{A}(t, \mathbf{x}) \rightarrow \mathbf{A}'(t, \mathbf{x}) = \mathbf{A}(t, \mathbf{x}) + \frac{\partial}{\partial \mathbf{x}} \chi(t, \mathbf{x}), \quad (\text{A.1})$$

$$\phi(t, \mathbf{x}) \rightarrow \phi'(t, \mathbf{x}) = \phi(t, \mathbf{x}) - \frac{1}{c} \frac{\partial}{\partial t} \chi(t, \mathbf{x}), \quad (\text{A.2})$$

Under the gauge transformation (A.1) and (A.2) the Lagrangian (3.7) is *not* invariant. It transforms like

$$\mathcal{L}\left(\mathbf{x}, \frac{d\mathbf{x}}{dt}, t\right) \rightarrow \mathcal{L}\left(\mathbf{x}, \frac{d\mathbf{x}}{dt}, t\right) + \frac{e}{c} \frac{d}{dt} \chi(t, \mathbf{x}(t)), \quad (\text{A.3})$$

where d/dt denotes the *total derivative*

$$\frac{d}{dt} := \frac{d\mathbf{x}}{dt} \cdot \frac{\partial}{\partial \mathbf{x}} + \frac{\partial}{\partial t}. \quad (\text{A.4})$$

Since the variation (A.3) of the Lagrangian is a total derivative of the function $e/c \chi(t, \mathbf{x}(t))$ it *does not* affect the classical equations of motion. It is interesting to mention that the gauge transformation can be treated as a canonical transformation

with the generating function

$$F(\mathbf{x}, \mathbf{P}, t) = \mathbf{x} \cdot \mathbf{P} - \Omega(t, \mathbf{x}(t)). \quad (\text{A.5})$$

A.2 Galilean Boosts

For small velocities we neglect $\mathcal{O}(V^2/c^2)$ and higher. A Lorentz boost, in the x direction, reduces to the Galilean transformation

$$t' = t, \quad x' = x - Vt, \quad y' = y, \quad z' = z, \quad (\text{A.6})$$

while the gauge potential will transform as

$$\phi' = \phi - \frac{V}{c} A_x, \quad A_x' = A_x - \frac{V}{c} \phi, \quad A_y' = A_y, \quad A_z' = A_z, \quad (\text{A.7})$$

Using (A.6) and (A.7) and keeping only the leading order V/c terms the Lagrangian (3.7) transforms as

$$\mathcal{L} \rightarrow \mathcal{L}' = \mathcal{L} - mV \frac{dx}{dt} - \frac{e}{c} V A_x + \frac{e}{c} V A_x + \frac{m}{2} V^2 + o(V/c) \quad (\text{A.8})$$

$$\Rightarrow \mathcal{L} - m \frac{d}{dt} \left(Vx - \frac{1}{2} V^2 t \right). \quad (\text{A.9})$$

Note that V is not infinitesimally small so terms $\mathcal{O}(V^2)$ survive. Therefore the Lagrangian is only invariant under a Galilean boost *up to a total derivative*. However, this change is important when considering a quantum treatment.

B. GENERAL BOUNDARY CONDITIONS

During the main body of the thesis we solved the equations of motion with the initial condition (3.55) when we could have solved for more general boundary conditions. Plugging the expression for the gauge potential (3.49) into the function $W(u, \Pi_\perp)$ from (3.25) we have

$$W(u, \Pi_\perp) = -\eta^2 m^2 c^2 (\epsilon^2 \cos^2 u + (1 - \epsilon^2) \sin^2 u) + 2\eta mc (\Pi_1 \cos u + \Pi_2 \sin u) .$$

The integral in (3.39) with this expression is an elliptic integral. Using the trigonometric substitution $x = \tan(u/2)$ it can be rewritten in the Weierstrass form (see [60] section 13.5):

$$t(s) = \frac{2}{\omega_L} \int_0^{\tan(\omega_L s/2)} dx \frac{1}{\sqrt{f(x)}} , \quad (\text{B.1})$$

with the fourth order polynomial

$$f(x) = a_0 x^4 + 4a_1 x^3 + 6a_2 x^2 + 4a_3 x + a_4 , \quad (\text{B.2})$$

whose coefficients are

$$a_0 := \beta_+^2 - \eta^2 \epsilon^2 - 2\eta \beta_1 , \quad a_1 := \eta \beta_2 , \quad a_3 := \eta \beta_2 , \quad (\text{B.3})$$

$$a_2 := \frac{1}{3} \beta_+^2 + \eta^2 \left(\epsilon^2 - \frac{2}{3} \right) , \quad a_4 := \beta_+^2 - \eta^2 \epsilon^2 + 2\eta \beta_1 . \quad (\text{B.4})$$

According to the classical result [59] attributed to Weierstrass, the integral (B.1) can be inverted:

$$\tan\left(\frac{\omega_L s}{2}\right) = \frac{\sqrt{f(0)} \wp'\left(\frac{\omega_L}{2} t\right) - \frac{1}{2} \left[\wp\left(\frac{\omega_L}{2} t\right) - \frac{1}{24} f''(0) \right] + \frac{1}{24} f(0) f'''(0)}{2 \left[\wp\left(\frac{\omega_L}{2} t\right) - \frac{1}{24} f''(0) \right]^2 - \frac{1}{48} f(0) f''''(0)}. \quad (\text{B.5})$$

Here the number of primes over the polynomial (B.2) denotes the order of the derivatives with respect to x . In (B.5) the Weierstrass double periodic function, $\wp(z; g_2, g_3)$ depends on two invariants (see [59] section 20.6 for details) g_2 and g_3 of the polynomial (B.2) which are

$$\begin{aligned} g_2 : &= 4\eta^4 \left(\varepsilon^4 - \varepsilon^2 + \frac{1}{3} \right) - 4\eta^2 \left(\frac{1}{3} \beta_+^2 + \beta_-^2 \right) + \frac{4}{3} \beta_+^4, \\ g_3 : &= \frac{4}{3} \eta^6 \left(\varepsilon^4 - \varepsilon^2 + \frac{2}{9} \right) - 4\eta^4 \left[\frac{2}{3} \varepsilon^4 \beta_+^2 + \varepsilon^2 \left(\beta_1^2 - \beta_2^2 - \frac{2}{3} \beta_+^2 \right) + \frac{1}{9} \beta_+^2 - \frac{2}{3} \beta_1^2 + \frac{1}{3} \beta_2^2 \right] \\ &\quad - \frac{4}{3} \eta^2 \beta_+^2 \left(\frac{1}{3} \beta_+^2 + \beta_-^2 \right) + \frac{8}{27} \beta_+^6. \end{aligned}$$

These equations show that the dependence of the trajectory on the initial conditions, contained within the invariants g_2 and g_3 is quite subtle.

C. JACOBIAN ELLIPTIC FUNCTIONS

Here, following the classical textbooks [59,60], we have collected the basic formulae describing the Jacobian elliptic functions which are extensively used in part I.

The *amplitude function* $\phi := \text{am}(z, \mu)$ is the *inverse* of the function defined by the integral

$$z(\phi) = \int_0^\phi d\vartheta \frac{1}{\sqrt{1 - \mu^2 \sin^2 \vartheta}}. \quad (\text{C.1})$$

The function $\text{am}(z, \mu)$ is defined on its principal domain which for real z is $(-\mathbb{K}, \mathbb{K})$. The value of constant, \mathbb{K} depends on *modulus* μ and is given by the *complete elliptic integral*, see (C.7) below.

Three *Jacobi elliptic functions*, $\text{sn}(z, \mu)$, $\text{cn}(z, \mu)$ and $\text{dn}(z, \mu)$ are analytical functions of the complex variable z everywhere except at the simple poles. They are expressed in terms of the amplitude function

$$\text{sn}(z, \mu) = \sin(\text{am}(z, \mu)), \quad \text{cn}(z, \mu) = \cos(\text{am}(z, \mu)), \quad \frac{d}{dz} \text{am}(z, \mu) = \text{dn}(z, \mu), \quad (\text{C.2})$$

and satisfy the basic algebraic equations

$$\text{sn}^2 z + \text{cn}^2 z = 1, \quad \mu^2 \text{sn}^2 z + \text{dn}^2 z = 1, \quad (\text{C.3})$$

and differential relations

$$\frac{d}{dz} \operatorname{sn}(z, \mu) = \operatorname{sn}(z, \mu) \operatorname{dn}(z, \mu), \quad (\text{C.4})$$

$$\frac{d}{dz} \operatorname{cn}(z, \mu) = -\operatorname{sn}(z, \mu) \operatorname{dn}(z, \mu), \quad (\text{C.5})$$

$$\frac{d}{dz} \operatorname{dn}(z, \mu) = -\mu^2 \operatorname{sn}(z, \mu) \operatorname{cn}(z, \mu), \quad (\text{C.6})$$

which shows their analogy to the trigonometric functions.

Functions $\operatorname{sn}(z, \mu)$, $\operatorname{cn}(z, \mu)$ and $\operatorname{dn}(z, \mu)$ are doubly periodic functions of z . Periods of $\operatorname{sn}(z, \mu)$ are $4\mathbb{K}$ and $2i\mathbb{K}'$ while periods of $\operatorname{cn}(z, \mu)$ are $4\mathbb{K}$ and $2\mathbb{K} + 2i\mathbb{K}'$. Function $\operatorname{dn}(z, \mu)$ has periods $2\mathbb{K}$ and $4i\mathbb{K}'$. The “real” (\mathbb{K}) and “imaginary” (\mathbb{K}') quarter periods are real numbers given by the complete elliptic integrals

$$\mathbb{K}(\mu) := \int_0^{\pi/2} d\vartheta \frac{1}{\sqrt{1 - \mu^2 \sin^2 \vartheta}}, \quad (\text{C.7})$$

$$i\mathbb{K}'(\mu) := i \int_0^{\pi/2} d\vartheta \frac{1}{\sqrt{1 - (1 - \mu^2) \sin^2 \vartheta}}. \quad (\text{C.8})$$

The Jacobian functions as functions of the modulus are single valued on the complex μ plane with two cuts $[1, \infty)$ and $(-\infty, 0]$.

The discrete symmetry. The Jacobian functions cn and dn are even functions, while sn is an odd function, they obey the relations

$$\operatorname{sn}(u + 2m\mathbb{K} + 2ni\mathbb{K}', \mu) = (-)^m \operatorname{sn}(u, \mu), \quad (\text{C.9})$$

$$\operatorname{cn}(u + 2m\mathbb{K} + 2ni\mathbb{K}', \mu) = (-)^{m+n} \operatorname{cn}(u, \mu),$$

$$\operatorname{dn}(u + 2m\mathbb{K} + 2ni\mathbb{K}', \mu) = (-)^n \operatorname{dn}(u, \mu),$$

with $n, m \in \mathbb{Z}$.

Two degenerate cases. The double periodic Jacobian functions degenerate into simpler functions when one of their periods becomes infinite, that if μ is 0 or 1.

When $\mu = 1$ the real quarter-period $\mathbb{K} = \infty$ and the Jacobian functions degenerate into the hyperbolic functions

$$\operatorname{sn}(u, 1) = \tanh u, \quad \operatorname{cn}(u, 1) = \frac{1}{\cosh u}, \quad \operatorname{dn}(u, 1) = \frac{1}{\cosh u}. \quad (\text{C.10})$$

If $\mu = 0$ the real quarter-period is finite, $\mathbb{K} = \pi/2$, but the imaginary quarter-period is infinite and the Jacobian functions degenerate into the trigonometric functions

$$\operatorname{sn}(u, 0) = \sin u, \quad \operatorname{cn}(u, 0) = \cos u, \quad \operatorname{dn}(u, 0) = 1. \quad (\text{C.11})$$

Small modulus expansions. When the modulus is small enough the Jacobian functions can be approximated by

$$\operatorname{am}(z, \mu) = z - \frac{1}{4} \mu^2 [z - \sin(z) \cos(z)] + o(\mu^4), \quad (\text{C.12})$$

$$\operatorname{sn}(z, \mu) = \sin(z) - \frac{1}{4} \mu^2 [z - \sin(z) \cos(z)] \cos(z) + o(\mu^4), \quad (\text{C.13})$$

$$\operatorname{cn}(z, \mu) = \cos(z) + \frac{1}{4} \mu^2 [z - \sin(z) \cos(z)] \cos(z) + o(\mu^4), \quad (\text{C.14})$$

$$\operatorname{dn}(z, \mu) = 1 - \frac{1}{2} \mu^2 \sin^2(z) + o(\mu^4). \quad (\text{C.15})$$

The quarter period \mathbb{K} with a small modulus may be expanded into the form

$$\mathbb{K} = \frac{\pi}{2} \left[1 + \left(\frac{1}{2} \right)^2 \mu^2 + \left(\frac{1 \cdot 3}{2 \cdot 4} \right)^2 \mu^4 + \left(\frac{1 \cdot 3 \cdot 5}{2 \cdot 4 \cdot 6} \right)^2 \mu^6 + \dots \right]. \quad (\text{C.16})$$

The Fourier series expansions:

$$\begin{aligned}\operatorname{sn}(z, \mu) &= \frac{2\pi}{\mu\mathbb{K}} \sum_{n=1}^{\infty} \frac{q^{n-1/2}}{1 - q^{2n-1}} \sin(2n-1) \frac{\pi z}{2\mathbb{K}}, \\ \operatorname{cn}(z, \mu) &= \frac{2\pi}{\mu\mathbb{K}} \sum_{n=1}^{\infty} \frac{q^{n-1/2}}{1 + q^{2n-1}} \cos(2n-1) \frac{\pi z}{2\mathbb{K}}, \\ \operatorname{dn}(z, \mu) &= \frac{2\pi}{\mathbb{K}} + \frac{2\pi}{\mathbb{K}} \sum_{n=1}^{\infty} \frac{q^n}{1 + q^{2n}} \cos 2n \frac{\pi z}{2\mathbb{K}},\end{aligned}\tag{C.17}$$

where the *nome*, or Jacobian parameter, is defined by $q := \exp(-\pi\mathbb{K}'/\mathbb{K})$. Similarly, since it is a function of the quarter periods the nome q can be expanded in powers of the modulus

$$q = \frac{\mu^2}{16} + 8 \left(\frac{\mu^2}{16} \right)^2 + 84 \left(\frac{\mu^2}{16} \right)^3 + \dots\tag{C.18}$$

The modular transformations. The doubly periodic elliptic functions with different periods can be expressed through each other. The following identities hold

$$\operatorname{sn}(iz, \mu') = i \frac{\operatorname{sn}(z, \mu)}{\operatorname{cn}(z, \mu)}, \quad \operatorname{cn}(iz, \mu') = \frac{1}{\operatorname{cn}(z, \mu)}, \quad \operatorname{dn}(iz, \mu') = \frac{\operatorname{dn}(z, \mu)}{\operatorname{cn}(z, \mu)},\tag{C.19}$$

$$\operatorname{sn}(\mu'z, \frac{i\mu}{\mu'}) = \mu' \frac{\operatorname{sn}(z, \mu)}{\operatorname{dn}(z, \mu)}, \quad \operatorname{cn}(\mu'z, \frac{i\mu}{\mu'}) = \frac{\operatorname{cn}(z, \mu)}{\operatorname{dn}(z, \mu)}, \quad \operatorname{dn}(\mu'z, \frac{i\mu}{\mu'}) = \frac{1}{\operatorname{dn}(z, \mu)},\tag{C.20}$$

$$\operatorname{sn}(\mu z, \underline{\mu}) = \mu \operatorname{sn}(z, \mu), \quad \operatorname{cn}(\mu z, \underline{\mu}) = \operatorname{dn}(z, \mu), \quad \operatorname{dn}(\mu z, \underline{\mu}) = \operatorname{cn}(z, \mu).\tag{C.21}$$

where $\underline{\mu} = 1/\mu$ and $\mu' := \sqrt{1 - \mu^2}$, which is called the *complementary modulus*.

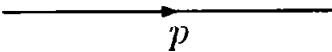
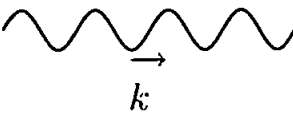
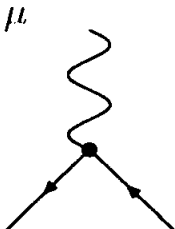
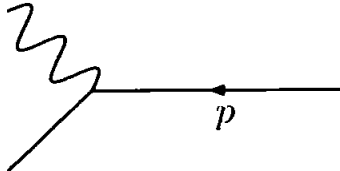
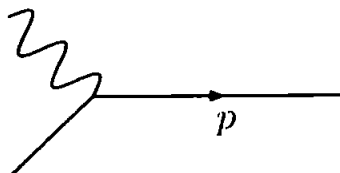
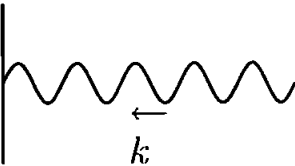
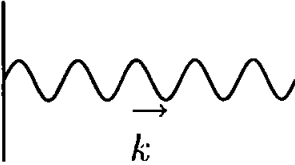
D. FEYNMAN RULES FOR QED

The QED Lagrangian is

$$\mathcal{L}_{\text{QED}} = -\frac{1}{4}F_{\mu\nu}F^{\mu\nu} + \bar{\psi}(i\not{D} - m)\psi + \mathcal{L}_{\text{G.F.}}. \quad (\text{D.1})$$

From this the Feynman rules use to calculate S -Matrix elements may be derived, they are give in table D. For an electron, in this thesis, the charge $Q = 1$. For the complete set of Feynman rules we should include anti-fermions too, but these are not needed for the calculations contained within this work. Momentum must be conserved at each vertex and virtual loop momentum are integrated over. Diagrams also have a symmetry factor but for many of the cases considered during this thesis it equals one.

Often we are considering processes which, at the level of the cross-section, may contribute via interference with a completely disconnected photon. The Feynman rule applied to these processes is given in figure 5.2.

Fermion propagator		$= \frac{i}{\not{p} - m + i\epsilon}$
Photon propagator		$= \frac{-ig_{\mu\nu}}{k^2 + i\epsilon}$
Vertex		$= iQe\gamma^\mu$
Initial external fermion		$= u^s(p)$
Final external fermion		$= \bar{u}^s(p)$
Initial external photon		$= \epsilon_\mu(k)$
Final external photon		$= \epsilon_\mu^*(k)$

Tab. D.1: Feynman rules for QED

E. SOME COLLINEAR APPROXIMATIONS

At various places in this thesis we make approximations based on collinearity. There are two classes of approximations that we will discuss in detail.

Type 1: Terms of the form $p \cdot k'$ that occur in a numerator where k' is not collinear with p , but is approximately collinear with p' . Here we want to understand how to relate the scalar product $p \cdot k'$ and $p \cdot p'$.

Type 2: Terms of the form $p_n \cdot k'$ that occur in a denominator where k' is approximately collinear with p_n , so the scalar product is very small. Here we want to understand how to relate the scalar product $p_n \cdot k'$ and $p \cdot k'$.

Type 1 approximations: Here we consider the non-vanishing $p \cdot k'$

$$p \cdot k' = E_p \omega' - |\mathbf{p}| |\mathbf{k}'| \cos(\theta_{k'}), \quad (\text{E.1})$$

where $\theta_{k'}$ is the large angle between the momenta \mathbf{p} and \mathbf{k}' . Neglecting terms of order m (which would be collinear finite) we can replace here $|\mathbf{k}'|$ by $|\mathbf{p}'| \omega' / E_{p'}$. Define $\theta_{p'}$ the angle between \mathbf{p} and \mathbf{p}' , then $\theta_{p'} = \theta_{k'} + \delta$ where δ is small. The angle in $\cos(\theta_{k'})$ may be replaced by $\cos(\theta_{p'})$ since the correction δ will only introduce finite corrections to our integrals. In this way we see that, for the divergent terms, we may rewrite the numerator using

$$p \cdot k' = p \cdot p' \frac{\omega'}{E'}. \quad (\text{E.2})$$

This manipulation allows us to express several divergent structures via a small number of integrals.

Type 2 approximations: We are interested in approximating $p_n \cdot k'$, where p_n and k' are on-shell but p is not. We are interested in the region where p_n is almost collinear with k' so these terms are small. Naively, we might expect that the simple identity

$$p_n \cdot k' = (p - nk') \cdot k' = p \cdot k', \quad (\text{E.3})$$

would suffice. However, in the text, we need to compare $p_n \cdot k'$ with $p \cdot k'$ where p is an on-shell momentum which is not the case in (E.3) except in the exactly collinear (and hence vanishing) limit. Thus a more careful argument is needed.

To proceed we need to relate the angles between the various vectors. Let θ_n be the small angle between p_n and k' , and let θ be the small angle between p and θ . Recall that $p_n = p - nk'$ and hence p is not on-shell. Indeed, it is straightforward to show that for small θ_n we have

$$p^2 = nE_n\omega'\theta_n^2. \quad (\text{E.4})$$

Similarly, writing p_n in terms of p and k' , we see that the on-shell condition for p_n implies that

$$0 = nE_n\omega'\theta_n^2 - 2nE\omega' + 2n|p|\omega'(1 - \frac{1}{2}\theta^2). \quad (\text{E.5})$$

Now the spatial component of p can be written as $\mathbf{p} = \mathbf{p}_n + n\mathbf{k}'$. Hence we can write

$$|p| = E - \frac{nE_n}{2E}\omega'\theta_n^2. \quad (\text{E.6})$$

Combining this result with (E.5) we find the approximation

$$E_n^2 \theta_n^2 = E^2 \theta^2. \quad (\text{E.7})$$

Using this result and the small angle approximation that

$$\frac{1}{p_n \cdot k'} = \frac{2}{\omega' E_n (\theta_n^2 + \frac{m^2}{E_n^2})}, \quad (\text{E.8})$$

it is now straightforward to show that

$$\frac{1}{p_n \cdot k'} \frac{E}{E_n} = \frac{1}{p \cdot k'}. \quad (\text{E.9})$$

BIBLIOGRAPHY

- [1] C. Itzykson and J. B. Zuber, Quantum Field Theory, McGraw-Hill, New York (1980).
- [2] F. Bloch and A. Nordsieck, Phys. Rev. **52**, 54 (1937).
- [3] P. P. Kulish and L. D. Faddeev, Theor. Math. Phys. **4**, 745 (1970).
- [4] T. Kinoshita, J. Math. Phys. **3**, 650 (1962).
- [5] T. D. Lee and M. Nauenberg, Phys. Rev. **133**, B1549 (1964).
- [6] V. Chung, Phys. Rev. **140**, B1110 (1965).
- [7] L. D. Landau and E. M. Lifshitz, Course of Theoretical Physics, Volume 2: The Classical Theory of Fields, Pergamon Press, Oxford, (1975).
- [8] E. S. Sarachik and G. T. Schappert, Phys. Rev. D **1**, A705 (1970).
- [9] N. Sengupta, Bull. Calcutta Math. Soc. **41** (1949).
- [10] M. Lavelle and D. McMullan, JHEP **03**, 026 (2006).
- [11] T. Kinoshita and D. R. Yennie, Adv. Ser. Direct. High Energy Phys. **7**, 1 (1990).
- [12] H. Reiss, Prog. Quant. Electron. **16** (1992).
- [13] N. Delone and V. Krainov, Atoms in Strong Light Fields, Springer Series in Chemical Physics, Vol. 28, Berlin, New York, Springer-Verlag, (1985).

-
- [14] N. Delone and V. Krainov, *Multiphoton Processes in Atoms*, Berlin, New York, Springer-Verlag, (2000).
- [15] F. Faisal, *Theory of Multiphoton Processes*, Plenum, New York, (1987).
- [16] M. Fedorov, *Electron in a Strong Optical Field*, Nauka, Moscow, (1991).
- [17] Y. I. Salamin, S. X. Hu, K. Z. Hatsagortsyan, and C. H. Keitel, *Phys. Rept.* **427**, 41 (2006).
- [18] T. T. G.A. Mourou and S. Bulanov, *Rev. Mod. Phys.* **78**, 309 (2006).
- [19] C. Bamber *et al.*, *Phys. Rev.* **D60**, 092004 (1999).
- [20] K. T. McDonald, Appeared in *Proc. of 2nd Workshop on Laser Acceleration of Particles*, Los Angeles, CA, Jan 7-18, (1985).
- [21] T. Heinzl and O. Schroeder, *J. Phys.* **A39**, 11623 (2006).
- [22] K. D. Shmakov, *Study of Nonlinear QED Effects in Interactions of Terawatt Laser with High Energy Electron Beam*, PhD thesis, SLAC-R-666, (1997).
- [23] J. Jackson, *Classical Electrodynamics*, New York , Wiley, (1999).
- [24] H. Reiss, *Phys. Rev. A* **63** (2000).
- [25] K. H. M. Klaiber and C. Keitel, *Phys. Rev. A* **75**, 063413 (2007).
- [26] Y. Salamin, *Phys. Rev. A* **56**, 4910 (1997).
- [27] L. Brown and T. Kibble, *Phys. Rev.* **133**, A705 (1964).
- [28] A. Nikishov and V. Ritus, *Zh. Eksp. Teor. Fiz.* **46**, 776 (1964).
- [29] H. Reiss, *J. Math. Phys.* **3**, 59 (1962).
- [30] J. Frenkel, *Z. Phys.* **32**, 27 (1925).

-
- [31] A. Taub, *Phys. Rev.* **73**, 768 (1948).
 - [32] J. Eberly and A. Sleeper, *Phys. Rev.* **176**, 1570 (1968).
 - [33] J. Kupersztych, *Phys. Rev.* **D17**, 629 (1978).
 - [34] R. W. Brown and K. L. Kowalski, *Phys. Rev. Lett.* **51**, 2355 (1983).
 - [35] Y. Salamin and F. Faisal, *Phys. Rev. A* **54**, 5 (1996).
 - [36] W. Thirring, *Classical Mathematical Physics: Dynamical Systems and Field Theories*, Springer , (1997).
 - [37] Vachaspati, *Phys. Rev* **128**, 664 (1962).
 - [38] I. Goldman, *Phys. Lett.* **8**, 103 (1964).
 - [39] J. Eberly, *Phys. Lett.* **19**, 284 (1965).
 - [40] V. Ritus, *Trud. Fiz. Inst. Acad. Nauk. SSSR* **111**, 5 (1979).
 - [41] M. Babzien, *Phys. Rev. Lett.* **96** (2006).
 - [42] M. Henneaux and C. Teitelboim, Princeton, USA: Univ. Pr. (1992).
 - [43] P. Dirac, *Lectures on Quantum Mechanics*, Belfer Graduate School of Science, Monographs Series Yeshiva University, New York, (1964).
 - [44] K. Sundermeyer, *Lect. Notes Phys. Constrained Dynamics* **169**, 1 (1982).
 - [45] L. H. Ryder, *Quantum Field Theory*, Cambridge, UK: Univ. Pr. (1985).
 - [46] H. Goldstein, *Classical Mechanics*, Addison-Wesley (1980).
 - [47] T. Tsang, *Statistical Mechanics*, Rinton Press, (2002).
 - [48] T. Heinzl, *Lect. Notes Phys.* **572**, 55 (2001).

-
- [49] W. Heitler, *The Quantum Theory of Radiation*, Oxford University Press, (1950).
- [50] F. Rohrlich, *Classical Charged Particles*, Addison-Wesley, Reading, Massachusetts, (1965).
- [51] J. Bergou and S. Varró, *J. Phys. A* **13**, 3553 (1980).
- [52] K. Drühl and J. McIver, *J. Math. Phys.* **24**, 705 (1983).
- [53] J. J. Sanderson, *Phys. Letters* **18**, 114 (1965).
- [54] A. D. Steiger and C. H. Woods, *Phys. Rev.* **D6**, 1468 (1972).
- [55] A. D. Steiger and C. H. Woods, *Phys. Rev.* **D5**, 2912 (1972).
- [56] E. Whittaker, *A Treatise on the Analytical Dynamics of Particles and Rigid bodies*, Third Ed., Cambridge University Press, Cambridge, (1927).
- [57] V. Arnold, *Mathematical Methods of Classical Mechanics*, Springer-Verlag, New-York, (1984).
- [58] R. Abraham and J. Marsden, *Foundations of Mechanics*, Second Ed., Benjamin/Cummings, Reading, Massachusetts, (1978).
- [59] E. T. Whittaker and G. N. Watson, *A Course of Modern Analysis*, Cambridge University Press, (1952).
- [60] H. Bateman, *Higher Transcendental Functions* vol. II, McGraw-Hill, New-York, (1953).
- [61] E. McMillan, *Phys. Rev.* **79**, 498 (1950).
- [62] T. Kibble, *Phys. Rev.* **138**, 1060 (1965).
- [63] M. Abramowitz and I. A. Stegun, *Handbook of Mathematical Functions with Formulas, Graphs, and Mathematical Tables*, (Dover, New York, 1964).

-
- [64] E. M. Stein and R. Shakarchi, *Princeton Lectures in Analysis: II Complex Analysis*, Princeton University Press, Princeton, (2003).
- [65] W. Rindler, *Introduction to Special Relativity*, Second Ed. Clarendon Press, Oxford, (1991).
- [66] CTEQ, J. Botts *et al.*, *Phys. Lett.* **B304**, 159 (1993).
- [67] K. G. Wilson and J. B. Kogut, *Phys. Rept.* **12**, 75 (1974).
- [68] M. E. Peskin and D. V. Schroeder, *An Introduction to Quantum Field Theory*, Addison-Wesley (1995).
- [69] E. Bagan, M. Lavelle, and D. McMullan, *Annals Phys.* **282**, 471 (2000).
- [70] J. D. Dollard, *J. Math. Phys.* **5**, 729 (1964).
- [71] R. Doria, J. Frenkel, and J. C. Taylor, *Nucl. Phys.* **B168**, 93 (1980).
- [72] C. Di'Lieto, S. Gendron, I. G. Halliday, and C. T. Sachrajda, *Nucl. Phys.* **B183**, 223 (1981).
- [73] A. A. Abrikosov, *Sov. Phys. JETP* **5**, 1174 (1957).
- [74] S. Weinberg, *Phys. Rev.* **140**, B516 (1965).
- [75] T. Muta and C. A. Nelson, *Phys. Rev.* **D25**, 2222 (1982).
- [76] A. Axelrod and C. A. Nelson, *Phys. Rev.* **D32**, 2385 (1985).
- [77] R. Akhoury, M. G. Sotiropoulos, and V. I. Zakharov, *Phys. Rev.* **D56**, 377 (1997).
- [78] H. F. Contopanagos and M. B. Einhorn, *Phys. Rev.* **D45**, 1291 (1992).
- [79] R. Jackiw, Presented at Les Houches Summer School on Theoretical Physics: Relativity Groups and Topology, Les Houches, France, Jun 27 - Aug 4, (1983).

-
- [80] N. Nakanishi and I. Ojima, *World Sci. Lect. Notes Phys.* **27** (1990).
- [81] F. Mandl and G. Shaw, *Quantum Field Theory*, Wiley, (1984).
- [82] R. Horan, M. Lavelle, and D. McMullan, *Pramana* **51**, 317 (1998).
- [83] J. Jauch and F. Rohrlich, *The Theory of Photons and Electrons: the Relativistic Quantum Field Theory of Charged Particles with Spin One-half*, Springer-Verlag, Heidelberg, (1976).
- [84] R. Horan, M. Lavelle, and D. McMullan, *J. Math. Phys.* **41**, 4437 (2000).
- [85] F. N. Havemann, Scanned version available at KEK library, (1985).
- [86] E. Bagan, M. Lavelle, and D. McMullan, *Annals Phys.* **282**, 503 (2000).
- [87] M. Lavelle and D. McMullan, *Phys. Rept.* **279**, 1 (1997).
- [88] S. Weinberg, *The Quantum Theory of Fields. Vol. 1: Foundations*, Cambridge University Press, (1995).
- [89] H. M. Fried, *Green's Functions and Ordered Exponentials*, Cambridge Univ Pr, (2002).
- [90] L. S. Brown, *Quantum Field Theory*, Cambridge Univ Pr, (1992).
- [91] H. Bethe and W. Heitler, *Proc. Roy. Soc. A* **146**, 83 (1934).
- [92] M. Bohm, A. Denner, and H. Joos, *Gauge Theories of the Strong and Electroweak Interaction*, Stuttgart, Germany: Teubner, (2001).
- [93] D. R. Yennie, S. C. Frautschi, and H. Suura, *Ann. Phys.* **13**, 379 (1961).
- [94] T. W. B. Kibble, *J. Math. Phys.* **9**, 315 (1968).
- [95] M. Lavelle and D. McMullan, (2006), hep-ph/0607262.

-
- [96] C. De Calan and G. Valent, Nucl. Phys. **B42**, 268 (1972).
 - [97] I. Ito, Prog. Theor. Phys. **65**, 1466 (1981).
 - [98] J. C. Taylor, Phys. Rev. **D54**, 2975 (1996).

Infrared Divergences from Soft and Collinear Gauge Bosons

Paul Jameson

School of Mathematics and Statistics

University of Plymouth

Plymouth, PL4 8AA, U.K.

1 Introduction

To compare with experiment it is vital that theoretical predictions are finite. Beyond leading order in perturbation theory many processes contain infrared divergences. It is often argued that these singularities are eliminated at the level of the inclusive cross-section [1, 2]. During this talk I will show that the infrared divergences are still poorly understood. I also expose some questionable assumptions which must be made to render the theoretical cross-section finite.

There are two types of infrared singularities – soft and collinear. Soft divergences are associated with low energy photons. Collinear divergences occur in high-energy or theories with massless charges. It is common practice to use the Bloch-Nordsieck trick [1] for the soft divergences. By adding the bremsstrahlung process to the cross-section with a virtual loop the overall cross-section is soft finite. Soft divergences can be regulated by dimensional regularisation where the number of dimensions, $D = 4 + 2\epsilon_{\text{IR}}$. Focusing on the infrared pole, the Bloch-Nordsieck trick is summarised diagrammatically at next-to-leading order by:

$$2 \left(\text{diagram 1} + \text{diagram 2} \right) + \left| \text{diagram 3} \right|^2 = -\frac{1}{\epsilon_{\text{IR}}} + \frac{1}{\epsilon_{\text{IR}}}, \quad (1)$$

up to an overall multiplicative constant. This sum corresponds to the idea that there may be low energy unobserved photons accompanying charges in the final state. Such processes are indistinguishable by experiment from an isolated charge. They are referred to as degenerate processes. The Bloch-Nordsieck trick, however, does not work for collinear divergences.

The standard approach to deal with collinear divergences was developed by Lee and Nauenberg [2]. Their quantum mechanical theorem states that the sum over all degenerate processes is infrared finite. In field theory one should thus include *both*

initial and final state degeneracies. In this talk I will analyse the Lee-Nauenberg theorem applied to high-energy QED. Collinear divergences will be regulated by the effectively small mass, m , of the electron and will appear as terms proportional to $\ln(m)$.

2 New Class of Collinear Divergences

It is assumed in [2] that soft divergences have been dealt with by the Bloch-Nordsieck trick and thus only collinear singularities produced by photons with energies greater than the experimental resolution Δ are considered. Recent work has shown that there is a class of divergences which were omitted in Lee and Nauenberg's paper [3]. These come from processes where low energy (soft) photons travelling parallel (collinearly) to the charges are emitted and/or absorbed. These processes contain $\Delta \ln(m)$ collinear singularities in their cross-section which, from now on, will be referred to as Δ -divergences. By inserting these divergences into the analysis conducted in [2] it may be seen that the cross-section cannot be simultaneously both soft and collinear finite. The reason for this failure may be traced back to the different ways soft and collinear singularities are dealt with.

The Lee-Nauenberg theorem states that one should consider initial state degeneracies. However, at first sight, including the absorption of low energy photons has the effect of reintroducing the soft divergences so that (1) becomes:

$$2 \left(\text{diagram 1} + \text{diagram 2} \right) + \left| \text{diagram 3} + \text{diagram 4} \right|^2 + \left| \text{diagram 5} + \text{diagram 6} \right|^2 = -\frac{1}{\epsilon_{\text{IR}}} + \frac{1}{\epsilon_{\text{IR}}} + \frac{1}{\epsilon_{\text{IR}}}. \quad (2)$$

However, all degeneracies must be considered and Lavelle and McMullan have shown that the residual soft divergences in (2) may be cancelled by including the following cross-section contributions:

$$2 \left(\text{diagram 7} + \dots + \text{diagram 8} \right) + \left| \text{diagram 9} + \text{diagram 10} \right|^2 = -\frac{2}{\epsilon_{\text{IR}}} + \frac{1}{\epsilon_{\text{IR}}}. \quad (3)$$

The striking thing here is the need for the disconnected processes in the application of the Lee-Nauenberg theorem. This was only briefly noted in the original paper [2].

Investigations, by a variety of authors [3-8], have shown the need to consider such disconnected processes as displayed above. The amplitudes which interfere with the disconnected ones are the emission and absorption of a photon which can take place with either electron leg. By including all the above processes the $\ln(m)$ and soft singularities are eliminated. However, in order to fully determine whether the cross-section is finite the Δ -divergences must also be studied. The aim of this work is to discover if the Coulomb scattering cross-section can be made simultaneously both soft and collinear infrared finite.

Lee and Nauenberg's theorem states that one should include all degenerate processes at each order of perturbation theory. However, at the same order of perturbation theory an infinite number of disconnected photons may be considered! Processes contributing to the next-to-leading order Coulomb scattering cross-section may be clustered into groups in which the soft singularities are eliminated:

$$\frac{1}{\varepsilon_{\text{IR}}} \left[\underbrace{-1 + 1}_{\text{Bloch-Nordsieck}} + \underbrace{(1 - 2 + 1)}_{\text{Lee-Nauenberg}} + \underbrace{(1 - 2 + 1)}_{\text{Lee-Nauenberg}} + \underbrace{(1 - 2 + 1)}_{\text{Lee-Nauenberg}} + \dots \right]. \quad (4)$$

For each additional disconnected photon there are three further processes to consider. By calculating the soft divergences one obtains another factor of $(1 - 2 + 1)$. Higher numbers of disconnected photons are *not* suppressed in this series so it will not converge. In practice this series is arbitrarily truncated at one of the finite stages to obtain a finite cross-section. Further discussion of this mathematically ill-defined procedure may be found in [3].

3 Cancellation of Δ -Divergences

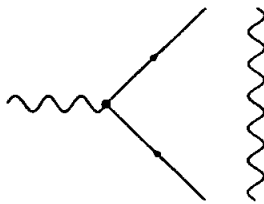


Figure 1: A process involving a disconnected photon.

The disconnected photon, displayed in Figure 1, cannot be collinear with the electron both before and after it has been scattered. Therefore, in order for it to contribute to Coulomb scattering (and not be identified as a different process) the photon's energy must be lower than the experiment's detector resolution. Disconnected processes provide contributions to the cross-section which can be soft *and*

collinear. Therefore they produce Δ -divergences. The question arises: do these Δ divergences cancel for the same combination of diagrams as the soft singularities (4)?

Photons may be detected by an experiment in two ways:

1. Directly, through a detector with resolution Δ ;
2. Indirectly, through a measurement of the electron's 'missing' energy.

A shift in the electron's energy puts an upper limit on the total energy contained by any number of soft photons. An electron energy detector is a powerful tool for determining whether a process is different from tree-level Coulomb scattering if multiple photons are contributing to the process. If the process contributes to Coulomb scattering then the photon's energy (or energies when including disconnected photons) is such that it cannot be detected by either of the above methods.

I have studied the next-to-leading order Coulomb scattering cross-section and evaluated all the Δ -divergences. The technical details will not be presented here (see [14]) and instead I will state the results. Removal of Δ -divergences from the cross-section may take place using exactly the same prescription as soft divergences (4). However, for this cancellation to take place the following assumptions are required.

1. All processes must have an inverted energy weighting¹. The exception to this rule is the emission process for which the usual Bethe-Heitler weighting is applied.
2. Experimentalists *must* observe photons *directly* through a photon detector i.e. they are *not* allowed to indirectly observe a photon through 'missing' electron energy.

The energy weighting applied is not supported by a physical motivation (other than the infrared finiteness which I am trying to prove). However, without this choice of weighting the Lee-Nauenberg theorem fails because the Δ -divergences are sensitive to the energy weighting. My calculations prove that in order for the Δ -divergences to cancel, the maximum photon energy must be the same for each of the processes being combined. If a photon is detected indirectly then the amplitudes which contain different numbers of soft photons will have different maximum photon energies. The

¹I have followed the lead set by Bethe and Heitler. They state that for the emission cross-section an *energy weighting* factor which is equal to the electron energy in the out-state divided by the electron energy in the in-state should be included. For references see section 5-2-4 in [9], p. 499 of [10], p. 244 of [11], p. 309 of [12] and the original paper [13]. Intuitively the probability for emission and absorption should be equivalent. This requirement leads to the introduction of an *inverted* energy weighting for the absorption process. In the literature the energy weighting has only been carefully considered for the emission process. Collinear Δ -divergences are highly sensitive to the energy weighting scheme used so it will be important while studying their cancellation.

processes required to cancel the soft singularities, displayed in equations (2) and (3), contain a different number of soft photons so the second assumption is necessary.

Weinberg has made his reservations clear on the application of the Lee-Nauenberg theorem. I quote from page 552 of [15] “... *to the best of my knowledge no one has given a complete demonstration that the sums of transition rates that are free of infrared divergences are the only ones that are experimentally measurable.*” Through this calculation I have shown that Weinberg’s reservations are well-founded since infrared finiteness places a condition on the way experiments are conducted.

In summary what I have seen is that not only does the Lee-Nauenberg approach to the infrared lead to an ill defined series of diagrams but there is no natural way to achieve infrared finiteness. Further research is urgently required.

I am grateful to Martin Lavelle and David McMullan for their advice and assistance during the conduct of this research.

References

- [1] F. Bloch and A. Nordsieck, Phys. Rev. **52**, 54 (1937).
- [2] T. D. Lee and M. Nauenberg, Phys. Rev. **133**, B1549 (1964).
- [3] M. Lavelle and D. McMullan, JHEP **03**, 026 (2006), hep-ph/0511314.
- [4] C. De Calan and G. Valent, Nucl. Phys. **B42**, 268 (1972).
- [5] I. Ito, Prog. Theor. Phys. **65**, 1466 (1981).
- [6] T. Muta and C. A. Nelson, Phys. Rev. **D25**, 2222 (1982).
- [7] A. Axelrod and C. A. Nelson, Phys. Rev. **D32**, 2385 (1985).
- [8] R. Akhoury, M. G. Sotiropoulos, and V. I. Zakharov, Phys. Rev. **D56**, 377 (1997), hep-ph/9702270.
- [9] C. Itzykson and J. B. Zuber, *Quantum Field Theory*, McGraw-Hill, New York (1980).
- [10] L. S. Brown, *Quantum field theory*, Cambridge, UK: Univ. Pr. (1992).
- [11] W. Heitler, *The Quantum Theory of Radiation*, Oxford University Press, (1950).
- [12] M. Bohm, A. Denner, and H. Joos, Stuttgart, Germany: Teubner (2001).
- [13] H. Bethe and W. Heitler, Proc. Roy. Soc. A **146**, 83 (1934).

- [14] P. Jameson, M. Lavelle and D. McMullan, in preparation.
- [15] S. Weinberg, *The Quantum Theory of Fields. Vol. 1: Foundations* , CUP, (1995)
609 p.